2013

Amalgamation of Nucleosides and Amino Acids in Antibiotic Biosynthesis

Sandra H. Barnard
University of Kentucky, sans4824@gmail.com

STUDENT AGREEMENT:

I represent that my thesis or dissertation and abstract are my original work. Proper attribution has been given to all outside sources. I understand that I am solely responsible for obtaining any needed copyright permissions. I have obtained and attached hereto needed written permission statements(s) from the owner(s) of each third-party copyrighted matter to be included in my work, allowing electronic distribution (if such use is not permitted by the fair use doctrine).

I hereby grant to The University of Kentucky and its agents the non-exclusive license to archive and make accessible my work in whole or in part in all forms of media, now or hereafter known. I agree that the document mentioned above may be made available immediately for worldwide access unless a preapproved embargo applies.

I retain all other ownership rights to the copyright of my work. I also retain the right to use in future works (such as articles or books) all or part of my work. I understand that I am free to register the copyright to my work.

REVIEW, APPROVAL AND ACCEPTANCE

The document mentioned above has been reviewed and accepted by the student's advisor, on behalf of the advisory committee, and by the Director of Graduate Studies (DGS), on behalf of the program; we verify that this is the final, approved version of the student's dissertation including all changes required by the advisory committee. The undersigned agree to abide by the statements above.

Sandra H. Barnard, Student

Dr. Steven Van Lanen, Major Professor

Dr. Jim Pauly, Director of Graduate Studies

Amalgamation of Nucleosides and Amino Acids in Antibiotic Biosynthesis

Dissertation

A dissertation submitted in partial fulfillment of the requirement
for the degree of Doctor of Philosophy in the College of Pharmacy
at the University of Kentucky
By

Sandra Hummel Barnard

Lexington, KY
Director: Dr. Steven Van Lanen
Assistant Professor of Pharmaceutical Sciences
Lexington, Kentucky
2013

Abstract of Dissertation

Amalgamation of Nucleosides and Amino Acids in Antibiotic Biosynthesis

The rapid increase in antibiotic resistance demands the identification of novel antibiotics with novel targets. One potential antibacterial target is the biosynthesis of peptidoglycan cell wall, which is both ubiquitous and necessary for bacterial survival. Both the caprazamycin-related compounds A-90289 and muraminomicin, as well as the capuramycin-related compounds A-503083 and A-102395 are potent inhibitors of the translocase I enzyme, one of the key enzymes required for cell wall biosynthesis. The caprazamycin-related compounds contain a core nonproteinogen β-hydroxy-α-amino acid referred to as 5'-*C*-glycyluridine (GlyU). Residing within the biosynthetic gene clusters of the aforementioned compounds is a shared open reading frame which encodes a putative serine hydroxymethyltransferase (SHMT). The revelation of this shared open reading frame resulted in the proposal that this putative SHMT catalyzes an aldol-type condensation reaction utilizing glycine and uridine-5'-aldehyde, resulting in the GlyU core. The enzyme LipK involved in A-90289 biosynthesis was used as a model to functionally assign this putative SHMT to reveal its functions as an L-threonine: uridine-5'-aldehyde transaldolases. Biochemical analysis indicates enzymatic activity is dependent upon pyridoxal-5'-phosphate, is non-reactive with alternative amino acids, and produces acetaldehyde as a co-product. Structural characterization of the enzymatic product is consistent with (5'*S*,6'*S*)-GlyU indicating that this enzyme orchestrates a C-C bond breaking and formation resulting in two new stereocenters to make a new L-α-amino acid. The same activity was demonstrated for the LipK homologues involved in the biosynthesis of muraminomicin, A-503083, and A-102395. This L-threonine: uridine-5'-aldehyde transaldolase was used with alternative aldehyde substrates to prepare unusual L-α-amino acids, suggesting the potential for exploiting this enzyme to make new compounds.

Sandra Hummel Barnard
2013

L-Threonine Transaldolase, C-C Bond, Caprazamycin, Capuramycin, Serine Hydroxymethyltransferase

Amalgamation of Nucleosides and Amino Acids in Antibiotic Biosynthesis

By

Sandra Hummel Barnard

Dr. Steven Van Lanen
(Director of Dissertation)

Dr. Jim Pauly
(Director of Graduate Studies)

2013

Dedicated to my Grandpa

Acknowledgments

I would like to take this chance to express my gratitude to all of those who have helped pave my path on this journey. First and foremost is my family, without which none of this dissertation would have been possible. Their constant support and example is the platform on which I stand and I am more grateful than words can express.

Second is Dr. Steven Van Lanen and my lab mates Xiuling Chi, Wenlong Cai, and Anwesha Goshwami, as well as everyone in Dr. Rohr's lab. They are some of the most amazing individuals I have ever met and the environment they provided me to live and learn is uncomproable, thank you so, so much. I would also like to thank my committee Dr. Dr. Jürgen Rohr, Dr. Kyung-Bo Kim, Dr. Robert Perry, and Dr. Natasha Kyprianou your advice and direction is invaluable and I greatly appreciate your time and patience over the years.

Finally I would like to thank all of my friends who, perhaps unintentionally, reminded me that laughter truly can be a "cure all" in the darkest situations

Table of Contents

Tables

Figures

ABBREVIATIONS

°C	Degree Celsius
M	Micro
Aa	Amino acids
Bp	Base pair
Da	Dalton
DMSO	dimethyl sulfoxide
DNA	deoxyribonucleic acid
DTT	1,4-dithiothreitol
E. coli	*Escherichia coli*
EDTA	ethylendiamine tetra-acetic acid
ESI	electrospray ionization
H	Hour
HCl	hydrochloric acid
His_6	Hexahistidine
HPLC	high performance liquid chromatography

HSQC	Heteronuclear Single Quantum Coherence
IPTG	isopropyl-*β*-thiogalactoside
k	kilo
KAc	potassium acetate
Kan	kanamycin
kb	kilo base pairs
kDa	kilo Dalton
Ki	inhibition constant
Km	Michaelis-Menten constant
L	litre
LB	Luria broth
M	molar
m	milli
MG	methylglutarate
min	minute
MS	mass spectrometry
MW	molecular weight

m/z	mass-to-charge ratio
n	nano
NADP	nicotine amide adenine dinucleotide phosphate
NaOH	sodium hydroxide
NMR	Nuclear magnetic resonance spectroscopy
nt	nucleotide
OD500	optical density at 500 nm
ORF	open reading frame
p	pico
PAGE	polyacrylamide gel electrophoresis
PCR	polymerase chain reaction
PEG	polyethylene glycol
PLP	pyridoxal phosphate
RBS	ribosome binding site
RNA	ribonucleic acid
RNase	ribonuclease

RP	reverse phase
rpm	revolutions per minute
s	second
S.	*Streptomyces*
SDS	sodium dodecyl sulfate
TEMED	N,N,N´,N´-tetramethylethylenediamine
TCA	Trichloracetic acid
TES	N-Tris-(hydroxymethyl)-methyl-2-aminoethanesulfonic acid
Thio	thiostrepton
TFA	Trifluoroacetic acid
Tris	2-amino-2-(hydroxymethyl)-1,3-propanediol
Tris-maleate	Tris-(hydroxymethyl)-aminomethane-maleate
U	unit
UA	Uridine-5′-aldehyde
UDP	uridine diphosphate

UV	ultraviolet
*V*max	maximal reaction velocity
WT	wild-type

Chapter One

INTRODUCTION

1.1 Searching for new antibiotics

The drastic increase in antibacterial resistance requires priority be given to the formation and discovery of novel antibacterial compounds. The limited shelf life of antibiotics is due in part to the natural or acquired resistance mechanism of the organism, which has been correlated to the quantity of antibiotic used, the frequency of use, the size of the population it's prescribed for, the resistance mechanisms for the drug already present in the organism, the quantity of mutations required for resistance in the organism, and the fitness of the resistant organism. Currently, an innovation gap exists in finding novel antibacterial structures that deviate from the main classes of antibiotics; the β-lactams, the macrolides, sulfonamides, and the fluoroquinolones (Fig. 1.1), the majority of which were discovered more than 60 years ago (1). Therefore, the search for novel antibacterial compounds continues.

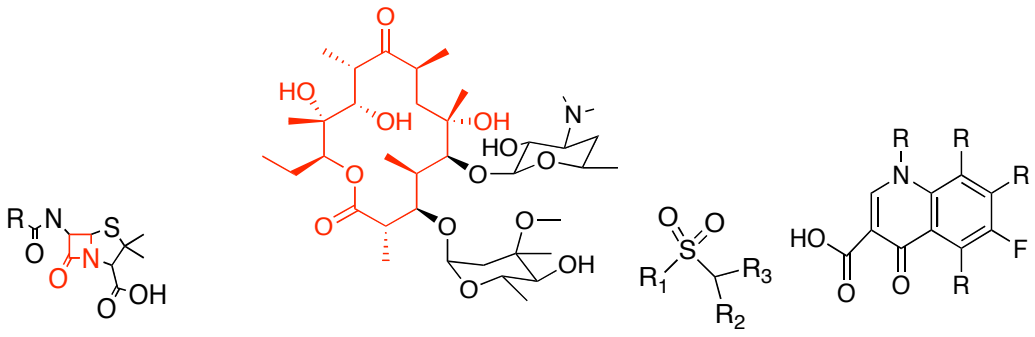

Figure 1.1 Structural examples of the main classes of antibiotics.

Natural products have been one of the leading sources of unprecedented bioactive compounds. Over the last 25 years, more than 60% of small-molecule compounds introduced as novel drugs were derived from natural products (2). However, as of late, pharmaceutical companies have focused on combinatorial chemistry, high-throughput screening of synthetic chemical libraries, and computer assisted design for novel drug compound development (3). While methods of identifying novel drug compounds vary over time, the consistency of natural products to unearth elaborate, novel compounds is still unequaled. Displaying complex scaffolds with richly deployed functional groups, natural products utilize enzymatic pathways which enable structural diversity that cannot be synthesized and is essential in drug development (4). One potential strategy to harness the unique capabilities of these unprecedented structures and optimize current drug compounds, is using a biosynthetic approach for production and discovery of these complex compounds.

1.1.1 Current antibacterial targets

Multiple sites in bacterial replication have proven effective targets for bacterial growth inhibition. Protein biosynthesis, DNA and RNA replication, thymine biosynthesis, cell surface decoration, isoprenoid biosynthesis, and peptidoglycan cell wall formation have all proven effective antibacterial targets. Protein biosynthesis targeting the bacterial ribosome within the organism is one primary target for antibiotics. The bacterial ribosome consists of two subunits (30S and 50S) of rRNA and protein. Antibiotics such as macrolides and oxazolidones bind

to the 50S unit while aminoglycosides and tetracyclines bind to the 30S unit inhibiting protein biosysnthesis (5-7). These inhibitors thus derail essential biosynthesis of proteins resulting in cell death.

DNA and RNA replication, as well as thymine biosynthesis are two more classical antibacterial targets. The antibiotics rifampin, ciprofloxacin, and the novobiocins successfully inhibit DNA and RNA formation during bacterial growth and therefore prevent antibacterial replication. Rifampin functions by binding to RNA polymerase and therefore inhibiting the polymerase from attaching to the DNA for transcription. Ciprofloxacin and novobiocins repress the introduction of supercoils in DNA by binding to DNA gyrase. By inhibiting DNA and RNA formation, the ability of the organism to survive is greatly reduced (6, 8). Thymine, generated by folate metabolism and utilized in DNA formation, is another successful target for antibitiotics such as sulfamethoxazole and trimethoprim. By depleting dihydropteroate, sulfamethoxazole inhibits dihydropteroate synthase by reducing the amount of dihydrofolate and thus folate. Trimethoprim, another antibacterial compound successful in inhibiting bacterial replication, inhibits the formation of tetrahydrofolate. By depleting dihdrofolate reductase, the compound trimethoprim successfully prohibits the formation of tetrahdyrofolate from dihydrofolate and therefore halts folate synthesis (9, 10).

Two more potential antibacterial targets are cell surface decoration and isoprenoid biosynthesis. Sortases, present in gram-positive bacteria, are enzymes which cleave cell surface proteins. These enzymes are anchored into the membrane by membrane spanning sequences containing an amino terminal and they covalently attach to the peptidoglycan cell wall by an amino terminal cleavage fragment of the surface protein (11). Another unique target not present in higher organisms is the non-classical (non-mevalonate) pathway of isoprenoid biosynthesis. Isotopic labeling studies have shown a divergence in the formation of isoprenoid units between most human pathogens and vertebrates. Vertebrates utilize the mevalonate pathway while most human pathogens incorporate isoprenoid units by means of the non-mevalonate pathway. This alternative pathway utilizes enzymes such as 1-deoxy-D-xylulose 5-phosphate reductoisomerase and 1-hydroxy-2-methyl-2-(E)-butenyl D-erythritol 2,4-cyclodiphosphate synthase which would be ideal targets for antibacterial compounds due to the lack of mammalian homologs (12, 13).

Finally, the peptidoglycan cell wall is a prime target due to its multiple inhibition sites, its presence in both gram-positive and gram-negative bacteria, and its necessity for the survival of nearly all bacteria. Peptidoglycan cell wall biosynthesis requires multiple enzymes, many of which are ideal targets for antibacterial inhibition. Peptidoglycan contains *N*-acetylglucosamine (glcNac) and *N*-acetyl-muramic acid (MurNAc), two hexoses forming the backbone of a cross-linked polymer. Lipids I and II are formed when the peptidoglycan units are

transferred to a carrier lipid which transports the precursors across the cellular membrane. One of the key enzymatic activities is that of transporting molecules aided by the translocase enzymes (14).

1.1.2 Formation of the Peptidoglycan cell wall

The biosynthesis of peptidoglycan cell wall has proven a viable target for antibacterial compounds. Drugs such as fosfomycin inhibiting MurA, ramoplanin inhibiting MurG, vancomycin inhibiting transglycolastion, and the β-lactams which inhibit the transpeptidation step have all been clinically used as antibiotics (15-18). The peptidoglycan cell wall is assembled by a series of enzymatic reactions within the cytoplasm as well as the periplasm that are depicted in Figure 1.2. The initial steps in the biosynthetic pathway are composed of stepwise additions of L-Ala, D-Glu, L-Lys or M-DAP, and D-Ala-D-Ala onto UDPMurNAc. This sequence is catalyzed by a series of ATP-dependent ligases MurC-F to form the precursor UDPMurNAc-pentapeptide. The pentapeptide then forms lipid I when it is transferred onto a lipid carrier undecaprenyl phosphate catalyzed by the enzyme bacterial translocase Ior MraY. Lipid II is subsequently formed when the product of MraY is tailored by the addition of a GlcNAc sugar onto the 4′-hydroxyl or MurNAc catalyzed by the enzyme MurG. The lipid-linked intermediate is then transported across the cytoplasmic membrane to the periplasm. Lipid II then undergoes transglycosylation to form a polysaccharide that is cross-linked by transpeptidation. The transglycosylation releases the undecaprenyl

pyrophosphate and then recycles it by means of dephosphorylation and “flipped” back to the cytoplasm to serve as a substrate for MraY (13) (Fig. 1.2).

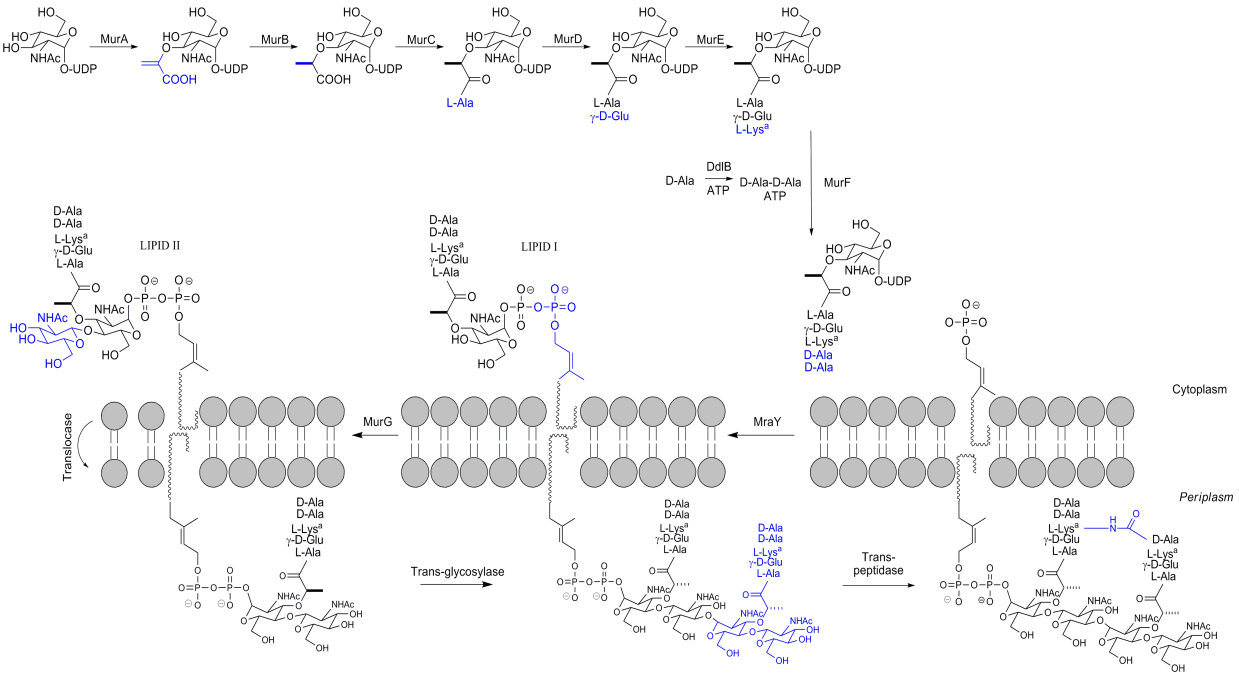

Figure 1.2 Step wise biosynthesis of the peptidoglycan cell wall within gram-positive and gram-negative bacteria. This residue is either an L-lysine in gram-positive bacteria or diaminopimelic acid in gram-negative bacteria.

1.2 Translocase I inhibitors

A key step in the biosynthesis of the peptidoglycan cell wall is the transfer of phosphor-*N*-acetylmuramic acid pentapeptide from UDP-*N*-acetylmuramic acid pentapeptide to undecaprenyl phosphate catalyzed by the enzyme MraY (Fig. 1.3)(19-21). The integral ten transmembrane, α-helical protein is ubiquitious

within bacteria, and lacks any mammalian homolog thus making it an ideal target for antibacterial compounds. However, while the identity of MraY was revealed in 1993, lack of tertiary structure and the refractory nature to overexpression and purification to homogeneity of this protein has rendered biochemical studies to be very difficult (13, 22). Fortunately, a small amount of *Bacillus subtilis* MraY has been purified to homogeneity and crude extracts of MraY from *Escherichia coli* and *Stapylococcus aureus,* have been obtained. Comparative analysis of the enzymes reveals five cytoplasmic and six perplasmic conserved domains. Alignment of the MraY cytoplasmic domains from *E. coli, B. subtilis,* and *S. aureus* maintain multiple highly conserved residues including three strictly conserved aspartic acid residues (Asp-115, Asp-116, and Asp-267) which may form the active site of the enzyme (23, 24).

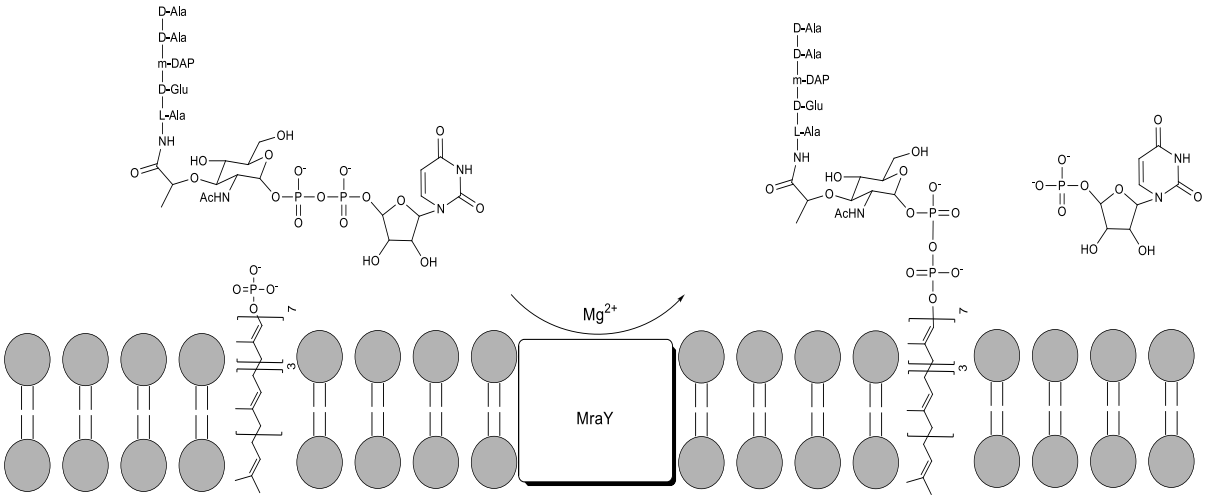

Figure 1.3. Enzymatic activity of the translocase I enzyme MraY. The Mg^{2+} dependent reaction initiates the phosphor-transfer of UDP-*N*-acetylmuramic acid to the isoprenoid unit embedded within the lipid wall subsequently forming UMP and lipid I.

Despite the difficulty associated with studying MraY, several screens over the past decade have discovered several classes of natural product antibiotics which have shown to inhibit MraY. Tunicamycins, mureidomycins, liposidomycin, muraymycin, capuramycin, and caprzamycin are examples of the classes of antibiotics which contain a uridine-like moiety with a high carbon furanoside (Fig. 1.4). Highlighted by a uridine disaccharide extended by a fatty acyl chain, the tunicamycins consist of one family of reversible, competitive MraY inhibitors. However, due to inhibition of GlcNAc-1-P transferase in glycoprotein biosynthesis, tunicamycins are toxic to mammals (25).

Two distinct classes of uridine-containing MraY inhibitors are the peptidyl nucleoside products mureidomycins and the liposidomycins. Mureidomycins contain a 3′-deoxyuridine sugar moiety and are highlighted by a unique peptide chain that is attached by means of an unusual enamide linkage. The peptide chain includes an *N*-methyl 2,3-diaminobutyric acid reside as well as a urea linked to a C-terminal aromatic amino acid of *meta*-tyrosine, Trp, or Phe. These slow binding inhibitors are believed to act by binding to the Mg^{2+} cofactor-binding site of MraY at the amino terminus (20). The liposidomycins consist of a sulfated aminoglycoside and fatty-acyl residues bonded to the uridine-containing core. These slow binding inhibitors show moderate activity against solubilized *E. coli* MraY. However, synthetic analogs of these compounds appear more promising due to better activity and increased spectrum of antibacterial activity (14, 19).

The muraymicyms represent another family of MraY inhibitors that contain an aminoribofuranoside monosaccharide connected to a peptide chain, that has an unusual urea linked to a C-terminal amino acid. These potent inhibitors show promising antibacterial activity against drug-resistant strains of *S. aureus* and *Enterococci*. Synthetic analogues of these compounds, which lack the aminoribofuranoside, have reduced *in vitro* activity, but retain some antibacterial activity (19, 26). The final two classes, the caprazamycin and capuramycin-related compounds, also inhibit the translocase I enzyme MraY and are the classes focused on in this dissertation (21).

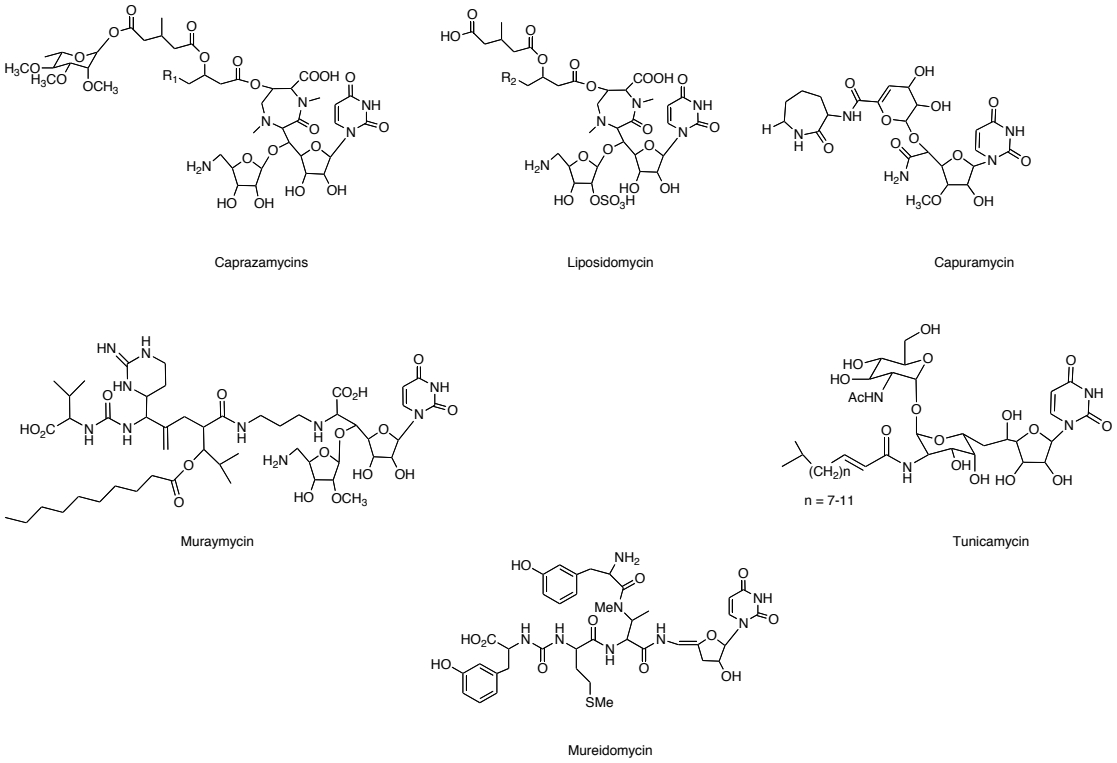

Figure 1.4. Families of known translocase I MraY inhibitor compounds.

1.2.1. Caprazamycin-related compounds

The liponucleoside antibiotics of the caprazamycin-related compounds show *in vitro* activity against gram-positive bacteria with no significant toxicity unlike tunicamycin, thus showing high potential as antibacterial compounds (27). Discovered in 2003 by specific enzymatic screening for MraY translocase I inhibition, the caprazamycin structure was established shortly thereafter in 2005 (28, 29). The core skeleton consists of an *N*-alkylated 5′-(β-*O*-aminoribosyl)-glycyluridine which is shared with that of closely related liposidomycins also shown to inhibit the formation of lipid I by inhibiting MraY translocase I (Fig. 1.5) (13, 30).

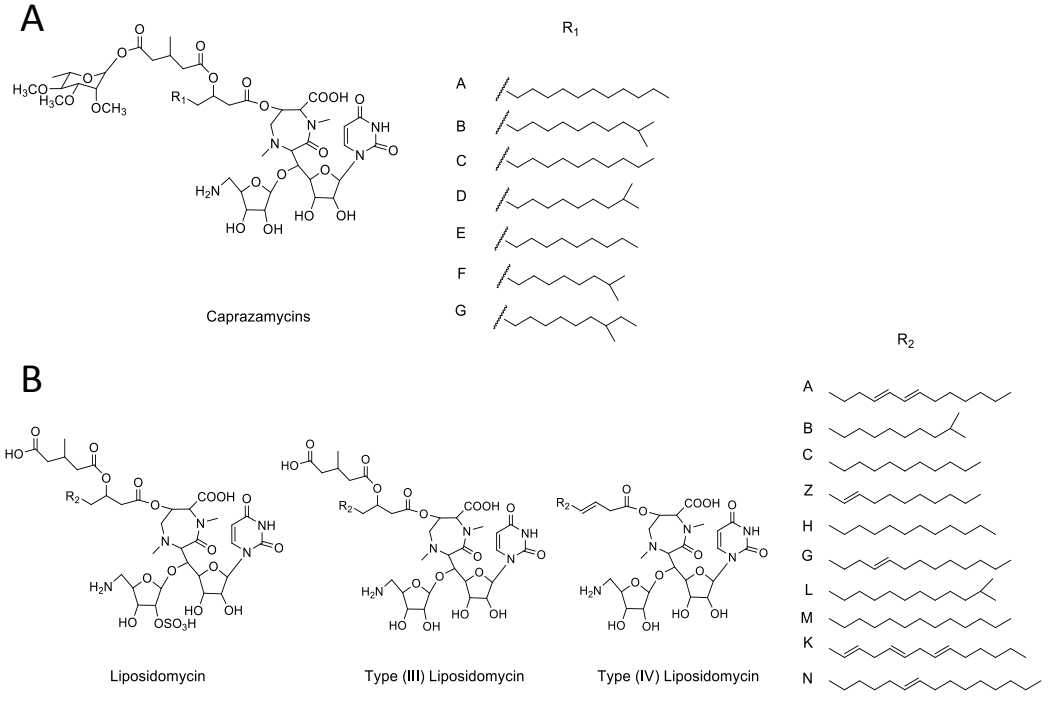

Figure 1.5. Nucleosid antibiotics of the translocase I inhibitor family highlighting the *N*-alkylated 5′-(β-*O*-aminoribosyl)-glycyluridine core. (A) The caprazamycin family of the MraY translocase I inhibitor family. (B) The liposidomycin family of the MraY translocase I inhibitor family.

1.2.2 Capuramycin-Related Compounds

The capuramycin analogs, also containing a uridine core with a high carbon furanose, show potent MraY translocase I inhibition with IC_{50} values within 10-20 nm. In contrast to the caprazamycin-related compounds, the capuramycin-related compounds are highlighted by a 5′-C-carbamoyluridine (CarU) core with an unusual unsaturated hexose attached via a glycosidic bond (19, 31). Initially discovered in 1986 by generic antibacterial activity screens, the specific analogs A-503083 and A-500359 were identified by specific enzymatic screens to identify inhibitors of MraY translocase I (Fig. 1.6) (31-34).

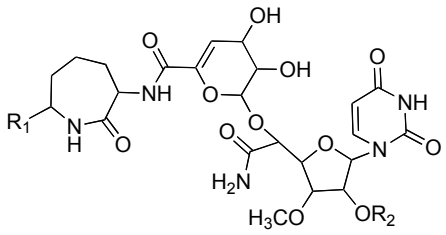

A-500359 A $R_1 = CH_3$, $R_2 = H$
A-500359 B $R_1 = R_2 = H$
A-503083 A $R_1 = CH_3$, $R_2 = CONH_2$
A-503083 B $R_1 = H$, $R_2 = CONH_2$
A-503083 E $R_1 = OCH_3$, $R_2 = CONH_2$
A-503083 F $R_1 = OH$, $R_2 = CONH_2$

Figure 1.6. Nucleoside antibiotics of the translocase I inhibitor family highlighting the 5′-*C*-carbamoyluridine.

We are interested in delineating the biosynthesis of the caprazamycin-like compounds A-90289 isolated from *Streptomyces* sp. SANK 60405, and muraminomicin isolated from *Streptosporangium amethystogenes* SANK 60709, as well capuramycin-like compounds A-503083 isolated from *Streptomyces* sp.

SANK 62799, and A-102395 isolated from *Amycolatopsis* sp. SANK 60206 (Fig. 1.7). All four compounds were discovered using an assay for identification of MraY activity *in vitro* and therefore are potential leads as antibiotics that target peptidoglycan cell wall biosynthesis (31, 35-37).

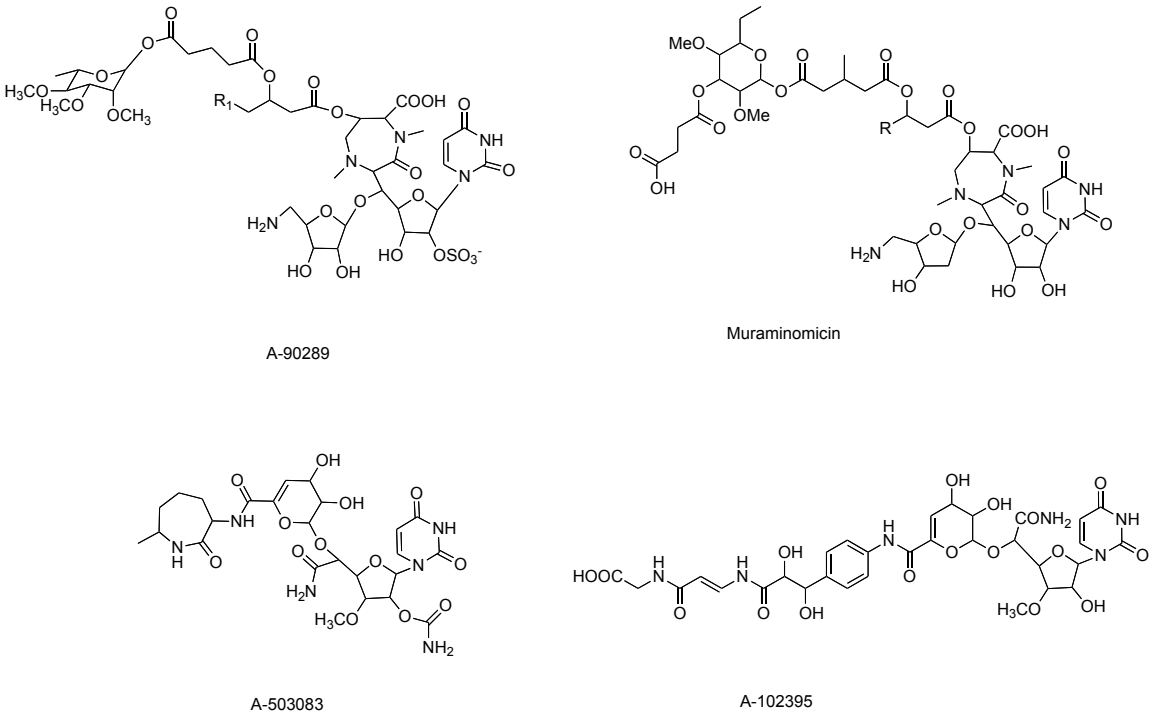

Figure 1.7. MraY translocase I inhibitor compounds discussed in this dissertation.

Previous work in our lab and others has identified the biosynthetic gene clusters for the lipopeptidyl nucleoside family including the compounds A-90289 (a caprazamycin-related compound), caprazamycins, and muraymycins. Each of

the compounds contains an aminoribosyl moiety attached by means of a 5′-O-glycosidic bond to a 5′-*C*-glycyluridine moiety. The putative open reading frames (*orfs*) shared within these clusters include those encoding a nonheme, Fe(II)-dependent dioxygenase (LipL), a putative nucleotidylyltransferase (LipM), a glycosyltransferase (LipN), an aminotransferase (LipO), a uridine phosporylase (LipP), and a serine hydroxymethyltransferase (LipK) hypothesized to form the 5′-*C*-glycyluridine (GlyU) core. Prior studies in our group have revealed LipL as a nonheme, Fe(II)-dependent dioxygenase converting UMP to uridine-5′-aldehyde (UA), LipO as an L-methionine:UA aminotransferase utilizing UA as a substrate, LipP as a low specificity phosphorylase, LipM as a primary amine-requiring nucleotidylyltransferase, and LipN as a 5-amino-5-deoxyribosyltransferase (Fig. 1.8) (38, 39). However, while five of the six shared genes have been shown to form the aminoribosyl moiety of the final compound, the putative serine hydroxymethyltransferase (SHMT) and its activity in forming the GlyU core was still in question.

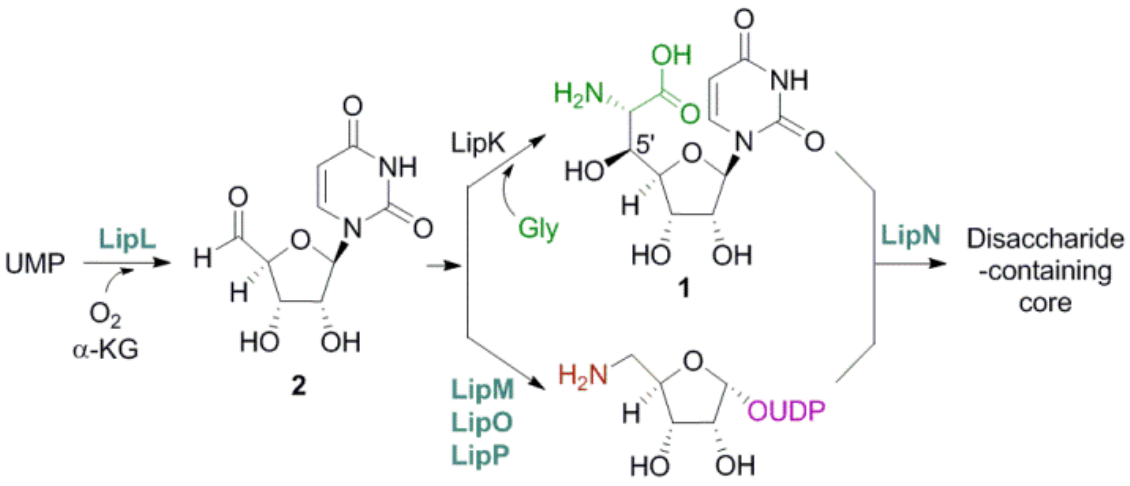

Figure 1.8. Biosynthesis of the disaccharide-containing nucleoside core of lipopeptidyl nucleoside antibiotics. Enzymes in blue have been functionally assigned.

Comparative bioinformatic analysis of the genes required for the formation of the caprazamycin-related compounds and the capuramycin-related compounds A-503083 and A-102395 revealed all of the clusters contain the *orfs* encoding the non-heme, Fe(II)-dependent α-ketoglutarate: UMP dioxygenase (LipL) as well as the putative SHMT. Gene deletion of the *orf* encoding the putative SHMTs from the biosynthetic gene clusters responsible for forming the caprazamycin-related compounds caused a failure to synthesize the final compound. Recently our lab has revealed the necessity of the putative SHMT within the biosynthetic pathway of A-102395 by showing the abolishment of production upon gene inactivation (27, 31, 35, 40). The lack of any detectable product formation without the presence of the putative SHMT within the biosynthetic gene cluster indicates necessity of the enzyme for biosynthesis. Also, the shared LipL homolog

amongst the biosynthetic gene clusters suggests that the UA product formed by LipL and its homologs is a shared intermediate and may be a precursor substrate for the putative SHMTs. These similarities prompted us to investigate the function of the putative SHMT and to define its role in the biosynthesis of the caprazamycin and capuramycin-related compounds.

The canonical SHMT is known primarily for its function in DNA biosynthesis by the inter-conversion of Ser and tetrahydrofolate (THF) to Gly and N^5, N^{10}-methylene-THF. However, the compound N^5, N^{10}-methylene-THF is known to be the donor of a single carbon group for use not only in thymidine biosynthesis, but also can be oxidized by to form the methenyl incorporated into purine biosynthesis, or be reduced to form the methyl group donated to sulfur during methionine biosynthesis (41, 42).

The formation of the single carbon donor N^5, N^{10}-methylene-THF is primarily dependent on the SHMT. The essential role of SHMT has spawned numerous reports describing the biochemistry, structure, and mechanism of this enzyme. Under the umbrella of the B_6-dependent (or PLP) enzymes, the SHMT is classified as a member of the type I fold, or α-family. This particular enzyme initiates a reaction by formation of an internal aldimine by binding a key Lys residue with the co-factor pyridoxal-5′-phosphate (PLP) which enables Ser to bind to PLP forming an external aldimine. The β-hydroxyl group is then deprotonated by a general base of the enzyme initiating an electron

rearrangement utilizing the PLP as an electron sink and forming formaldehyde and a Gly bound PLP product. The formaldehyde group is then incorporated onto THF in a series of reactions forming N^5, N^{10}-methylene-THF (Fig. 1.9) (4, 43).

While the *in vivo* role of canonical SHMTs in transferring the Cβ of Ser to THF is well established, several studies have revealed that these SHMTs are also able to catalyze numerous reactions in the absence of THF. Decarboxylation, transamination, retroaldol cleavage, and racemization reactions have all been seen at rates sometimes approaching or even surpassing those of physiological reactions when THF is absent (44, 45). These *in vitro* studies of SHMTs raise interesting questions about the role that the putative SHMTs play in the biosynthesis of MraY inhibitors.

Another enzyme of great interest due to its similarity to the canonical SHMT is L-threonine aldolase (LTA or LTAE). Also a type I fold PLP dependent enzyme, the canonical LTA catalyzes the interconversion of L-Thr to Gly and acetaldehyde. SHMT and LTA share similar catalytic properties and are able to catalyze similar reactions including the retroaldol cleavage of varying L-3-hydroxyamino acids, the transamination and the racemization of D- and L-alanine, and the exchange of the α-proton of Gly with solvent. While both enzymes show similar enzymatic activity, LTA and SHMT appear to have modest specificity for

the retroaldol cleavage of L-allo-threonine and the Cβ of serine to H_4PteGlu respectively (4, 46).

Due to the intriguing chemistry catalyzed by SHMTs and LTAEs, including the alternative reactions observed, we set out to establish the putative SHMTs function within the biosynthetic gene clusters of the caprazamycin and capuramycin-related compounds. We envisioned that the results would not only provide a definitive biosynthetic pathway of the known MraY inhibitor compounds, but also serve as a genetic fingerprint for identifying future antibiotics.

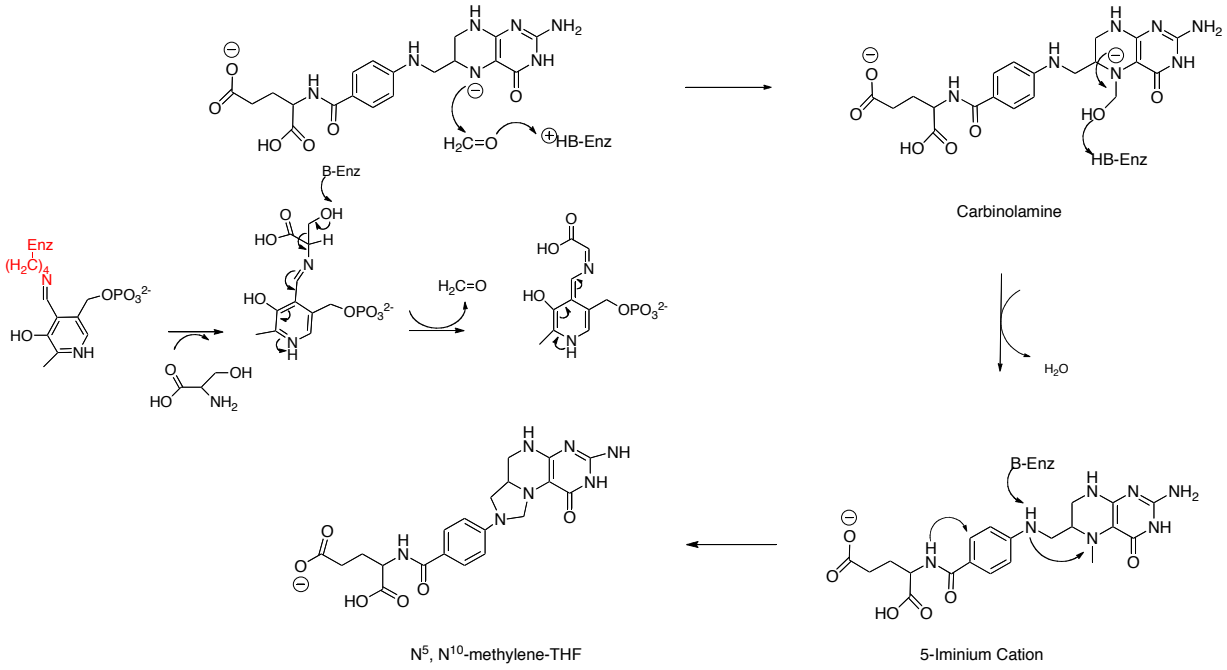

Figure 1.9. Reaction mechanism of the canonical SHMT utilizing Ser and THF as substrates in the transfer of a single carbon unit.

1.3. Aims of this study

The overarching objective of this study is to identify the enzymatic activity of the putative SHMT shared among the A-90289, muraminomicin, A-102395, and A-503083 biosynthetic gene clusters of the caprazamycin and capuramycin- related compounds. We hypothesize d that these SHMT-like enzymes catalyze a PLP dependent aldol-like condensation reaction incorporating the amino acid Gly onto the known intermediate UA. This C-C bond formation would enable the elongation of the furanoside and formation of the intermediate GlyU.

To interrogate this hypothesis, three specific aims were developed.
Aim I: Isolation and purification of SHMT. This objective was achieved by cloning of the gene, confirming the identity by sequencing, obtaining soluble protein from a heterologous host, and optimizing the purification process.

Aim II: Functional characterization of the putative SHMT. Characterization of the putative SHMT would lead to identification of the enzymatic role played in the biosynthesis of the final compounds. This role can also reveal novel chemistry associated with C-C bond formation necessary in more complex antibacterial compounds. This objective was achieved by identifying required co-factors, determining viable substrates, identification of the putative SHMT product, and optimization of reaction conditions for kinetic analysis of the enzymatic activity.

Aim III: Verification of the expected activity of the putative SHMT *in vivo*. Due to the novel chemistry associated with the putative SHMT and its preferred substrates, identification of specific amino acids *in vivo* verifies the enzymatic activity and necessity in C-C bond formation and the development of the high carbon furanoside in caprazamycin and capuramycin-related antibacterial biosynthesis. This task was accomplished by feeding isotopically enriched Gly and L-Thr precursosrs to the producing strain of A-503083 and identifying incorporation into the CarU core.

The canonical SHMT and LTA were used to compare with the newly characterized putative SHMT from the caprazamycin and capuramycin-related biosynthetic gene clusters. The results described here reveal new mechanistic information for all three groups of enzyme catalysts.

Chapter Two

Materials and Methods

2.1 Chemicals.

L-Thr [(*2S,3R*)-2-amino-3-hydroxybutyric acid], D-Thr [(*2R,3S*)-2-amino-3-hydroxybutyric acid], L-*allo*-Thr [(*2S,3S*)-2-amino-3-hydroxybutyric acid],DL-*allo*-Thr,*N*-methyl-L-Thr, *O*-phospho-L-Thr, proteinogenic amino acids, uridine-5'-monophoshate (UMP), uridine, α-ketoglutartate (αKG),β-nicotinamide adenine dinucleotide (β-NAD^+), potassium-activated aldehyde dehydrogenase (ADH) from baker's yeast, 2,4-dinitrophenylhydrazone (DPNH), tetrahydrofolic acid (THF), pyridoxal-5'-phosphate (PLP), various aldehyde substrates, and buffers were purchased from Sigma. Synthetic oligonucleotides were purchased from Integrated DNA Technologies. DNA sequencing was performed using the BigDye™Terminator version 3.1 Cycle Sequencing kit from Applied Biosystems, Inc. (Foster City, CA) and analyzed at the University of Kentucky Advanced Genetic Technologies Center.

2.2 Instrumentation.

UV/Vis spectroscopy was performed with a Bio-Tek µQuant microplate reader using Microtest™ 96-well plates (BD Biosciences) or a Shimadzu UV/Vis-1800 Spectrophotometer equipped with a TCC-240A thermoelectrically temperature controlled cell holder. PCR was performed with a Veriti® 96-well thermal cycler

from Applied Biosystems. Analytic HPLC was performed with one of three systems: an Agilent 1200 Series Quaternary LC system equipped with a diode array detector and an Eclipse XDB-C18 column (250mm x 4.6 mm, 5 μm), a Dionex Ultimate 3000 Focused separation module (Bannockburn, IL) equipped with a DAD-3000 (RS) and MWD-3000 (RS) diode array detector and an Acclaim 120 C-18 column (4.6 mm x 100 mm, 3 μm), or a Waters Alliance 2695 separation module (Milford, MA) equipped with a Waters 2998 diode array detector and an analytical Apollo C-18 column (250 mm x 4.6 mm, 5 μm) purchased from Grace (Deerfield, IL).

Semipreparative HPLC was performed with a Waters 600 controller and pump (Milford, MA) equipped with a 996 diode array detector, 717plus autosampler, and an Apollo C-18 column (250 mm x 10 mm, 5 mm) purchased from Grace (Deerfield, IL). LC-electrospray ionization (ESI)-mass spectroscopy (MS) was performed using an Agilent 6120 Quadrupole MSD mass spectrometer (Agilent Technologies, Santa Clara, CA) equipped with an Agilent 1200 Series Quaternary LC system and an Eclipse XDB-C18 column (150mm x 4.6 mm, 5 mm, 80Å).High resolution (HR)-MS was performed at the Department of Chemistry Mass Spectrometry Service Laboratory, University of Minnesota, using a Bruker BioTOF II. NMR data were collected using a Varian Unity Inova 400 or 500 MHz spectrometer (Varian, Inc., Palo Alto, CA) or a Bruker AVANCE 500 MHz spectrometer (Bruker Biospin Corporation, Billerica, MA).

2.3 Enzymes, strains, and growth media.

Escherichia coli JM109 was purchased from Takara Bio Inc. (Shiga, Japan). Restriction enzymes and DNA modifying enzymes were purchased from Takara Bio Inc. or New England BioLabs Inc. (Ipswich, MA). Proteases and nucleases for genomic DNA preparation were purchased from Sigma-Aldrich. Media, growth conditions, genomic DNA isolation, and recombinant DNA techniques for *E. coli* (*31*) and actinomycetes (*32*) were performed as described. *Streptomyces avermitilis* ATCC 31267 and *Streptomyces coelicolor* A3(2) ATCC BAA-471 were obtained from the American Type Culture Collection (ATCC). *Streptomyces griseus* IFO13350 was obtained from the Institute of Fermentation, Osaka (IFO). *Saccharopolyspora erythraea* NRRL 3887 and *Streptomyces* sp. NRRL 30471 were obtained from the Agricultural Research Service Culture Collection (NRRL). *Streptomyces lividans* TK21 was a gift from the John Innes Centre. *Streptomyces albus* was a gift from Prof. José A. Salas, Universidad de Oviedo. The remaining strains are part of the culture collection maintained at Daiichi-Sankyo Co., Ltd.

A-503083 B and A-503083 F were isolated from *Streptomyces* sp. SANK 62799 and purified as previously reported (31). Muraminomicin F was isolated as previously described (47). MS and ^{1}H-and ^{13}C-NMR spectra (Fig. 2.1) were consistent with this report.

^{1}H-NMR in DMSO-*d*6

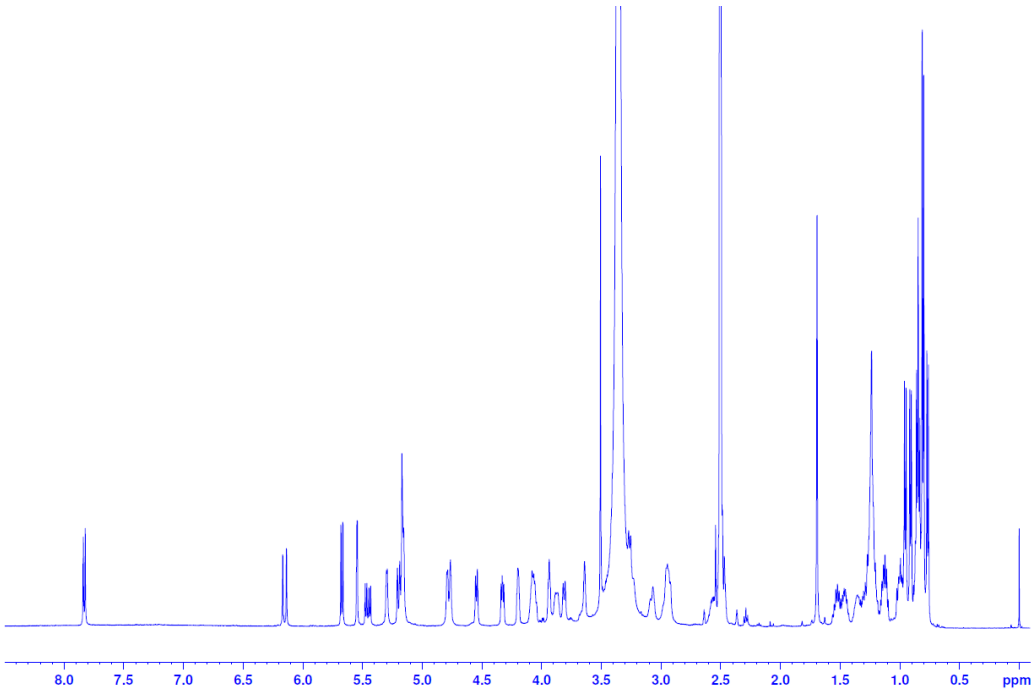

^{13}C-NMR in DMSO-*d*6

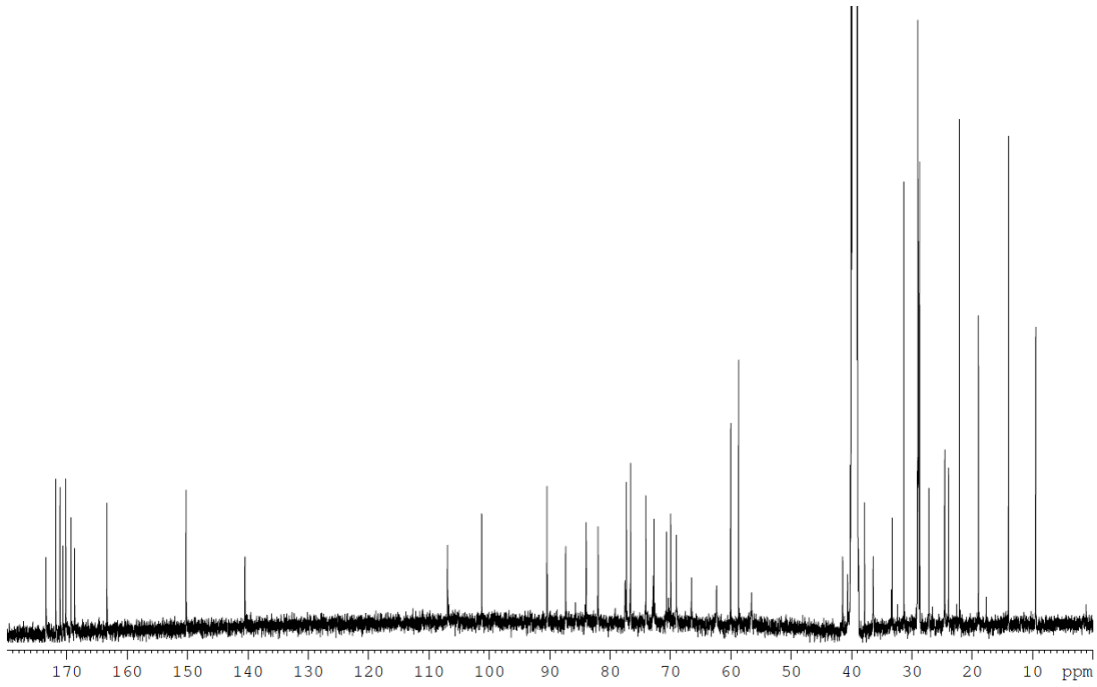

Figure 2.1. ^{1}H-and ^{13}C-NMR spectra of muraminomicin F.

2.4 Synthesis of 5'-*C*-glycyluridinediastereomers.

The synthesis of (5*S*,6*S*)-5'-*C*-glycyluridine, (5*R*,6*S*)-5'-*C*-glycyluridine, and (5*S*,6*R*)-5'-*C*-glycyluridine is reported in detail elsewhere (*36*). ESI-MS analysis of (5*S*,6*S*)-5'-*C*-glycyluridineyieldedan [M+Na]+ion of m/z = 340.1, consistent with the expected molecular formula of C11H15N3O8Na . NMR spectroscopic analysis was obtained at neutral pH (zwitterionic form). 1H-NMR(600 MHz, D2O, 35 °C): δ = 4.30 (d, *J* = 3.1 Hz, 1 H, 6'-H), 4.40 (dd, *J* = 5.7 Hz, *J* = 1.5 Hz, 1 H, 4'-H), 4.45 (dd, *J* = 5.7 Hz, *J* = 5.3 Hz, 1 H, 3'-H), 4.48 (dd, *J* = 5.3 Hz, *J* = 3.7 Hz, 1 H, 2'-H), 4.64 (dd, *J* = 3.1 Hz, *J* = 1.5 Hz, 1 H, 5'-H), 6.00 (d, *J* = 8.2 Hz, 1 H, 5-H), 6.05 (d, *J* = 3.7 Hz, 1 H, 1'-H), 8.16 (d, *J* = 8.2 Hz, 1 H, 6-H). 13C-NMR(126 MHz, D2O, 35 °C): δ = 60.04 (C-6'), 69.36 (C-5'), 72.85 (C-3'), 75.85 (C-2'), 87.57 (C-4'), 92.43 (C-1'), 104.81 (C-5), 144.47 (C-6), 154.09 (C-2), 168.59 (C-4), 173.35 (C-7')

2.5 Cloning of genes for heterologous expression.

Genes were amplified by PCR using Expand Long Template PCR System from Roche (Indianapolis, IN) with supplied Buffer 2, 200 mM dNTPs, 5% DMSO, 10 ng DNA template, 5 U DNA polymerase, and 200 nM each of the following primer pairs: *EcglyA* (forward) 5'-GGTATTGAGGGTCGCATGTTAAAGCGTGAAATGAACATTG-3'/ (reverse) 5'-AGAGGAGAGTTAGAGCCTTATGCGTAAACCGGGTAACG -3'; *EcLTA* (forward) 5'-GGTATTGAGGGTCGCATGTCCGTGCTGGGGCGG-3'/ (reverse) 5'-

AGAGGAGAGTTAGAGCCTTAACGCGCCAGGAATGCAC-3'; *lipK* (forward) 5'-GGTATTGAGGGTCGCATGACGGTGGGGGCTGGTG-3'/ (reverse) 5'-AGAGGAGAGTTAGAGCCTCACAGCCCGGCCTCCACTT-3'; *orf25* (forward) 5'-GGTATTGAGGGTCGCATGACTGACACTAACGAGTTACGG -3'/ (reverse) 5'-AGAGGAGAGTTAGAGCCTCATGGGTAATCGACGAAGTGGAA -3'; *capH* (forward) 5'-GGTATTGAGGGTCGCATGACTGATATCAGGGAGCTCCGCAAG-3'/ (reverse) 5'-AGAGGAGAGTTAGAGCCTCAGGAGAACTCGACGAAATAGAAGGGAG-3'; and *Mra14* (forward) 5'-GGTATTGAGGGTCGCAGCTAGTGGCAAGACATCTTTGGGCG-3'/ (reverse) 5'-AGAGGAGAGTTAGAGCCTTGTAGAAGTCGGAACCCAGTGGCAGTG-3'. DNA templates for PCR cloning were *E. coli* DH5α genomic DNA for *EcglyA and EcLTA*, cosmid pN1 for *lipK (48)*, cosmid pNCap02 for *orf25*, cosmid pMra02 for *Mra14*, and cosmid N-4 for *capH* (49). The PCR program included an initial hold at 94 °C for 2 min, followed by 30 cycles of 94 °C for 10 s, 56 °C for 15 s, and 68 °C for 60s per kb DNA. The gel-purified PCR product was inserted into pET-30 Xa/LIC using ligation-independent cloning as described in the provided protocol to yield pET30-*EcglycA*, pET30-*EcLTA,* pET30-*lipK*, pET30-*orf25*, pET30-*mra14*, and pET30-*capH*. The genes were sequenced to confirm PCR fidelity.

2.6 Site-directed mutagenesis.

A K235A point mutation of LipK was generated by PCR amplification using pET30-*lipK* as a template and the Expand Long Template PCR system (RocheAppliedScience). Reactions were performed using the manufacturer's provided Buffer 2 with 5% DMSO, primers of 5'-CTTCGGCGGATCGACTCACGCGTCCTTCCCCGGGCCCC-3' and the reverse complement (the engineered Ala codon is underlined), and a PCR program consisting of an initial hold at 94°C for 2 min followed by 20 cycles of 94°C for 10s, 56°C for 20s, and 68°C for 7min. The template DNA was digested with 10 units of *Dpn*I (NewEngland Biolabs) for 1h at 37°C and transformed into *E.coli* NovaBlue competent cells. The introduction of the correct point mutation and the sequence of the entire gene including 200bp upstream and downstream were confirmed by DNA sequencing to yield pET30-*lipK* (K235A).

2.7 Heterologous production of proteins in *E. coli*.

Plasmids pET30-*EcglycA* and pET30-*Eclta*, were introduced into *E. coli* BL21(DE3) cells, and the transformed strains were grown in LB supplemented with 30 mg/mL kanamycin. Following inoculation of 500 mL of LB with 30 mg/mL kanamycin, the cultures were grown at 18 °C until the cell density reached an OD600~ 0.5 when expression was induced with 0.1 mM IPTG. Cells were harvested after an overnight incubation at 18 °C and lysed in 100 mM Tris-HCl (pH 8) and 300 mM KCl using a French Press with one pass at 15000 psi.

Following centrifugation the protein was purified using affinity chromatography with Ni-NTA agarose from Qiagen (Valencia, CA), and the recombinant proteins were desalted into 50 mM phosphate (pH 7.5)(for *Ec*GlyA and *Ec*LTA), 100 mM KCl, and 5 % glycerol using a PD-10 desalting column (GE Healthcare). The purified protein was concentrated using an Amicon Ultra 10000 MWCO centrifugal filter (Millipore) and stored as glycerol stocks (40%) at -20 °C. Protein purity was assessed by 12% acrylamide SDS-PAGE; His6-tagged proteins were utilized without further modifications. Protein concentration was determined using Bradford protein assay or extension coefficients calculated using the ProtParam tool available from ExPASY (LipK, ε280= 28,880 $M^{-1}cm^{-1}$; CapH, ε280= 30,940 $M^{-1}cm^{-1}$; *Ec*GlyA, ε280= 46,300 $M^{-1}cm^{-1}$; *Ec*LTA, ε280= 36,900 $M^{-1}\,cm^{-1}$.

2.8 Subcloning and expression in *Streptomyces lividans* TK-64 or *Streptomyces albus*.

Plasmids pET30-*lipK*, pET30-*lipK*(K235A), pET30-*orf25*, and pET30-*mra14* were digested with *Nde*I-*Hind*III and the DNA fragment of the expected size was purified and ligated to the identical sites of pUWL201pw to yield pUWL201pw-*lipK*, pUWL201pw-*lipK*(K235A), pUWL201pw-*capH*, pUWL201pw-*orf25*, and pUWL201pw-*mra14* respectively. The resulting plasmids were transformed into *S. lividans* TK-64 using PEG-mediated protoplast transformation and plated on M_2CaO or R2YE. After 14 h at 28 °C, the plates were overlaid with 1 mL of water supplemented with 200 mg of thiostrepton. Single colonies were transferred to fresh M_2CaO or R2YE plates supplemented with 10 mg/mL thiostrepton, and

after 4 days at 28 °C positive transformants were confirmed by colony PCR using InstaGene Matrix from Bio-Rad (Hercules, CA) and LA-Taq polymerase with GC buffer II from Takara Bio Inc. (Shiga, Japan).

The recombinant strain was utilized to inoculate 50 mL R2YE containing 10 μg/mL thiostrepton, grown for 2 days at 28 °C at 250 rpm, and 2 mL transferred to fresh 100 mL containing 10 μg/mL thiostrepton. Following growth for 3 days at 28 °C at 250 rpm, the cells from 400 mL of culture were collected by centrifugation and washed with 60 mL of 100 mM potassium phosphate (pH 7.4), 300 mM KCl, and 1 mM PMSF and stored on ice for 10 min. Following centrifugation at 4,000 rpm for 15 min at 4^{o}C,the pellet was thoroughly resuspended in 60 mL ice-cold 100 mM potassium phosphate (pH 7.4), 300 mM KCl, and 1 mM PMSF and ~25 mg of lysozyme was subsequently added to the suspension. After incubation on ice for 30 minutes, the suspension was mixed by pipeting and subjected to one pass through a French press at 18,000 psi. The cell debris was removed by centrifugation (17,500 rpm for 45 min), the cell-free extract filtered using a 0.45 mm PVDF syringe filter, and the clarified extract was loaded onto a gravity column containing 0.5 mL Ni-NTA resin that was pre-equilibrated with 100 mM potassium phosphate (pH 7.4) containing 300mM KCl. The resin was washed with 10 volumes 100 mM potassium phosphate (pH 7.4) containing 300 mM KCl followed by 10 volumes of 100 mM potassium phosphate (pH 7.4) containing 300 mM KCl and 20 mM imidazole. The His_6-tagged protein was eluted with 10 volumes of 100 mM potassium phosphate (pH 7.4) containing

300 mM KCl and 250 mM imidazole and concentrated to < 2.5 mL using an Amicon Ultra 10k MWCO. The sample was desalted into 35 mM potassium phosphate (pH 7.4) containing 100 mM KCl using a gravity flow PD-10 column following the manufacturer's instructions. The purified protein was re-concentrated and stored as a 40% glycerol stock at -20°C.

2.9 Subcloning and expression of CapH into *S. lividans* TK-64.

Plasmid pET30-CapH was digested with *Nde*I-*Hind*III and the DNA fragment of the expected size was purified and ligated to the identical sites of pUWL201pw to yield pUWL201pw-CapH. The resulting plasmids was transformed into *S. lividans* TK-64 using PEG-mediated protoplast transformation and plated on M_2CaO agar plates. After 16 hr at 28 °C, the plates were overlaid with 1 mL of nutrient agar supplemented with 200 mg of thiostrepton. Single colonies were transferred to fresh M_2CaO plates supplemented with 25mg/mL thiostrepton, and after 4 days at 28 °C positive transformants were confirmed by colony PCR using InstaGene Matrix from Bio-Rad (Hercules, CA) and LA-Taq polymerase with GC buffer II from Takara Bio Inc. (Shiga, Japan).

The recombinant strain was utilized to inoculate 50 mL M_2CaO containing 10 mg/mL thiostrepton, grown for 2 days at 28 °C at 250 rpm, and 2 mL transferred to fresh 100 mL containing 10 mg/mL thiostrepton. Following growth for 3 days at

28 °C at 250 rpm, the cells from 1000 mL of culture were collected by centrifugation at 4,000 rpm for 15 min at 4^{o}C, the pellet was thoroughly re-suspended in ice-cold and re-suspended with 250 mL of 100 mM potassium phosphate pH 7.4, 300 mM KCl and stored on ice. After incubation on ice for 30 minutes, the cell suspension was mixed by pipeting and subjected to one pass through a French press at 18,000 psi. The cell debris was removed by centrifugation (17,500 rpm for 45 min), the cell-free extract filtered using a 0.45 mm PVDF syringe filter, and the clarified extract was loaded onto a gravity column containing 0.5 mL Ni-NTA resin that was pre-equilibrated with 100 mM potassium phosphate containing 300 mM KCl. The resin was washed with 10 volumes 100 mM potassium phosphate pH 7.4 containing 300 mM KCl (Buffer A) followed by 10 volumes of Buffer A containing 20 mM imidazole. The His-tagged protein was eluted with 10 volumes of Buffer A containing 250 mM imidazole and concentrated to < 2.5 mL using an Amicon Ultra 10k MWCO. The sample was desalted into 35 mM potassium phosphate pH 7.4 containing 100 mM KCl using a gravity flow PD-10 column following the manufacturer's instructions. The purified protein was re-concentrated and stored as a 40% glycerol stock at -20 ^{o}C.

2.10 HPLC analysis of the reactions catalyzed by LipK, CapH, Orf 25, and Mra14. Routine reactions for LipK, CapH, Orf25, and Mra14 consisted of 50 mM HEPES or TES (pH 7.5), 2 mM UA, 5 mM co-substrate, 0.1 mM PLP, and 3.5 mM LipK at 30 °Cat the indicated time points. Following removal of the protein by

ultrafiltration or TCA precipitation (7%), the reaction components were analyzed using reverse-phase chromatography using the Agilent 1200 series HPLC equipped with an Eclipse XDB-C18 column or a Dionex Ultimate 3000 Focused separation module (Bannockburn, IL) equipped with a DAD-3000(RS) and MWD-3000(RS) diode array detector and an Acclaim 120 C-18 column (4.6 mm x 100 mm, 3 mm). A series of linear gradients was developed from 0.1 % TFA in 0.5 % acetonitrile (A) to 0.1% TFA in 90% acetonitrile (B) in the following manner (beginning time and ending time with linear increase to % B): 0-8 min, 100% B; 8-28 min, 100% B; 28-32 min, 100% B; and 32-35 min, 0% B. The flow rate was kept constant at 1 mL/min, and elution was monitored at 260 nm.

2.11 Isolation of the LipK product.

A large scale reaction (33 mL) consisted of 50 mM TES (pH 7.5), 100 mM KCl, 0.1 mM PLP, 1 mM DTT, 10 mM L-Thr, 2.5 mM uridine-5'-aldehyde, 3 mM NAD, 10 U ADH, and 5 mM LipK. Following incubation for 24 h at 30 °C, protein was removed by ultra filtration and the product was partially purified by HPLC using a C-18 reverse-phase semi-preparative column. A series of linear gradients was developed from A to B in the following manner (beginning time and ending time with linear increase to % B): 0-4 min, 100% B; 4-24 min, 50% B; 24-26 min, 100% B; 26-32 min, 100% B; and 32-35 min, 0% B. The flow rate was kept constant at 3.5 mL/min, and elution was monitored at 260 nm. Fractions containing the desired product eluting near the column void volume were combined and lyophilized to yield a viscous, clear solution. The amount of

product was estimated using 262 nm = 10,100 M^{-1} (50). Partially purified GlyU was resuspended in 5 mL of 200 mM ammonium acetate (pH 8.8) and loaded onto a column containing 1 mL of immobilized boronic acid resin (Thermo-Fisher) that was equilibrated in 10 mL of 200 mM ammonium acetate (pH 8.8). Following a 3 mL wash with the same buffer, the bound GlyU was eluted with 12 mL of 0.1 M formic acid. The purified sample was lyophilized prior to spectroscopic analysis.

2.12 Phosgene modification of GlyU.

Phosgene modification of β-hydroxy-α-amino acids was carried out as previously described (51). Approximately 20 mg of partially purified GlyU was dissolved in 1 M potassium hydroxide (6.5 mL), and the solution cooled to 5°C prior to the addition of 6 mL of a 20% solution of phosgene in toluene. Following 5 min with rigorous stirring, the mixture was acidified with 10 drops of concentrated HCl, and the aqueous phase was removed and subjected to HPLC for purification using a C-18 reverse-phase semi-preparative column following the above conditions. The purified product was lyophilized and subjected to spectroscopic analysis. 1H-NMR (D2O, 500 MHz): *δ*7.56 (d, *J*= 8.5 Hz, 1H), 5.95 (d, *J*= 5.0 Hz, 1H), 5.90 (d, *J*= 8.0 Hz, 1H), 5.08 (dd, *J*= 5.0 Hz,*J*= 2.5 Hz,1H),4.55 (d, *J*= 5.5Hz, 1H), 4.45 (t, *J*= 5.25Hz, 1H),4.41 (t, *J*= 5.0Hz, 1H), 4.30 (dd, *J*= 5.25Hz, *J*= 2.5 Hz,1H). 13C-NMR (D2O, 100 MHz): *δ* 173.54, 165.85, 159.98, 151.51, 141.03, 102.60, 89.09, 83.33, 77.59, 72.71, 69.24, 62.38, 55.83.

For analytical analysis of synthetic GlyU diastereomers, a 2 mM solution (50 mL) of pure diastereomer was prepared and chilled on ice for 5 min. After addition of 10 mL of 5 M KOH, the reaction was initiated by adding 50 mL of 20% phosgene in toluene. After a 1 h incubation on ice with periodic mixing, the organic phase was removed and the aqueous phase analyzed by HPLC using the Agilent 1200 series HPLC Agilent 1200 Series equipped with an Eclipse XDB-C18 column and gradient conditions described above for isolation of the LipK product.

2.13 Modification of aldehydes with DPNH.

LipK reaction components were modified with DPNH as previously described (52). Following protein removal by centrifugation, the modified components were analyzed using reverse-phase chromatography using the Agilent 1200 series HPLC Agilent 1200 Series equipped with an Eclipse XDB-C18 column. A series of linear gradients was developed from A to B in the following manner (beginning time and ending time with linear increase to % B): 0-8 min, 100% B; 8-28 min, 100% B; 28-32 min, 100% B; and 32-35 min, 0% B. The flow rate was kept constant at 1 mL/min, and elution was monitored at 430 nm.

2.14 Kinetic analysis of LipK and CapH.

Single-substrate kinetic analysis was carried out by monitoring the reduction of β-NAD^+ using $\varepsilon 340 = 6220\ M^{-1}cm^{-1}$. Reaction mixtures (90 mL) consisting of 100 mM TES (pH 7.5), 100 mM KCl, 1 mM DTT, 30 mM L-Thr, 0.1 mM PLP, 2 mM β-

NAD, and variable UA (1.0-125 mM) were incubated at 30 ^{o}C for 1 min prior to initiation with a mixture (10 mL) consisting of 50 mM TES (pH 7.5), 100 mM KCl, 1 mM DTT, 2 mM β-NAD, 1 U ADH, and 250 nM LipK or CapH. Reactions were carried out for 10 min, and rates were calculated using linear regression analysis with data obtained under initial velocity conditions (< 10% product). Data were fitted to the Michaelis-Menten equation using GraphPad Prism 5.0.4 (GraphPad Software, Inc., La Jolla, CA). Each data point represents the average of a minimum of three independent measurements.

Bi-substrate kinetic analysis for LipK were performed using reactions as described above with variable UA (1.0 -60 mM) and L-Thr (62 mM –15.6 mM). For mechanistic determination (ping pong versus sequential mechanism) the inverse data (1/[S] versus1/v) were analyzed by simple linear regression analysis. If data are fitted to an equation (Fig. 2.2*; (53)*) describing a random sequential mechanism as described for serine hydroxymethyltransferases (54), the global fit yields a kinetic constant of K_m= 31 mM with respect to L-Thr and α= 0.88 (α is the factor by which the binding of one substrate alters the dissociation constant for the remaining substrate; an αvalue of unity indicates substrate binding has no effect on the binding of the respective substrate).

$$\frac{1}{v} = \frac{\propto K_B}{V_{max}}\left(1 + \frac{K_A}{[A]}\right)\frac{1}{[B]} + \frac{1}{V_{max}}\left(1 + \frac{\propto K_A}{[A]}\right)$$

Figure 2.2 Equation for simple linear regression analysis.

2.15 Isotopic Enrichment.

Fermentation media and growth conditions for *Streptomyces* sp. SANK 62799 were as previously described (31). A seed culture was incubated at 28 ^{o}C for 48 h when 1.5 mL was used to inoculate fresh media (50 mL liquid medium in a 250 mL flask). After fermentation for 70 h, 25 mg of filter-sterilized [1-^{13}C]Gly, [2-^{13}C]Gly, or L-[$^{13}C_4$,^{15}N]Thr was added to each flask. Fermentation was continued an additional 72 h. An equal volume of methanol was added directly to the culture and mixed vigorously prior to centrifugation to remove cell debris. The supernatant was lyophilized and the dried powder was resuspended in water (100 mg/mL) for HPLC analysis using a C-18 reverse-phase semi-preparative column. A series of linear gradients was developed from A to B in the following manner (beginning time and ending time with linear increase to % B): 0-6 min, 0% B; 6-26 min, 100% B; 26-30min, 100% B; 30-34 min, 0% B; and 34-35 min, 0% B. The flow rate was kept constant at 3.5 mL/min, and elution was monitored at 260 nm. Relative peak intensities were assigned based on the relative intensity of C -2''and C-3'' from the natural abundance spectrum.

2.16 HPLC analysis of the reactions catalyzed by *Ec*GlyA and *Ec*LTA with 2-pyridinde-carboxaldehyde and L-Thr.

Routine reactions *Ec*GlyA and *Ec*LTA consisted of 50 mM potassium phosphate (pH 7.5), 2 mM 2-pyridine-carboxaldehyde, 5 mM L-Thr, 0.1 mM PLP, and 5.0 mM *Ec*GlyA or *Ec*LTA at 30 °C for the indicated time points. Following removal of

the protein by ultrafiltration, the reaction components were analyzed using reverse-phase chromatography using the Dionex Ultimate 3000 Focused separation module (Bannockburn, IL) equipped with a DAD-3000(RS) and MWD-3000(RS) diode array detector and an Acclaim 120 C-18 column (4.6 mm x 100 mm, 3 mm). A series of linear gradients was developed from 0.1 % TFA in 0.5 % acetonitrile (A) to 0.1% TFA in 90% acetonitrile (B) in the following manner (beginning time and ending time with linear increase to % B): 0-8 min, 100% B; 8-28 min, 100% B; 28-32 min, 100% B; and 32-35 min, 0% B. The flow rate was kept constant at 1 mL/min, and elution was monitored at 260 nm.

Chapter Three

RESULTS and Discussion

3.1. Heterologous expression of putative serine hydroxymethyltransferases (SHMT)

The uniqueness of the C-C bond formation involved in SHMT activity and the presence of a single putative SHMT within the biosynthetic gene clusters of the caprazamycin and capuramycin-related compounds under investigation prompted inquiry into the function of these putative enzymes. However, initial investigation of the putative SHMTs required the isolation of the initial DNA, insertion into the selected vector system, and expression of a soluble protein.

3.1.1 Isolation of the putative SHMTs from cosmid DNA

Bioinformatic analysis of each of the biosynthetic gene clusters of muraminomicin, A-90289, A-503083, and A-102395 previously revealed the presence of a putative SHMT within each cluster. The moderate sequence similarity/identity of the putative SHMTs to each suggested a shared function of each enzyme in the biosynthesis of the final compounds (Table 3.1). In order to elucidate the function of the putative SHMTs and their mechanism in the biosynthesis of the caprazamycin-related and capuramycin-related compounds,

we cloned and expressed the genes from cosmid DNA generously provided by Daiichi Sankyo Novare.

Primers for amplification of the putative SHMTs for the caprazamycin-related compounds muraminomicin and A-90289 were designed from the sequence, and the genes of interest were then amplified by PCR from the cosmid DNA pMra02 and pLip02 respectively. The putative SHMTs for the capuramycin-related compounds A-503083 and A-102395 were amplified form the cosmid DNA N-1 and NCap02 respectively. After agarose gel purification, the DNA was then inserted into the pET30 Xa/LIC vector and sequentially transformed into NovaBlue cells purchased from Novagen. Individual colonies were then selected and grown in a 3.0 mL LB culture containing the antibiotic selection marker kanamycin. The cells were collected and the plasmid was purified. The gene of the purified plasmid was sequenced to ensure 100% identity to the expected sequence.

Table 3.1. Putative SHMT DNA comparison. Comparison of the DNA sequence of the individual putative SHMTs. %Identical/%Similar.

	lipK	***capH***	***mra14***	***orf25***
lipK	X	54/68	55/68	55/79
capH	54/68	X	62/64	81/82
mra14	55/68	62/64	X	62/64
orf25	55/79	81/82	62/64	x

3.1.2 Protein expression of putative SHMTs

After sequencing to confirm the identity, the plasmids encoding the putative SHMTs were tested for their ability to produce soluble, recombinant protein. Cell lines for pET30-*lipK*, pET30- *capH*, pET30-*mra14*, and pET30-*orf25* were created by transformation of each respective vector into *E. coli* BL21(DE3) cells. The cells were then plated and cultured in LB broth with the antibiotic selection marker kanamycin. A one-liter culture was grown for each of the above cell lines and gene expression induced with IPTG. Unfortunately none of the above proteins were soluble in the *E. coli* strain, therefore an alternative expression system was chosen. The pET30 Xa/LIC vectors containing the cloned genes were digested with the restriction enzymes *NdeI* and *HindIII* to remove the putative SHMT genes including the engineered sequence for an N-terminal His_6-tag. The DNA fragment was then purified by agarose gel electrophoresis, ligated into the pUWL201pw vector, and transformed into *S. lividans* TK64 protoplasts. The plasmid encoding the model enzyme LipK was also used to transform a different host, *Streptomyces albus (S. albus)*. The respective *S. lividans* or *S. albus* strain was then cultured in R2YE media with the selective antibiotic thiostrepton and the recombinant proteins were partially purified by nickel affinity column (Fig. 3.1A-D and F). All five proteins proved soluble in *S. lividans*; LipK was also soluble in *S. albus*.

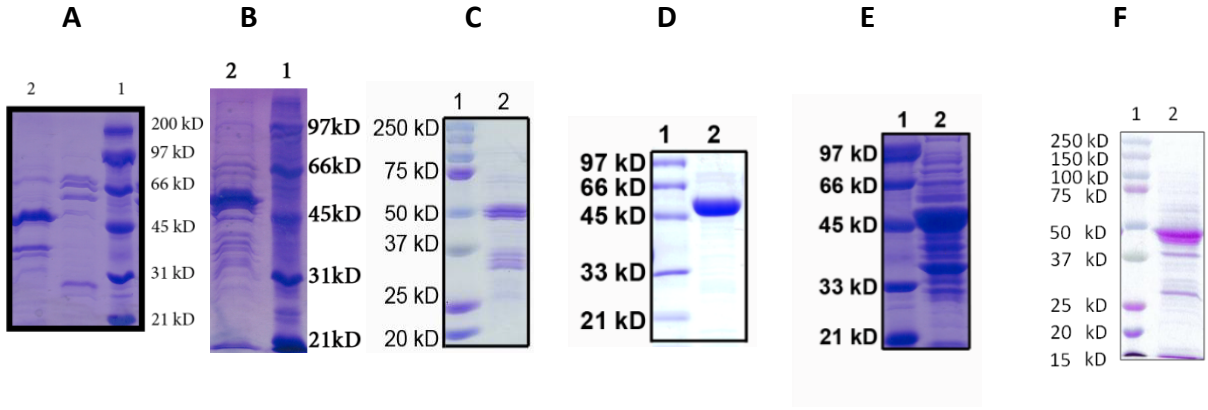

Figure 3.1. Expression of recombinant putative SHMTs. (**A**) SDS-PAGE analysis of partially purified His_6-Orf25 from *Streptomyces lividans* TK64 (lane 2, expected MW of 50.24 kD). (**B**) SDS-PAGE analysis of partially purified His_6-Mra14 from *Streptomyces lividans* TK64 (lane 2, expected MW of 50.1 kD). (**C**) SDS-PAGE analysis of partially purified His_6-CapH from *Streptomyces lividans* TK64 (lane 2, expected MW of 50.4 kD). (**D**) SDS-PAGE analysis of purified His_6-LipK from *Streptomyces lividans* TK64 (lane 2, expected MW of 50.1 kD). (**E**) SDS-PAGE analysis of partially purified His_6-LipK(K235A) (lane 2, expected MW of 50.1 kD). (**F**) SDS-PAGE analysis of partially purified His_6-LipK from *Streptomyces albus* (lane 2, expected MW of 50.1 kD). The expected molecular weight for each of the above proteins was calculated to include an engineered N-terminal His6-tag (5 kD) and lane 1 represents molecular weight standards purchased from BioRad.

3.1.3 Site directed mutagenesis of the model enzyme LipK

Due to the importance of the Lys residue in the formation of the PLP binding motif in SHMT reactions, a His_6-LipK(K235A) mutant was generated. PLP dependent enzymes follow a mechanistic pathway that can be monitored by UV/Vis spectroscopy. Both the known SHMTs and LTAs involve the formation of an internal aldimine (holo-enzyme) upon which an amino acid then binds forming an external aldimine. Both the internal and external aldimine display a unique

absorbance at 425 nm. (4, 43) Mutation of the lysine residue would obliterate formation of the PLP bound intermediate and formation of the external aldimine to yield an inactive enzyme. The *lipK*-(K235A) mutant was generated from pET30-*lipK* using Quikchange technology and sequenced to 100% identity. The *lipK*-(K235A) plasmid was then digested with *NdeI* and *HindIII* and ligated into the pUW201pw vector for transformation into *S. lividans* TK64 protoplasts. The generated LipK(K235A) mutant was heterologously expressed in *S. lividans* TK-64 and also proved to be soluble (Fig. 3.1E).

3.2. Characterization of theoretical SHMTs

With the soluble proteins in hand, we were able to test for enzymatic activity and determine the role of the putative SHMTs in the biosynthesis of icaprazamycin and capuramycin-like compounds. Previous work in our lab has indicated that the precursor for the putative SHMTs was likely uridine-5′-aldehyde (UA), the product of the α-ketoglutarage:UMP dioxygenase LipL (38). We hypothesized that these enzymes used UA to add a glycyl unit to produce 5′-*C*-glycyluridine (GlyU) (Fig. 3.2).

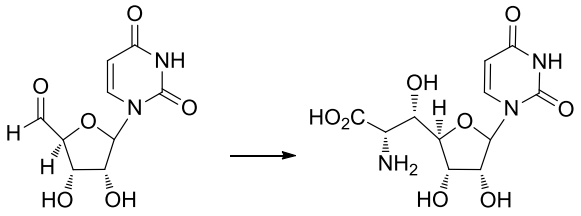

2 1

Figure 3.2 Reaction of putative SHMTs in caprazamycin and capuramycin-related compound biosynthesis. The formation of GlyU (1) utilizing uridine-5′-aldehyde (2) as a substrate and the putative SHMTs.

3.2.1.1 Substrate and activity testing of the putative SHMTs Mra14, LipK, CapH, and Orf25

In order to test The hypothesized function of the putative SHMTs, we synthesized the potential substrate UA (Fig. 3.3) and incubated it with 5 μM of each putative SHMT Mra14, LipK, Orf25, and CapH, with Gly, or other L-amino acids as potential co-substrates.

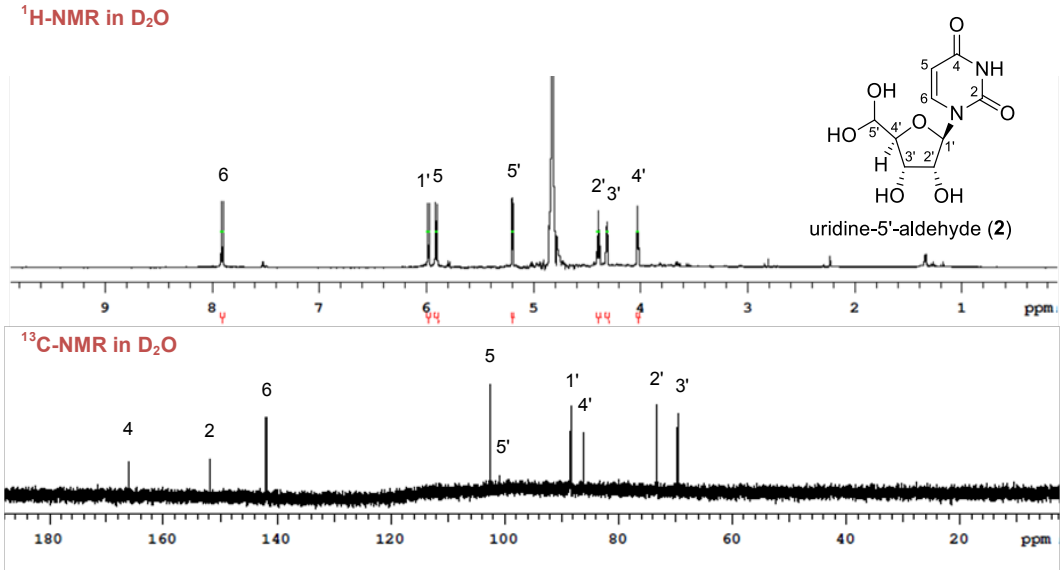

Figure 3.3. The substrate Uridine-5′-aldehyde NMR. The synthesis of uridine-5′-aldehdye followed a two-step procedure that was previously described.(38) MS and ^{1}H- and ^{13}C-NMR spectra (above) were consistent with this report.

3.2.1.2 Substrates and enzymatic activity of the putative SHMTs from caprazamycin-like compounds muraminomicin and A-90289.

The caprazamycin-related compounds has a core structure of a β-hydroxy-α-amino acid 5′-*C*-glycyluridine (GlyU). Due to the SHMTs C-C bond forming ability, the putative SHMTs Mra14 and LipK from caprazamycin-related compounds were initially tested for enzymatic activity using UA as well as the co-factor PLP with the expectation that GlyU would be formed. Gly and Ser were initially tested as glycyl unit donors for incorporation onto the UA intermediate.

3.2.1.2a Substrates and enzymatic activity of Mra14

Enzymatic activity of the putative SHMT Mra14 from the muraminomicin biosynthetic gene cluster was tested using 2.0 mM UA, 0.1 mM PLP, and 10.0 mM of a variety of amino acid donors in 50 mM potassium phosphate buffer (pH 7.5). Individual reactions were prepared and incubated at 30°C for 2 hr, 6 hr, and 18 hr and terminated by spin column filtration. The reactions were then analyzed by reverse-phase HPLC utilizing a linear acetonitrile gradient. No activity was observed with Gly or Ser as amino acid donors. In contrast, enzymatic activity was found using UA and L-Thr as the donor with PLP as a co-factor (Fig. 3.4A).

3.2.1.2b Substrates and enzymatic activity of LipK

The putative SHMT LipK from the A-90289 biosynthetic gene cluster was also tested for activity using 2.0 mM UA, 0.1 mM PLP, and 10.0 mM of a variety of amino acid donors in 50 mM potassium phosphate buffer (pH 7.5). Once again, the individual reactions were prepared and incubated at 30°C for 2 hr, 6 hr, and 18 hr and terminated by spin column filtration and analyzed by reverse-phase HPLC utilizing a linear acetonitrile gradient. Identical to Mra14, the only enzymatic activity was seen utilizing UA, and L-Thr as substrates with co-factor PLP (Fig. 3.4B).

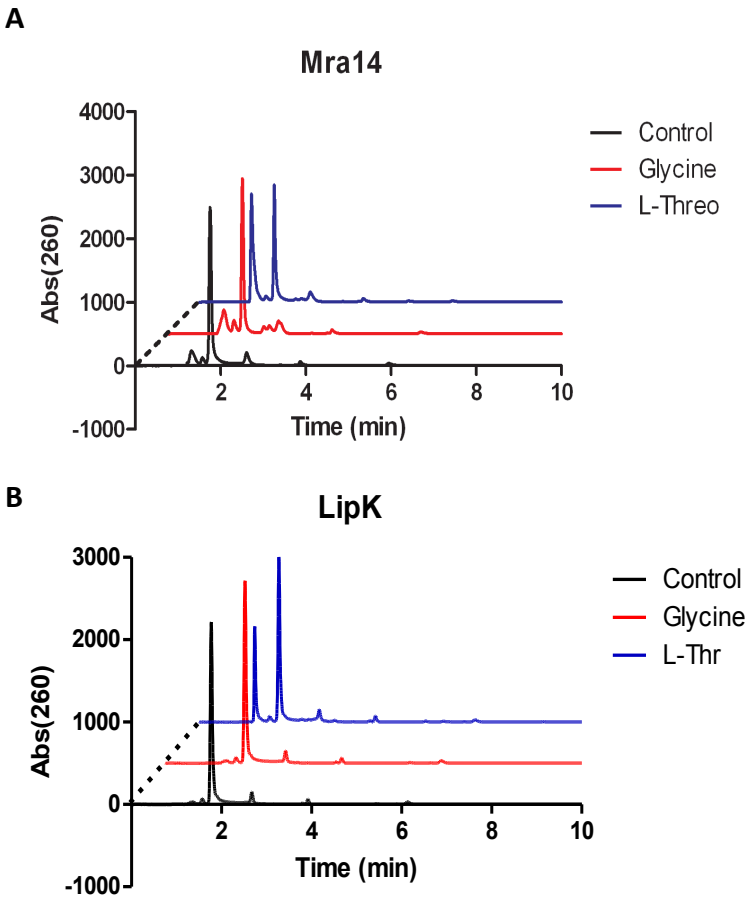

Figure 3.4. Verification of enzymatic activity of the putative SHMTs isolated from the biosynthetic gene cluster of caprazamycin-related compounds. Reactions were carried out in 50 mM potassium phosphate buffer (pH 7.5), 0.1mM PLP, 10 mM L-Thr or Gly, and 2.0 mM UA. (**A**) Enzymatic activity involving the putative 5 μM SHMT, Mra14, from the muraminomicin biosynthetic gene cluster. No activity was seen with the amino acid donor Gly while product formation was observed at 1.28 min with L-Thr. (**B**) Enzymatic activity involving the putative 5 μM SHMT, LipK, from A-90289 biosynthetic gene cluster. Again, no activity was seen with the amino acid donor Gly while product formation was observed at 1.28 min with L-Thr.

3.2.2 Characterization of enzymatic product using LipK as the model enzyme

HPLC analysis revealed the formation of a new peak, but only with the substrates UA, L-Thr, and the cofactor PLP. In contrast incubation of the mutant protein LipK(K235A) with UA, L-Thr, PLP, and other amino acids in place of L-Thr revealed no new peak. The lack of activity and utilization of any other amino acid donor verifies the specificity of this enzyme mutagenesis of the lysine residue indicates the necessity of PLP binding and internal aldimine formation to initiate the catalytic mechanism (Fig. 3.5 and Fig. 3.20). Using a large-scale reaction with LipK, the product was partially purified by reverse-phase HPLC. Subsequentially, a boronic acid affinity column was utilized to bind the *cis*-hydroxyl groups located on the 2′ and 3′ positions of the ribose of the expected enzymatic product.

3.2.2.1 LC-MS anaylsis of LipK product

The purified product was verified for purity by HPLC analysis and submitted for LC-MS analysis (Fig. 3.6). LC-MS revealed a $(M - H)^-$ ion at *m/z* = 315.9 consistent with the molecular formula $C_{11}H_{13}N_3O_8$ of GlyU (expected *m/z* = 316.1) (Fig. 3.6B and Fig. 3.6C).

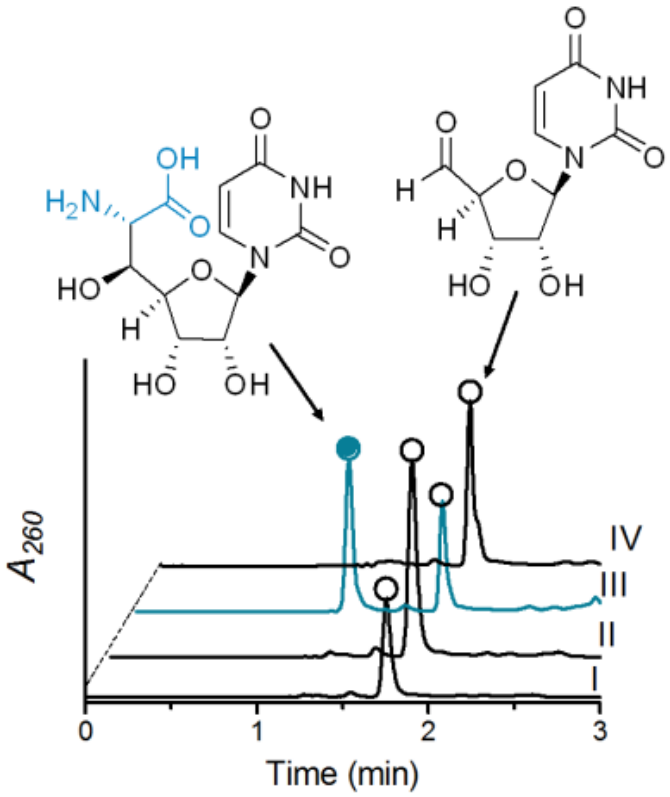

Figure 3.5. HPLC analysis of the reaction catalyzed by LipK. Using 2 with co-substrate Gly or Ser (I), L-Thr without exogenous PLP (II), L-Thr (III), and L-Thr with LipK (K235A) (IV). AU, absorbance units; A_{260}, absorbance at 260 nm.

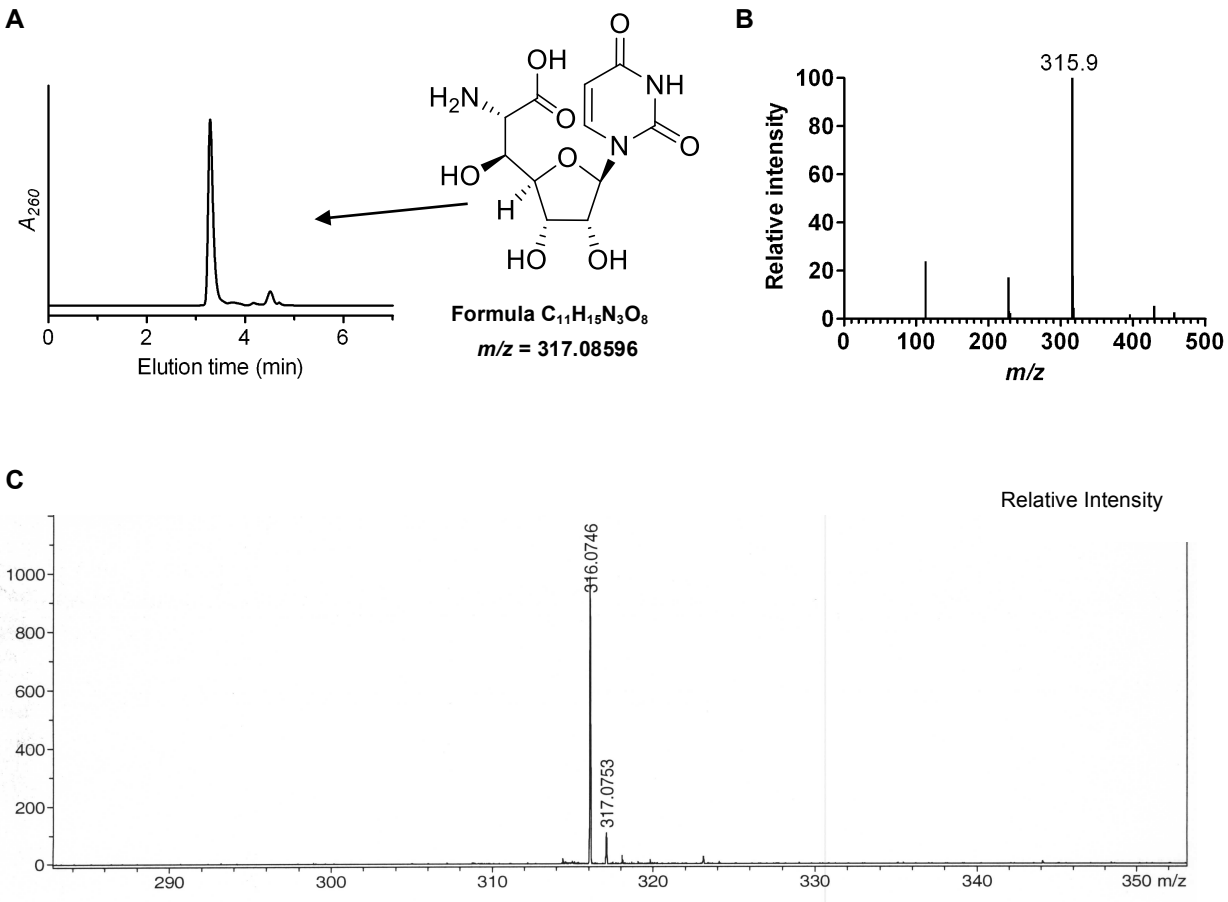

Figure 3.6. LC-MS analysis of the LipK product, 1. (A) HPLC trace of enzymatically prepared product following purification using reverse-phase chromatography and boronic acid affinity chromatography. (B) Mass spectrum for the peak eluting at t = 3.3 min yielding an $(M - H)^-$ ion consistent with the molecular formula of **1**. (C) High resolution mass spectrum of purified **1** yielding an $(M - H)^-$ ion consistent with the molecular formula of **1**. A_{260}, absorbance at 260 nm.

3.2.2.2 1D and 2D NMR spectroscopic analysis

Approximatedly 10 mg of purified product was lyophilized and re-suspended in DMSO for 1D and 2D NMR analysis.

3.2.2.2a 1D Spectroscopic analysis

In an effort to easily identify the 1′, 5, 5′, and 2′ peaks, a DMSO solvent was chosen as the solvent (Fig. 3.7). The spectroscopic analysis is consistent with that of the expected product (5'*S*, 6'*S*)-GlyU (Fig. 3.7 – 3.9) which was compared to synthetic NMR data acquired with (5'*S*, 6'*S*)-GlyU.

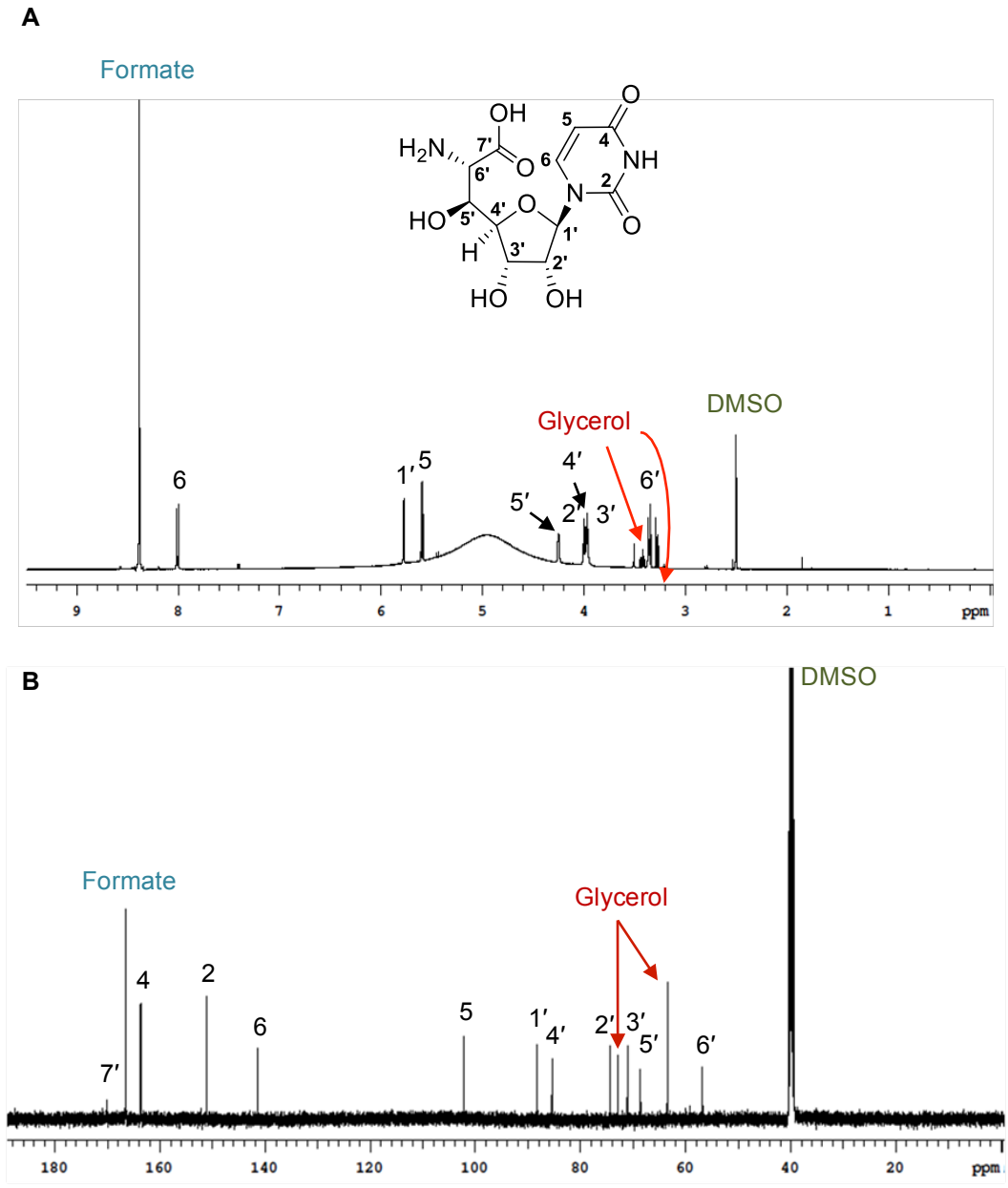

Figure 3.7. 1D NMR spectra of the LipK product, 1. (A) ^{1}H-NMR spectrum of **1** following a two-step purification of reverse-phase chromatography and boronic acid affinity chromatography. DMSO was utilized as a solvent to minimize the interference of the water peak that was difficult to avoid due to the highly hygroscopic nature of **1**. (B) ^{13}C-NMR spectrum of **1** with contaminating glycerol that originated from the enzyme storage solution and formate that was used to elute **1** from the immobilized boronic acid resin.

3.2.2.2b 2D Spectroscopic analysis

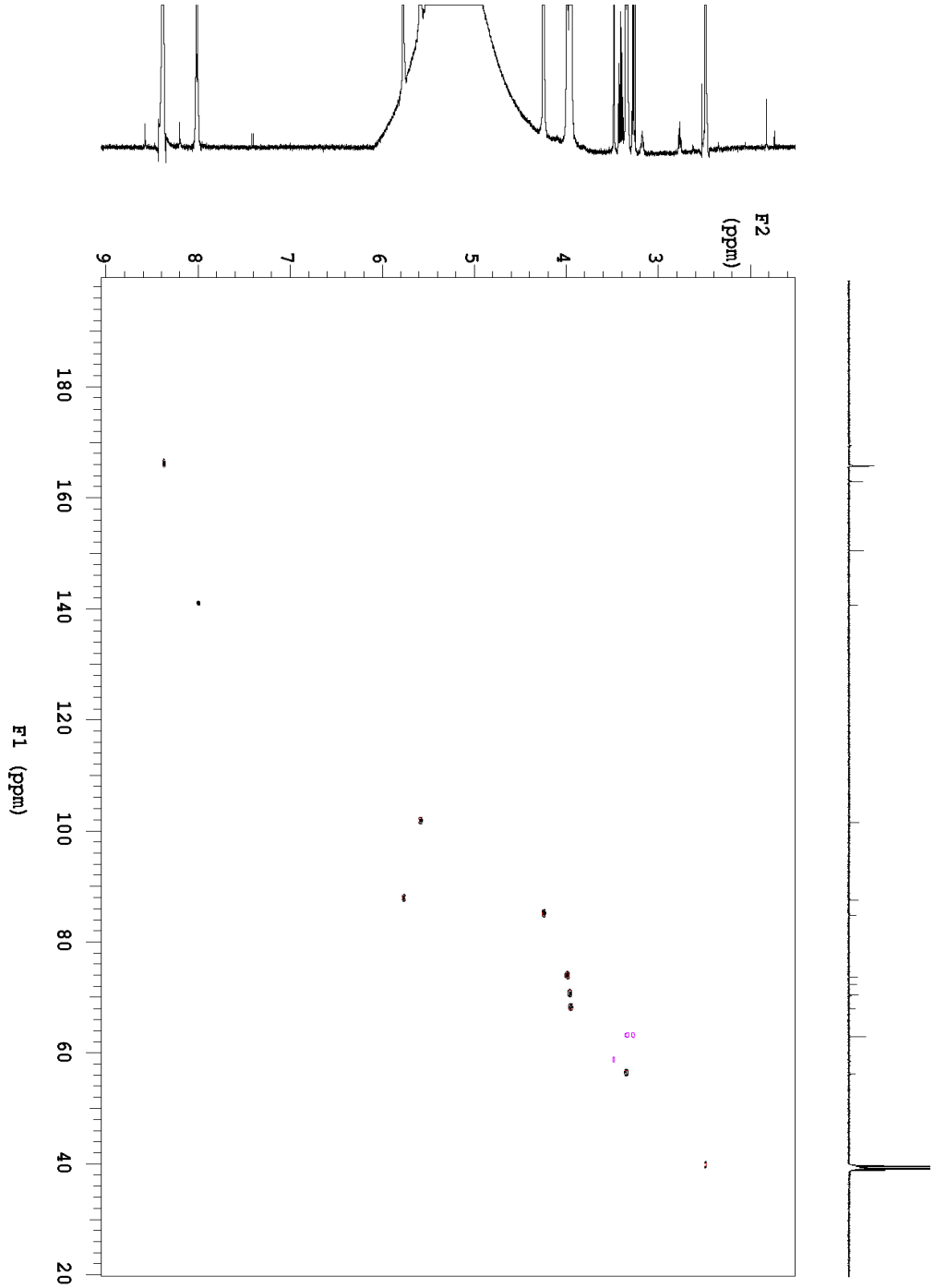

Figure 3.8. ^{1}H-^{13}C gHSQC NMR spectrum of the LipK product, 1.

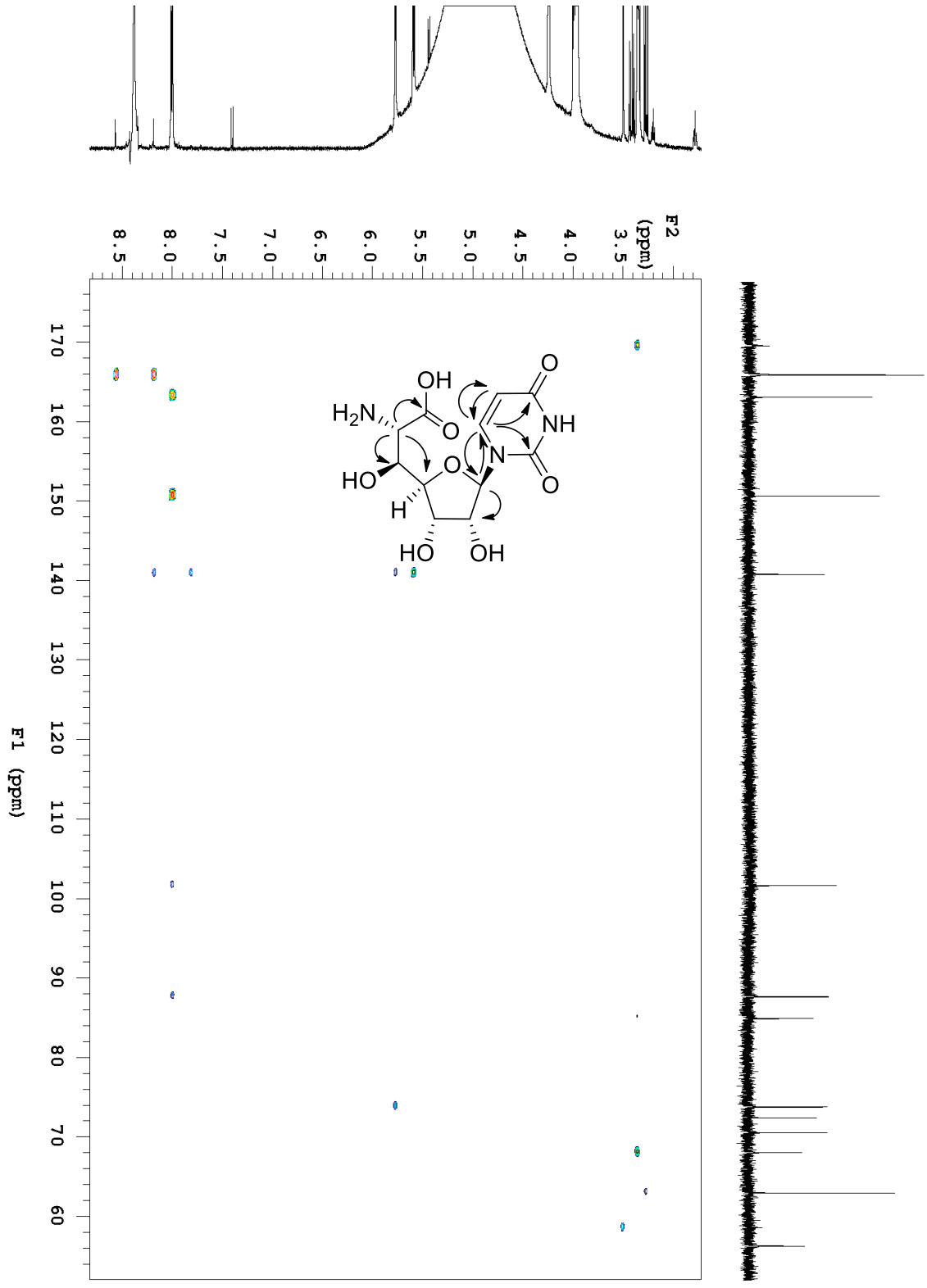

Figure 3.9. ^{1}H-^{13}C gHMBC NMR spectrum of the LipK product, 1.

3.2.3 Phosgene modification and HR-ESI-MS, 1D, and 2D spectroscopic analysis of the LipK enzymatic product and synthetic controls

Further stereochemical assignment of the 5' and 6' position of the enzymatic LipK product by phosgene modification was done. Phosgene ($COCl_2$), known primarily for its use in WWI as a poisonous choking agent and for its use in polyurethane synthesis, has the ability to lock in the stereochemistry of β-hydroxy-α-amino acids, and therefore compound 1 by reacting with primary amine and adjacent oxygen center. Phosgene initially reacts with the nitrogen lone pair forming a collapsible intermediate, which gives a stable carbomoyl chloride derivative and can sequentially undergo dehydrohalogenation. Reactions with α-amino acids and phosgene afford oxazolidine-2,5-diones, commonly called N-carboxy anhydrides or Leuchs' anhydrides without altering the stereochemistry of the original stereocenters of the initial substrate (55, 56).

Synthetic controls of the (5'*S*, 6'*S*)-GlyU, (5'*S*, 6'*R*)-GlyU, and (5'*R*, 6'*S*)-GlyU compound were obtained from the lab of Dr. Christian Ducho. Both the synthetic and enzymatic LipK product were modified with phosgene and were then analyzed by HPLC and NMR spectroscopy (Fig. 3.10 – 3.14).

3.2.3.1 HPLC and MS analysis of phosgene modified 1 controls and the LipK enzymatic product

HPLC analysis of the phosgene-modified compounds revealed identical elution times of the phosgene-modified enzymatic product and that of the phosgene modified (5'*S*, 6'*S*)-GlyU diastereomer (Fig. 3.10). The new peaks were collected and subjected to MS analysis. The new peaks revealed $(M - H)^-$ ions of *m/z* = 341.7 and 367.6. These masses are consistent with that of either a single phosgene modification (*m/z* = 343) or a double phosgene modification (*m/z* = 369) (Fig. 3.11).

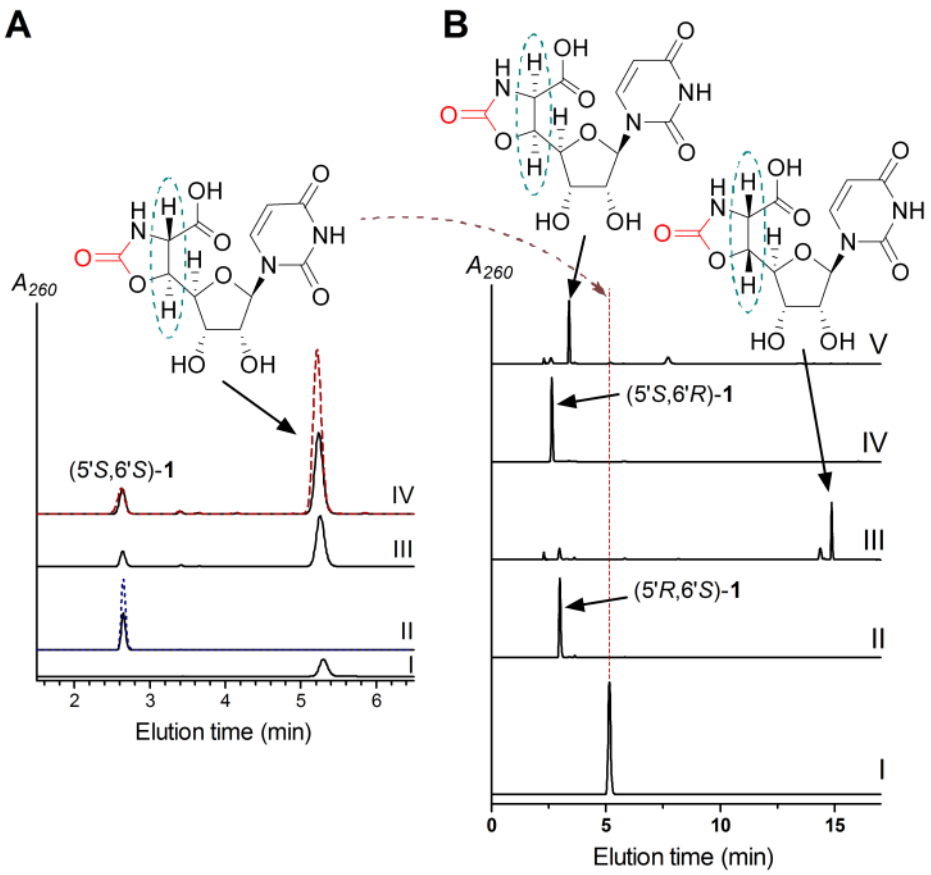

Figure 3.10. Comparative analysis of enzymatic and synthetic 1 diastereomers. (A) HPLC analysis of pure phosgene-modified (5'*S*,6'*S*)-1 that was prepared by enzymatic synthesis and confirmed by NMR spectroscopy (I), (5'*S*,6'*S*)-1 prepared by chemical synthesis (black, solid line) and spiked with an equimolar amount of enzymatic (5'*S*,6'*S*)-1 (blue, dashed line) (II), crude mixture of (5'*S*,6'*S*)-GlyU that was prepared by enzymatic synthesis and modified with phosgene (III), crude mixture of (5'*S*,6'*S*)-1 that was prepared by chemical synthesis and modified with phosgene (black, solid line) and spiked with authentic, enzymatically produced phosgene-modified (5'*S*,6'*S*)-1 (red, dashed line) (IV). (B) HPLC analysis of pure phosgene-modified (5'*S*,6′*S*)-1 (I), synthetic (5'*R*,6'*S*)-1 (II), phosgene-modified (5′*R*,6'*S*)-1 (III), synthetic (5'*S*,6'*R*)-1 (IV), and phosgene-modified (5'*S*,6'*R*)-1 (V). A_{260}, absorbance at 260 nm.

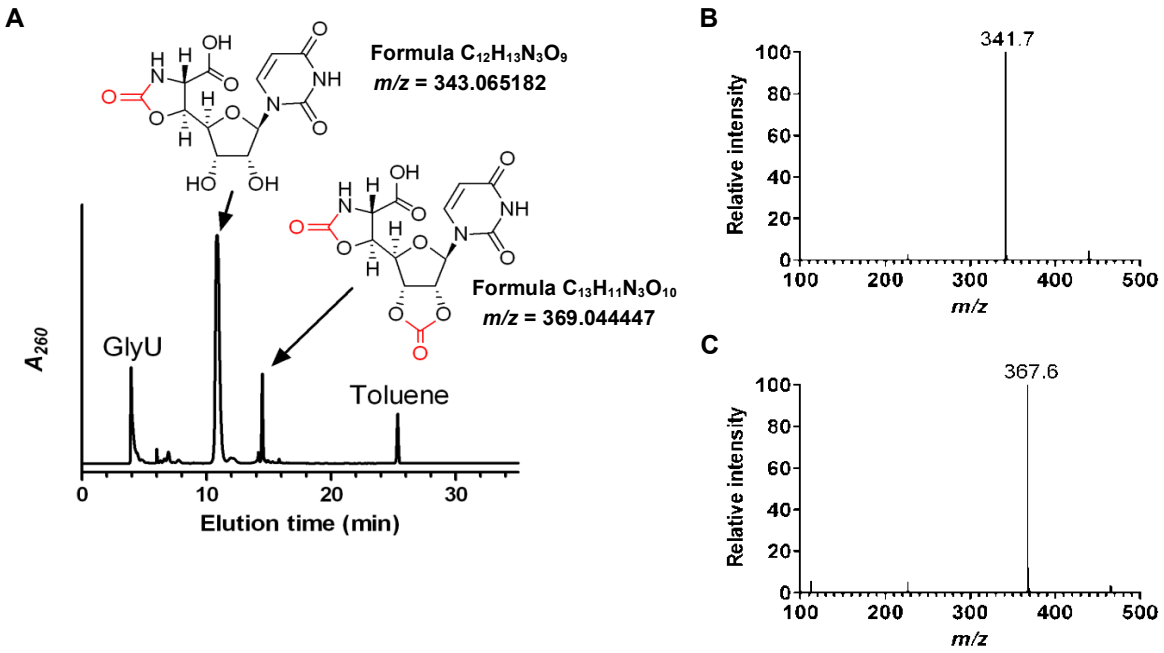

Figure 3.11. Phosgene modification of 1. (A) Semipreparative HPLC analysis of purified **1** prepared enzymatically that was reacted with phosgene to yield two major products with the expected mass spectrum for modification with (B) one or (C) two molecules of phosgene. A_{260}, absorbance at 260 nm.

3.2.3.2 1D NMR analysis of the phosgene modified LipK enzymatic product

^{1}H-NMR analysis of the phosgene-modified enzymatic product indicated a *J* coupling of ~5 Hz which is consistent with the MM2 ChemBio3D prediction suggesting a dihedral angle of 112° for phosgene-modified *threo* diastereomer (5'*S*,6'*S*)-GlyU under acidic conditions. In contrast, the erythro diastereomers are predicted to contain dihedral angles of ≤32° which is approximate to J values >8 Hz. The remaining (5'*R*, 6'*R*) threo diastereomer was ruled out due to the necessity of the dihedral angle of 160° which correlates to a ~12 Hz coupling constant (Fig. 3.12).

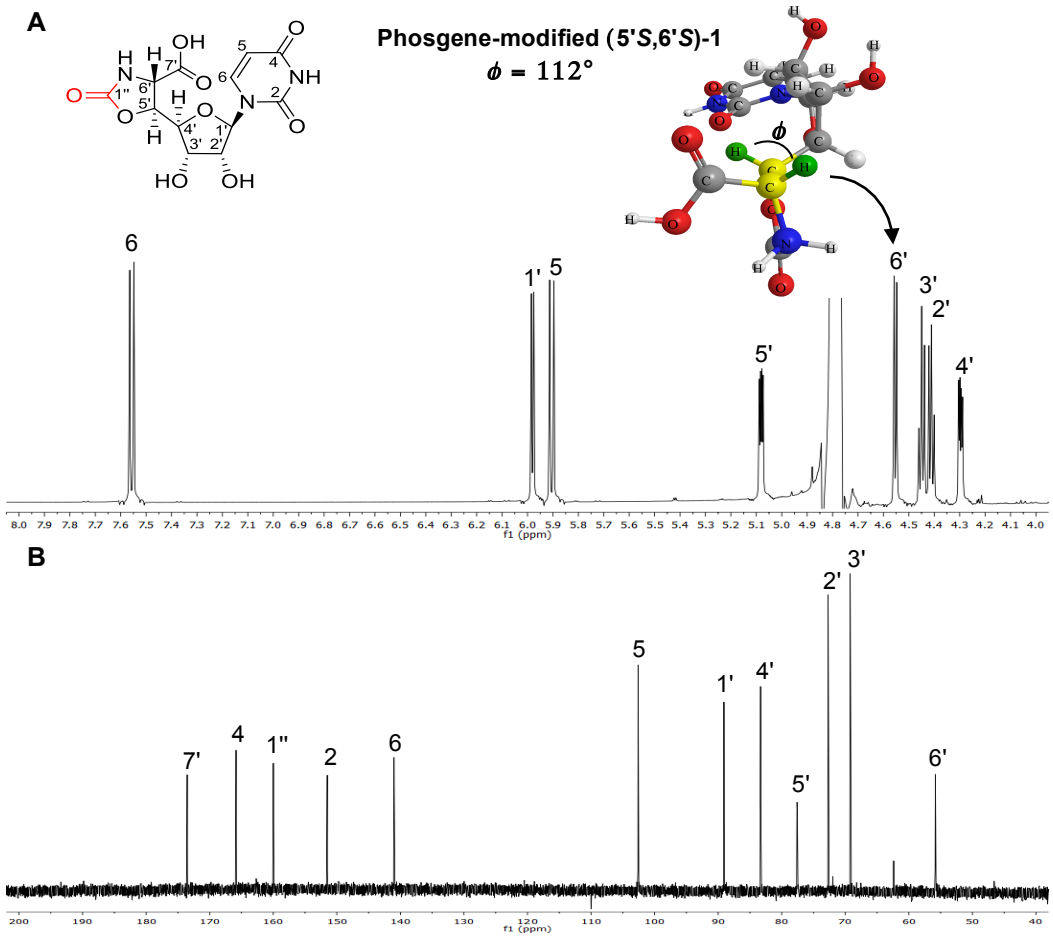

Figure 3.12. 1D NMR spectrum of phosgene-modified (5'*S*,6'*S*)-1. (A) ^{1}H NMR spectrum of (5'*S*,6'*S*)-**1** prepared enzymatically and modified with phosgene. Predictions following MM2 energy minimization with ChemBio3D suggest a dihedral angle of 112° for phosgene-modified (5'*S*,6'*S*)-**1** under acidic conditions that were utilized to obtain purified material for NMR. This dihedral angle is consistent with the *J* value of 5 Hz obtained from the ^{1}H-NMR spectrum, suggesting a *threo* configuration and overall stereochemical assignment as (5'*S*,6'*S*)-**1**. [Note that the ribofuranose component changes the priority at C-5' compared to C-3 of (2*S*,3*R*)-Thr, the *threo* diastereomer of L-Thr that serves as the substrate for LipK]. The *erythro* diastereomers are predicted to have dihedral angles of ≤ 32° that would yield *J* values of > 8 Hz, and the remaining *threo* diastereomer [(5'*R*,6'*R*)-**1**] is predicted to have a dihedral angle of 160° that would yield a *J* value of ~12 Hz. (B) ^{13}C NMR spectrum of (5'*S*,6'*S*)-**1** prepared enzymatically and modified with phosgene.

3.2.3.3 2D NMR analysis of the phosgene modified LipK enzymatic product

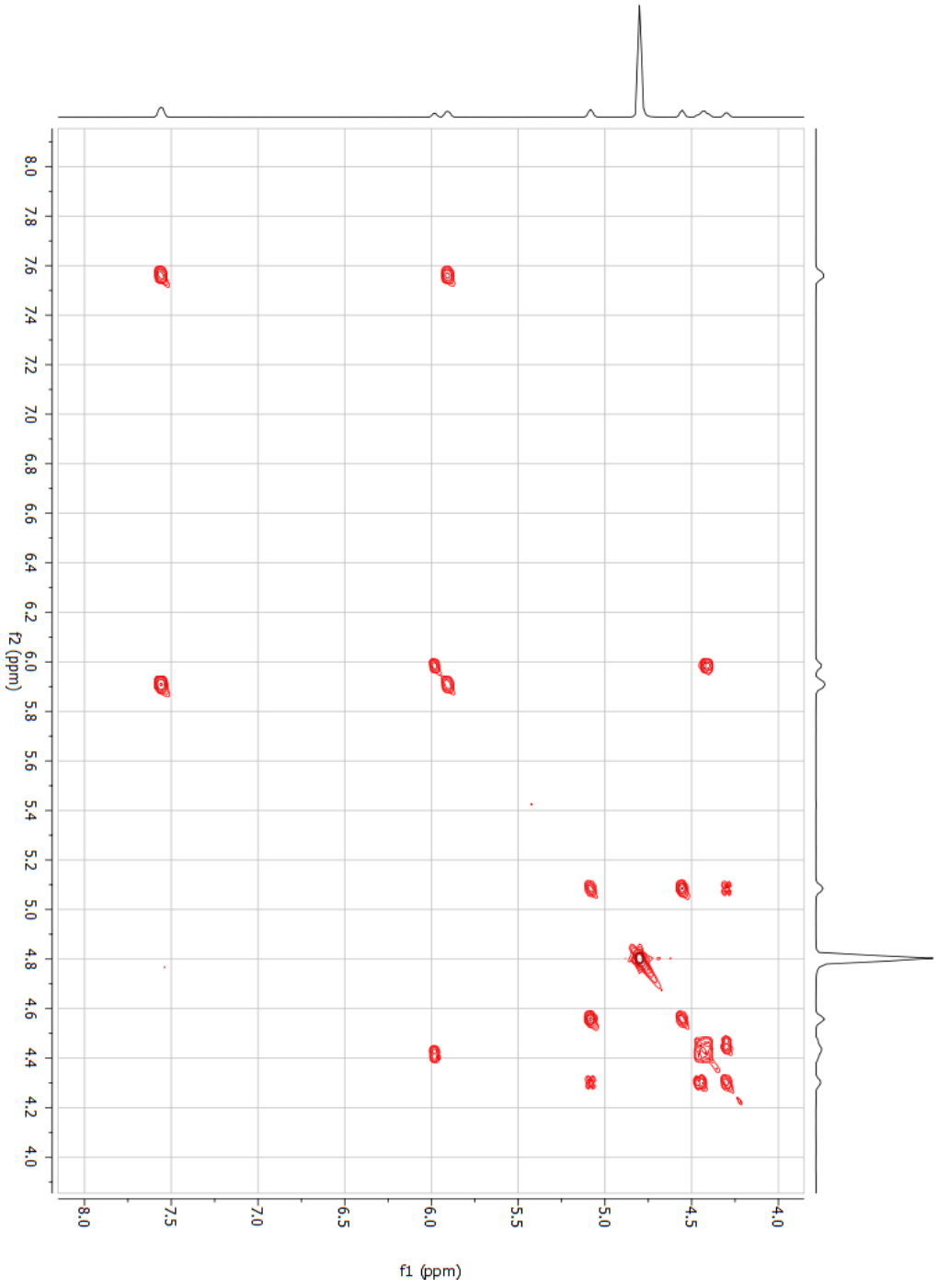

Figure 3.13. gCOSY NMR spectrum of phosgene-modified (5'*S*,6'*S*)-1.

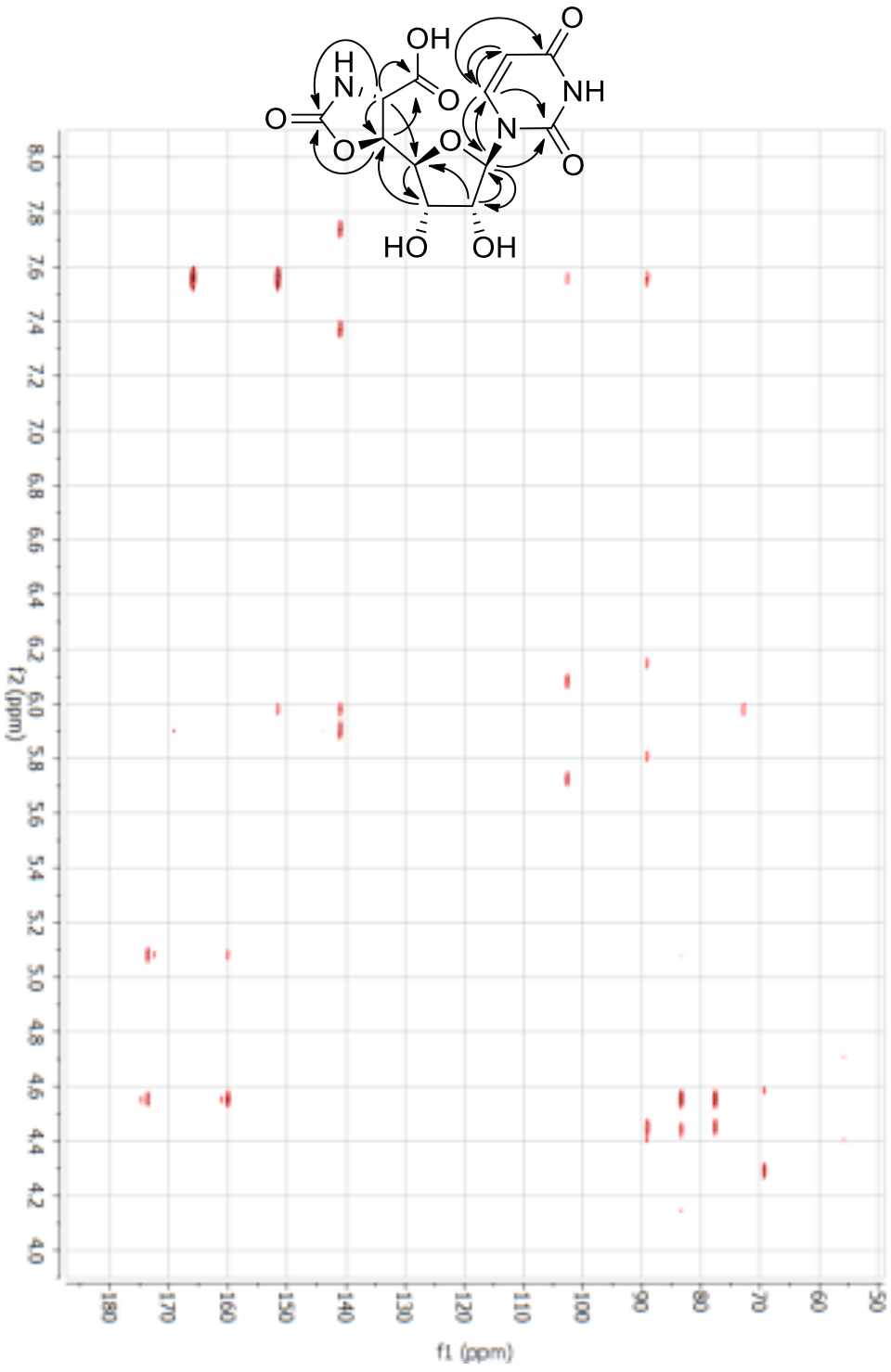

Figure 3.14. ^{1}H-^{13}C **gHMBC NMR spectrum of phosgene-modified (5'*S*,6'*S*)-1.**

3.2.4 Identification of enzymatic activity with capuramycin-related compounds by HPLC analysis

Bioinformatic analysis revealed both the caprazamycin and capuramycin-related compounds contain *lipL* and an *orf* encoding the putative SHMT homolog. This suggests a strong correlation in the biosynthesis of the core structures where GlyU is an intermediate of the uridine-5′--carboxamide (CarU) found in capuramycin-related antibiotics.

3.2.4.1 Substrates and enzymatic activity of Orf25

The putative SHMT, Orf25, from the capuramycin-like compound A-102395, was tested for activity using 2.0 mM UA, 0.1 mM PLP, and 10.0 mM of a variety of amino acid donors in 50 mM potassium phosphate buffer (pH 7.5). Individual reactions were incubated at 30°C and terminated by spin column filtration at 2 hr, 6 hr, and 18 hr time points. The control reaction and subsequent reactions containing 5 μM of Orf25 were then analyzed by reverse-phase HPLC using a linear gradient of water to acetonitrile. The control reaction containing all the components except enzyme showed elution of the UA substrate at ~1.98 min. Similarly to LipK and Mra14, there was no activity seen with the amino acids Gly or Ser, the primary hypothetical amino acid donor. However, a new peak was seen with the partially purified Orf25 when using L-Thr as previously observed with the other enzymes. HPLC analysis revealed the enzymatic product eluted at ~1.28 min (Fig. 3.15A).

3.2.4.2 Substrates and enzymatic activity of CapH

The next putative SHMT of interest from the capuramycin-like compound A-503083 biosynthetic gene cluster, CapH, was tested for activity. Again, 2.0 mM UA, 0.1 mM PLP, and 10.0 mM of a variety of amino acid donors in 50 mM potassium phosphate buffer (pH 7.5) containing 5 μM of CapH were tested for enzymatic activity. Individual reactions were prepared and incubated at 30°C for 2 hr, 6 hr, and 18 hr and terminated by spin column filtration. The reactions were then analyzed by reverse-phase HPLC utilizing a linear acetonitrile gradient. Once again, the control reaction containing all substituents except enzyme showed elution of the UA substrate at ~1.98 min and the primary hypothetical amino acid donors Gly or Ser showed no activity in any of the reactions. In contrast, and similarly to Orf25, HPLC analysis again revealed enzymatic activity with the amino acid L-Thr with the enzymatic product eluting at ~1.28 min (Fig. 3.15B), consisten with GlyU as the product.

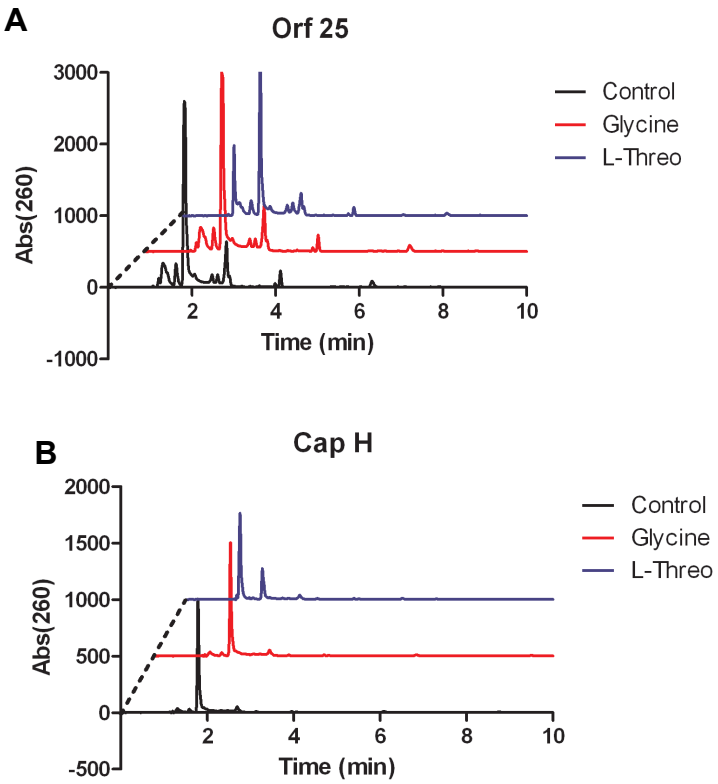

Figure 3.15. Verification of enzymatic activity of the putative SHMTs isolated from the biosynthetic gene cluster of capuramycin-related compounds. Reactions were carried out in 50 mM potassium phosphate buffer (pH 7.5), 0.1mM PLP, 10 mM L-Thr or Gly, and 2.0 mM UA. (**A**) Enzymatic activity involving the putative 5 μM SHMT, Orf25, from A-102395 biosynthetic gene cluster. No activity was seen with the amino acid donor Gly while product formation was observed at 1.28 min with L-Thr. (**B**) Enzymatic activity involving the putative 5 μM SHMT, CapH, from A-503083 biosynthetic gene cluster. Again, no activity was seen with the amino acid donor Gly while product formation was observed at 1.28 min with L-Thr.

3.2.5 Comparison of enzymatic activity of putative SHMTs

Due to the high similarity in amino acid sequence, as well as a key lysine residue located at ~235 aa found in each enzyme, the selection of preferred substrates by each enzyme indicates an identical catalytic function of the putative SHMTs

(Table 3.2). Comparison of the putative SHMTs utilizing UA, and L-Thr as substrates and PLP as a co-factor indeed gave identical HPLC chromatographs (Fig. 3.16). This is further evidence that the putative SHMTs are involved in the biosynthesis of the core unit of both the caprazamycin and capuramycin-related compounds GlyU and CarU respectively. Importantly, the results in total have led us to functionally assign these enzymes as LP-dependent UA: L-Thr transaldolases.

Table 3.2. Transaldolase sequence comparison. Comparison of the amino acid sequence of the individual putative SHMTs. %Identical/%Similar.

	LipK	**CapH**	**Mra14**	**Orf25**
LipK	X	45/47	81/82	45/47
CapH	45/47	X	46/48	79/80
Mra14	81/82	46/48	X	45/47
Orf25	45/47	79/80	45/47	X

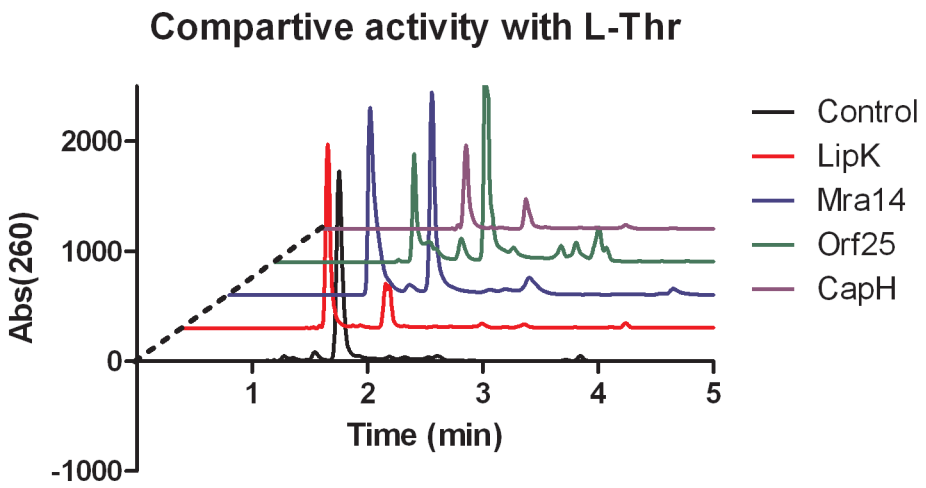

Figure 3.16. Transaldolase activity utilizing L-Thr and UA as primary substrates. Reactions were carried out in 50 mM potassium phosphate buffer (pH 7.5), 0.1mM PLP, 10 mM L-Thr or Gly, and 2.0 mM UA. The control reaction reflects reaction conditions lacking any enzyme. LipK, Mra14, Orf25, and CapH were individually tested by addition of 5 μM, run at 30°C, and terminated by spin column after 18 hours. The substrate UA elutes at ~1.89 min while the enzymatic product of each of the afore mentioned enzymes elutes at ~1.29 min. No activity was seen utilizing any other amino acid donor.

3.3. Isotopic feeding experiments for the capuramycin-like compound A-503083

The results suggest GlyU is an intermediate in the biosynthesis of the uridine-5′-carboxamide (CarU) core in the capuramycin-related compound biosynthesis. In order to provide additional evidence for the shared biosynthetic mechanism in capuramycin and carazamycin-related compounds, isotopic tracer experiments were executed employing the strain that produces A-503083. [1-^{13}C]Gly or [2-^{13}C]Gly and L-[$^{13}C_4$, ^{15}N]Thr were used with the expectation that the first two would serve as negative controls while the last would lead to enrichment

3.3.1 Isotopic feeding of [1-^{13}C]Gly or [2-^{13}C]Gly to the A-503083 B strain

The isotopically labeled Gly was fed into the producing strain of A-503083 B, the aminocaprolactam-containing and major congener of the A-503083 compounds (Fig. 3.17A). There was no significant enrichment observed for A-503083 B except for a 6% enrichment of the 3′-*O*-methyl group when fed the [2-^{13}C]Gly into the producing strain (Fig. 3.17B-D). This result is consistent with previous Gly tracer studies for other *Streptomyces O*-methylated metabolites (57).

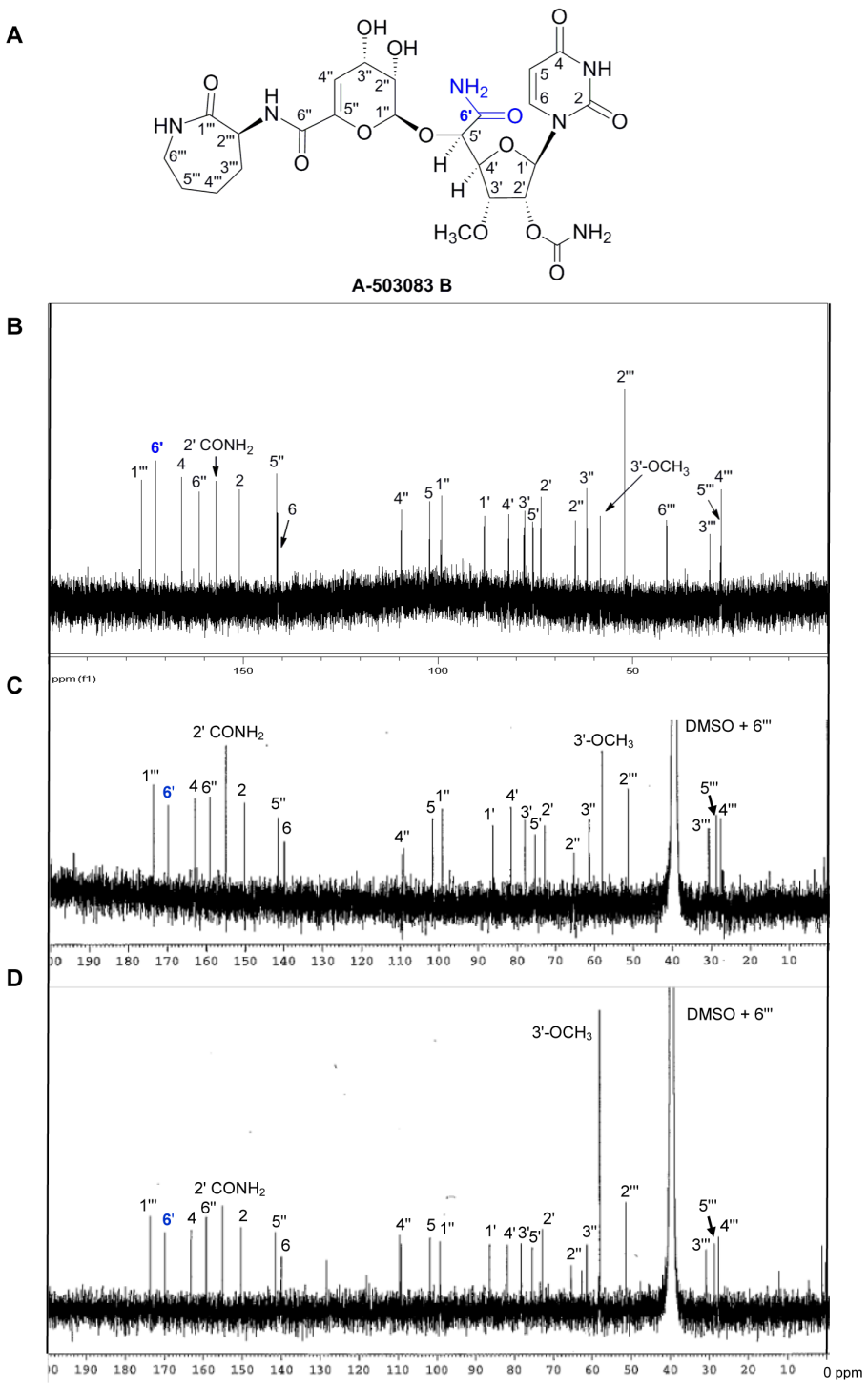

Figure 3.17. Isotopic tracer experiments using ^{13}C-Gly. (**A**) Structure of A-503083 B, the 6'''-desmethyl derivative of A-503083 A. (**B**) ^{13}C-NMR spectrum of A-503083 B obtained without feeding (natural abundance ^{13}C). (**C**) ^{13}C-NMR spectrum of A-503083 B obtained with [1-^{13}C]Gly feeding. (**D**) ^{13}C NMR spectrum of A-503083 B obtained with [2-^{13}C]Gly feeding.

3.3.2 Isotopic feeding of L-[$^{13}C_4$, ^{15}N]Thr into the strain producing A-503083 F

The isotopically labeled compound L-[$^{13}C_4$, ^{15}N]Thr was fed into the producing strain of A-503083 F, the deaminocaprolactam derivative of A-503083 B and a minor congener produced by the strain (Fig. 3.18A). In contrast to the [1-^{13}C]Gly and [2-^{13}C]Gly experiment, there was a 15% enrichment at the C-6′ position (Fig. 3.18B-D). Incorporation at this position is consistent with the direct incorporation of L-Thr by means of a transaldolase mechanism. We also observed a C-6′ doublet within the ^{13}C spectrum (J_{CN} = 18 Hz) indicative of a preserved C-N bond from L-Thr during biosynthesis of CarU (Fig. 3.18E).

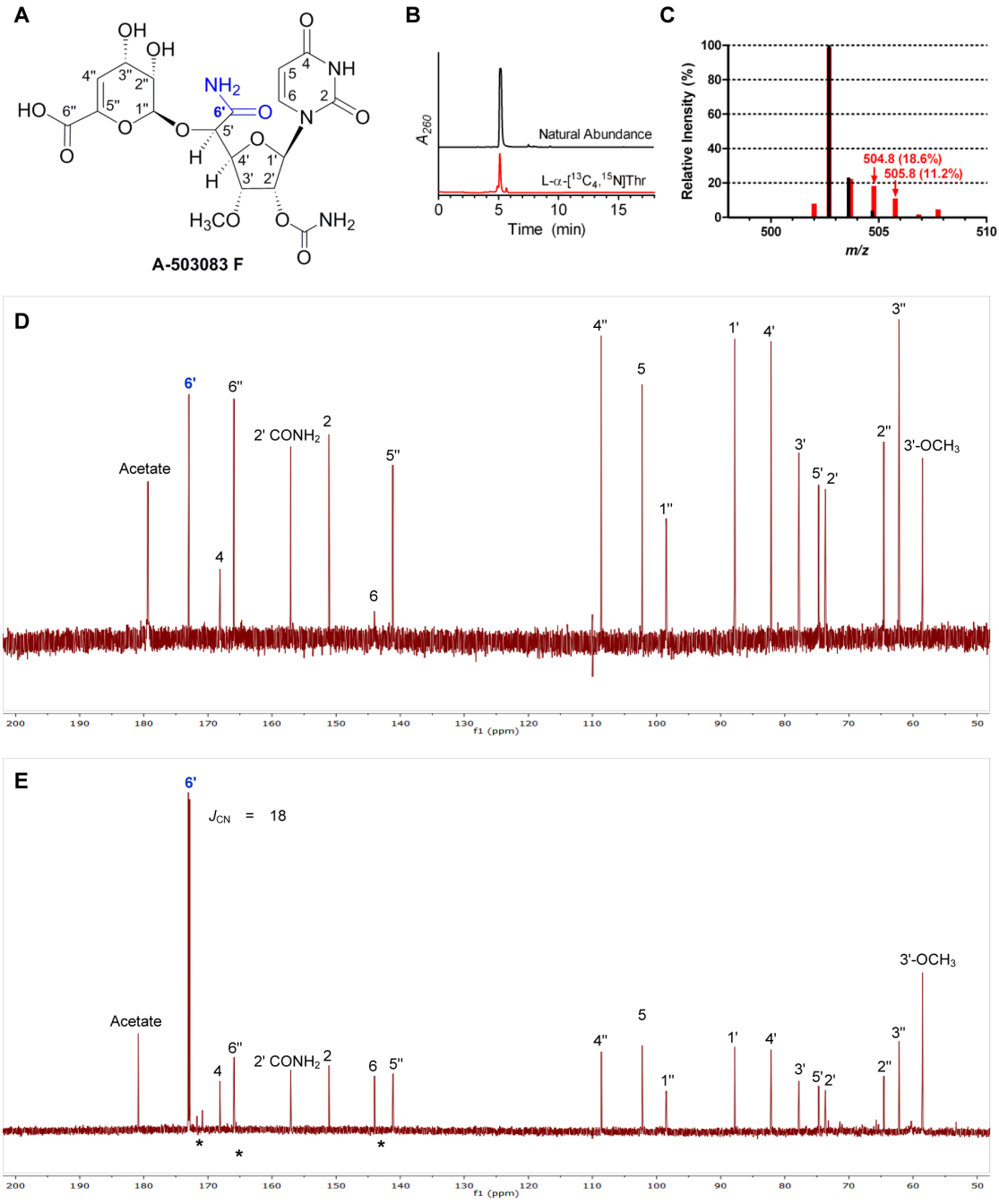

Figure 3.18. Isotopic tracer experiments using L-[^{13}C4,^{15}N]Thr. (**A**) Structure of A-503083 F, the deaminocaprolactam derivative of A-503083 A. (**B**) HPLC analysis of the purified A-503083 F obtained without feeding (natural abundance ^{13}C) and with L-[^{13}C4,^{15}N]Thr feeding. (**C**) Mass spectra for the peak eluting at t = 5.2 min, comparing A-503083 F isolated without feeding (**black**bars) and with L-[^{13}C4,^{15}N]Thr feeding (**red**bars). (**D**) ^{13}C-NMR spectrum of A-503083 F obtained without feeding (natural abundance ^{13}C). (**E**) ^{13}C-NMR spectrum of A-503083 F obtained withL-[^{13}C4,^{15}N]Thr feeding.

3.4. Biochemical analysis of the model enzyme LipK

3.4.1 Co-factor determination of the model enzyme of LipK

A useful characteristic of PLP-dependent enzymes is the unique UV/VIS spectrum associated with the binding of the co-factor and formation of catalytic intermediates. During the reaction coordinate formation of the internal aldimine, or holo-enzyme, followed by amino acid binding to form the external aldimine exhibits a UV maximum near 425 nm. Both SHMTs and LTAs elicit a UV maximum near 425 nm upon binding of the B_6 derived cofactor PLP and formation of the internal aldimine (Fig.3.19A). (4, 43). Contrastingly, LTA forms a quininoid intermediate upon Cα abstraction of Gly shifting the UV_{max} to 492 nm, while SHMTs retaining the same profile until THF binding to form a ternary complex, thus shifting the maximum to 500 nm (Fig. 3.19A).

Analysis of *Ec*GlyA, *Ec*LTA, and LipK revealed a UV/Vis spectra consistent with PLP bound to the protein as purified. The model enzyme LipK originating from both *S. lividans* TK64 and *S. albus* displayed a UV_{max} at 416 nm (Fig. 3.19B and Fig. 3.19F) which was absent in the LipK(K235A) mutant (Fig. 3.19F). The *Ec*LTA displayed a maximum absorbance at 421 nm (Fig. 3.19C), while the *Ec*GlyA at 425 nm (Fig. 3.19D). As expected, upon addition of Gly, the *Ec*LTA shifted the UVmax to 492 nm (Fig. 3.19C) and the *Ec*GlyA UV_{max} shifted to 500 nm upon the addition of both THF and Gly (Fig. 3.19D). These shifts in UV_{max}

are both consistent with the formation of a quininoid intermediate. In contrast, addition of either Gly, THF, or both did not alter the UV_{max} of LipK (Fig. 3.19E). This data suggests that LipK has unique catalytic properties differing from those of *Ec*GlyA and *Ec*LTA.

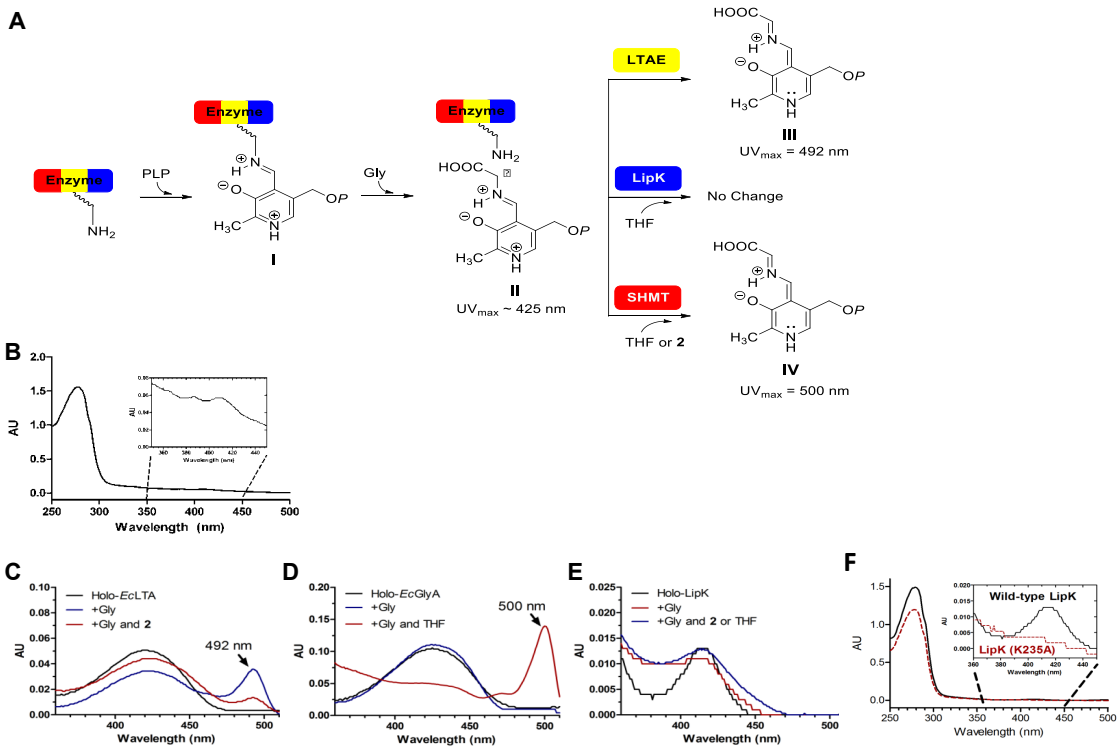

Figure 3.19. UV/Vis spectra for intermediates and the potential intermediates of the PLP-dependent enzymes under analysis. (**A**) Formation of the internal aldimine with the binding of the apo-enzymes to PLP generating the holo-enzyme (**I**) followed external aldimine formation by Gly binding (**II**). A quininoid intermediate is observed by UV/VIS spectroscopy due to deprotonation at the α-carbon within the active site of LTA. (**III**). In contrast, SHMT binding of the substrate analogues of N^5,N^{10}-methylene tetrahydrofolate (THF) such as THF to form a ternary complex that undergoes deprotonation at the α-carbon of Gly to yield a quininoid intermediate (**IV**). However, no UV/Vis spectral changes were identified with LipK therefore precluding the assignment of any intermediates that are depicted. (**B**) UV/Vis spectrum of LipK isolated from *Streptomyces albus*. (C) UV/Vis spectrum of *Ec*LTA as isolated (holo-*Ec*LTA), following the addition of Gly (+Gly), and following addition of Gly with **2** (+Gly and **2**). The reduction in the peak at 492 nm following the addition of **2** suggests either a reaction is occurring or **2** binding is promoting re-formation of aldimine **II**, in both cases preventing the accumulation of a quininoid intermediate. As subsequently determined, the inability to observe any product by HPLC is consistent with the latter. (D) UV/Vis spectrum of *Ec*GlyA as isolated (holo-*Ec*GlyA), following the addition of Gly (+Gly), and following addition of Gly with THF (+Gly and THF). (E) UV/Vis spectrum of LipK as isolated (holo-LipK), following the addition of Gly (+Gly), and following addition of Gly with **2** or THF (+Gly and **2** or THF). (F) The UV/Vis spectra of recombinant LipK and point mutant isolated from *S. lividans* TK64. AU, absorbance units.

3.4.2 Specificity and biochemical properties of LipK

In order to develop assays capable of measuring LipK activity, optimal reaction conditions were determined. By identifying optimal pH, buffer conditions, and potential substrates, we were able to determine conditions suitable for kinetic analysis. Kinetic analysis utilized the formation of a secondary product during the LipK reaction, acetaldehyde.

3.4.2.1 Optimization of LipK enzymatic activity

3.4.2.1a L-Thr specificity for LipK activity

We first explored LipK activity with different α-amino acids and detection by HPLC. The only activity seen was that utilizing L-Thr as the amino acid donor. The lack of activity with proteinogenic α-amino acids, commercially available L-Thr diasteromers, and Thr analogues (Fig. 3.20) indicates the high specificity for L-Thr.

3.4.2.1b Optimal pH and buffer for LipK activity

A variety of buffers capable of maintaining various pH profiles was tested to determine the optimal pH for activity. Succinate, citrate, phosphate, Tes, Hepes, and Tris buffers were prepared in pH profiles ranging from 3-10 and tested. The pH profile for LipK resembles a bell shaped curve under initial velocity conditions and maintained an optimal pH activity at 7.5 with the optimal buffer being Tes (Fig. 3.21A).

3.4.2.1c Optimal salt concentration for LipK activity

The monovalent cations K+ and Na+ have shown activation of enzymatic activity by enhancing the affinity of the enzyme for the substrate (58). Therefore, monovalent cation concentration was tested between 0.001-10000 mM. Monovalent ions slightly changed the activity up to 100mM and then began to decrease activity (Fig. 3.21B).

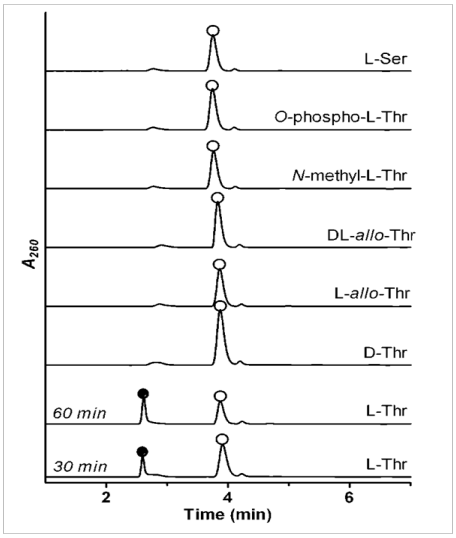

Figure 3.20. HPLC analysis to probe the substrate specificity of LipK. The reactions were carried out in 50 mM HEPES (pH 7.5), 2 mM **2**, 5 mM indicated co-substrate (all α-amino acids), 0.1 mM PLP, and 2 μM LipK at 30 °C for 1 h prior to termination. Product formation was monitored using the Agilent HPLC system with an Eclipse XDB-C18 column. (o) **2** (•) **1**. $A_{260,}$ absorbance at 260 nm.

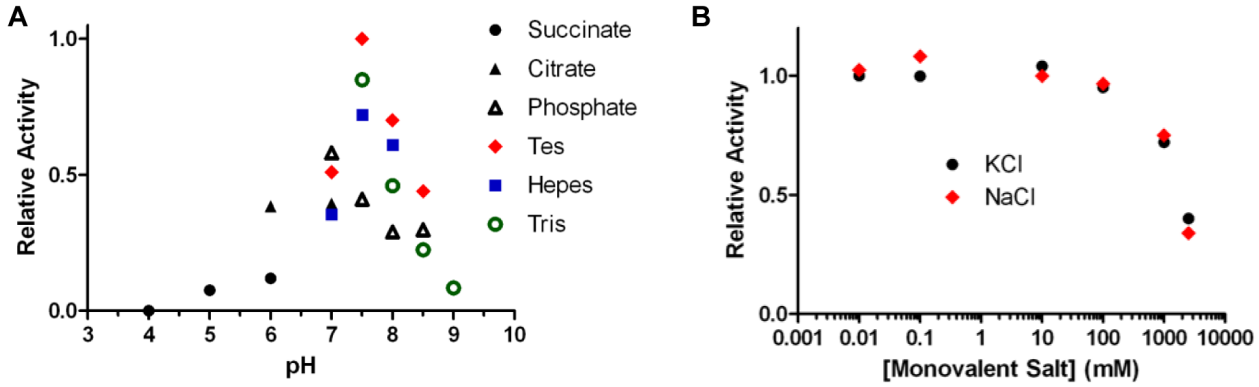

Figure 3.21. Activity optimization for LipK. (**A**) pH profile of LipK. The activity was assessed in reactions containing 50 mM buffer,2 mM uridine-5'-aldehyde, 5 mM L-Thr,0.1 mM PLP, and 2 μM LipK at 30 °C under initial velocity conditions. Product formation was assessed by HPLC. (**B**)Activity of LipK with monovalent salts using 50 mM TES (pH 7.5)and the conditions indicated in **A**.

3.4.2.2 Assay development for enzymatic activity

After optimizing conditions for enzymatic activity for LipK, we tested for L-Thr dependent retro-aldol activity in which we utilized the formation of acetaldehyde during the reaction to develop an assay amicable to kinetic analysis. *Saccharomyces cerevisiae* aldehyde dehydrogenase (ADH, EC 1.2.1.3) efficiently utilizes acetaldehyde as a substrate for oxidation by reduction of β-NAD^+ (Fig. 3.22). To verify the formation of acetaldehyde, we also compared results to that of *Ec*LTA and *Ec*GlyA.

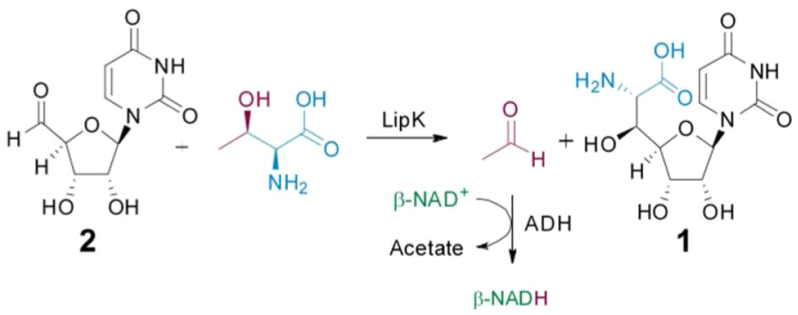

Figure 3.22. The LipK-catalyzed reaction and coupling with aldehyde dehydrogenase (ADH).

First, we ensured conditions for ADH activity did not interfere with the activity of the LipK, *Ec*LTA, and *Ec*GlyA (Fig. 3.23). This assay revealed that a retro-aldol reaction was catalyzed solely with L-Thr and LipK, *Ec*LTA, and *Ec*GlyA yielding activities of (1.3 ± 0.2) x 10^{-2}, 1.2 ± 0.2, and (5.7 ± 0.4) x 10^{-4} μmol/min/mg, respectively (Fig. 3.24 and 3.25A).

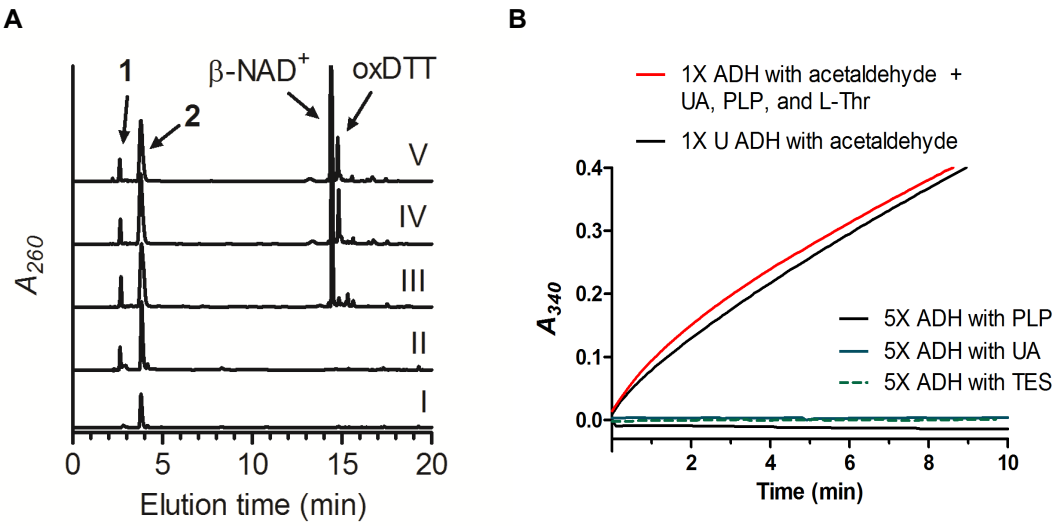

Figure 3.23. Assay Development for LipK. (A) HPLC analysis of the LipK reaction starting with **2** after 2 h reactions with omission of L-Thr (I), all necessary reaction components (II), reaction components plus 1 mM β-NAD^+ (III), reaction components plus 1 mM β-NAD^+ and 1 mM DTT (IV), reaction components plus 1 mM β-NAD^+, 1 mM DTT, and 100 mM KCl (V). The results demonstrate that LipK activity is not affected by β-NAD^+, DTT, or KCl at these concentrations. Reactions were monitored using the Agilent HPLC system with an Eclipse XDB-C18 column. β-NAD^+, β–nicotinamide adenine dinucleotide, oxidized form; oxDTT, oxidized dithiothreitol; A_{260}, absorbance at 260 nm. (B) UV/Vis spectroscopic analysis of the LipK and aldehyde dehydrogenase (ADH)-coupled reaction monitoring the reduction of β-NAD^+. ADH did not oxidize **2**, pyridoxal-5'-phosphate (PLP), nor TES buffer, and oxidation activity of acetaldehyde was not affected by the necessary components for LipK activity. 1X corresponds to 0.004 U of ADH. A_{340}, absorbance at 340 nm.

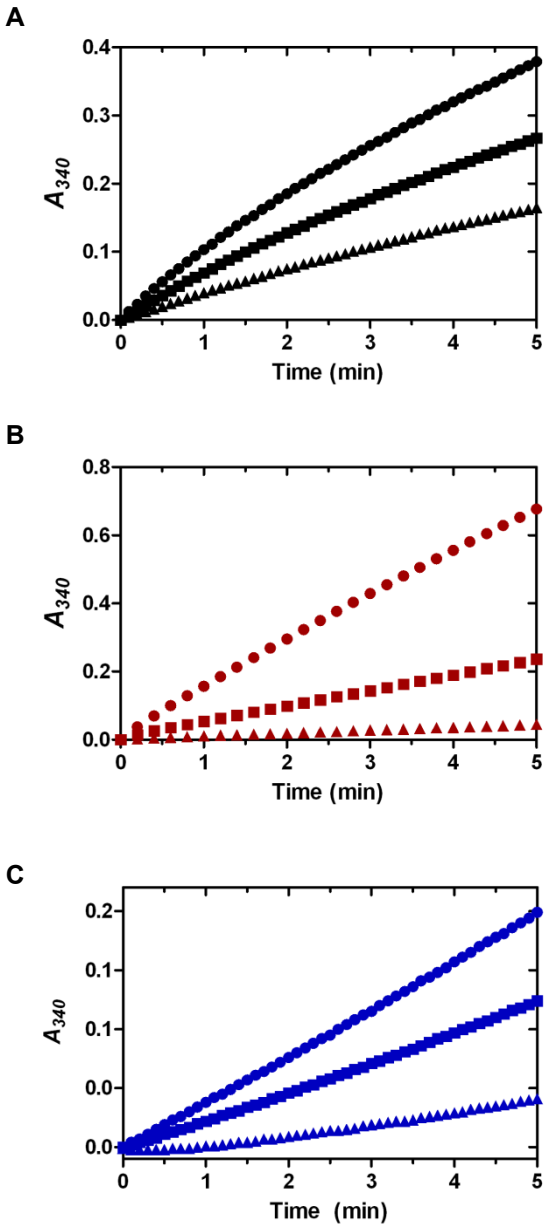

Figure 3.24. L-Thr aldolase activity. Reactions were conducted in 50 mM TES (pH 7.5), 100 mM KCl, 1 mM DTT, 0.1 mM PLP, 10 mM L-Thr, 2 mM β-NAD^+ at 30 °C (A) LipK at 33 μg (▲), 62.5 μg (■) and 96 μg (●) yielding a specific activity of (1.3 ± 0.2) x 10^{-2} μmol/min/mg. (B) *Ec*LTA at 0.12 μg (▲), 0.5 μg (■) and 1.7 μg (●) yielding a specific activity of 1.2 ± 0.2 μmol/min/mg. (C) *Ec*GlyA at 300 μg (▲), 750 μg (■) and 1180 μg (●) yielding a specific activity of (5.7 ± 0.4) x 10^{-4} μmol/min/mg. A_{340}, absorbance at 340 nm.

Although the detection of acetaldehyde with LipK was surprising, the rate of retro-aldol activity catalyzed by LipK was significantly increased upon an equimolar addition of UA (Fig. 3.25A), which suggests that the normal catalytic cycle involves an initial binding of L-Thr and formation of a ternary complex. The single-substrate kinetics experiments utilizing LipK displayed the typical Michaelis-Menten kinetics in regards to UA and yielded constants of K_m = 29.2 ± 9.5 mM and k_{cat} = 40 ± 4 min^{-1} (Fig. 3.25B). However, while the high K_m for UA precluded an accurate single-substrate kinetic analysis with respect to varied L-Thr, the bisubstrate kinetic analysis was consistent with LipK utilizing a sequential mechanism more characteristic of bona fide SHMTs despite the production of acetaldehyde in the absence of UA (Fig. 3.25C) (54).

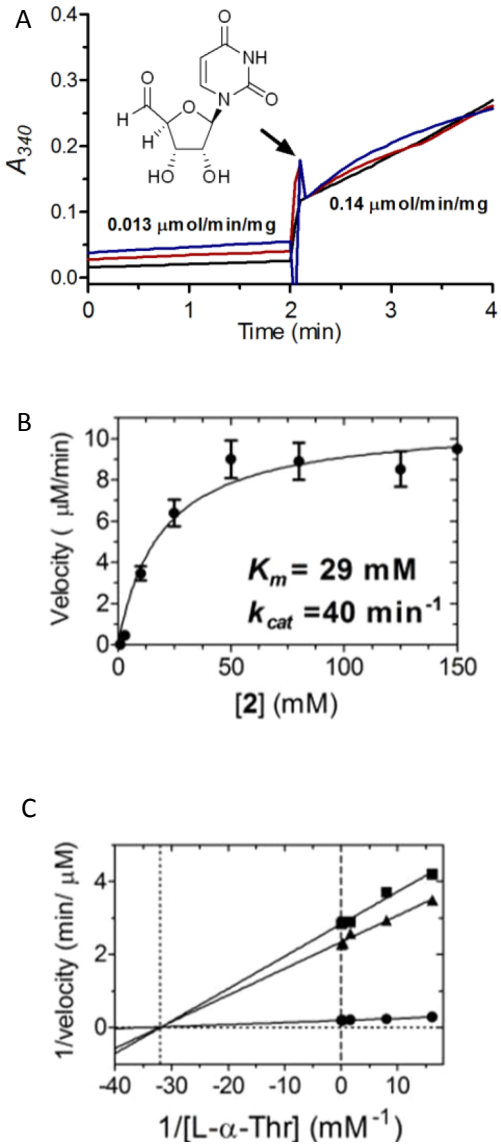

Figure 3.25. Kinetic analysis of LipK. (A) UV/Vis spectroscopic analysis of the L-Thr retro-aldol-type reaction catalyzed by LipK in the absence or presence of 10 mM **2**. Each line represents an independent reaction with **2** added at the indicated time. A_{340}, absorbance at 340 nm. (B) Single-substrate kinetic analysis with 30 mM L-Thr and variable **2**. (C) Bisubstrate kinetic analysis using 1 mM (■), 3 mM (▲), and 60 mM (●) **2**.

3.5. Exploration of *Ec*GlyA and *Ec*LTA as L-threonine Transaldolases

The initial bioinformatics analysis of the four enzymes studied in this dissertation gave the highest similarity to PLP dependent serine hydroxymethyltransferases. However, the actual function is revealed to be an L-Thr transaldolase. Knowing that the putative SHMT LipK is actually a transaldolase, we decided to test both *Ec*GlyA and *Ec*LTA, well characterized SHMT and LTA respectively, for transaldolase activity.

3.5.1 Enzymatic activity with L-Thr and UA as primary substrates

The initial experiment combined PLP, TES buffer, Gly, and UA with either *Ec*Gly*A* or *Ec*LTA and subjected to HPLC analysis. (43, 59) Initial screening revealed no activity with Gly, however a low amount of activity with L-Thr was observed (Fig. 3.26). The new peaks had identical retention time and UV spectrum to the LipK product, GlyU. The stereochemistry of this reaction product is under investigation.

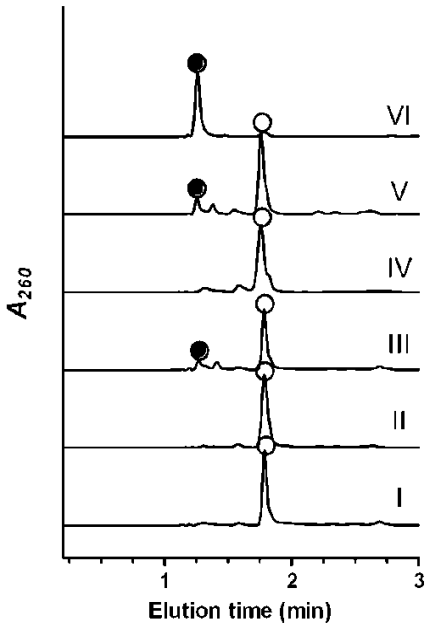

Figure 3.26. Detection of potential (trans)aldolase activity of *Ec*GlyA and *Ec*LTA. HPLC analysis of 18 h reactions containing 5 μM enzyme and **2** with control (no enzyme, I), *Ec*LTA with Gly (II), *Ec*LTA with L-Thr (III), *Ec*GlyA with Gly (IV), *Ec*GlyA with L-Thr (V), and LipK with L-Thr (VI). (o) **2**, (●) new peak co-eluting with **1**. $A_{260,}$ absorbance at 260 nm.

3.5.2 Enzymatic activity with L-Thr and 2-pyridine-carboxaldehyde as primary substrates

Due to the enzymatic activity seen with UA and L-Thr, with either *Ec*GlyA and *Ec*LTA in comparison to LipK, the potential L-Threonine transaldolase activity of *Ec*GlyA and *Ec*LTA was further explored with the alternative aldehyde substrates. The commercially available substrates 2-pyridine-carboxaldehyde and L-Thr were tested for enzymatic activity with *Ec*GlyA and *Ec*LTA, using reverse-phase HPLC and MS for detection and analysis.

3.5.2.1 HPLC analysis of enzymatic reactions involving *Ec*GlyA (EcSHMT), *Ec*LTA, and 2-pyridine-carboxaldehyde

Reactions incorporating 0.1 mM PLP, 10.0 mM L-Thr, 2.0 mM 2-pyridine-carboxaldehyde, and 5 μM enzyme were incubated for 18 h. The reactions were analyzed by reverse-phase HPLC chromatography following a linear acetonitrile gradient. The control reaction lacking any enzyme shows elution of the 2-pyridine-carboxaldehyde at ~1.93 min. Reactions containing 5 μM of the specified enzyme indicate enzymatic activity by the formation of a new peak at ~1.53 min. Both *Ec*GlyA and *Ec*LTA show identical chromatographs to that of the reaction containing LipK (Fig. 3.27A).

3.5.2.2 MS analysis of enzymatic reactions involving *Ec*GlyA, *Ec*LTA, and 2-pyridine-carboxaldehyde.

The new peak was collected and subject to HPLC analysis for purity and MS analysis for preliminary identification of the product. The *Ec*GlyA product appeared pure while the *Ec*LTA product showed only minor contamination in the chromatograph (Fig. 3.27D and Fig. 3.27E). Interestingly, both the *Ec*GlyA product and the *Ec*LTA product showed a $(M - H)^+$ ion at *m/z* = 183.2 (Fig. 3.27B and Fig. 3.27C), consistent with that of **4** (expect *m/z* = 182), the L-Thr transaldolase product of 2-pyridine-carboxaldehyde and L-Thr (Fig. 3.27F). The structure and stereochemical assignment of the product is under investigation.

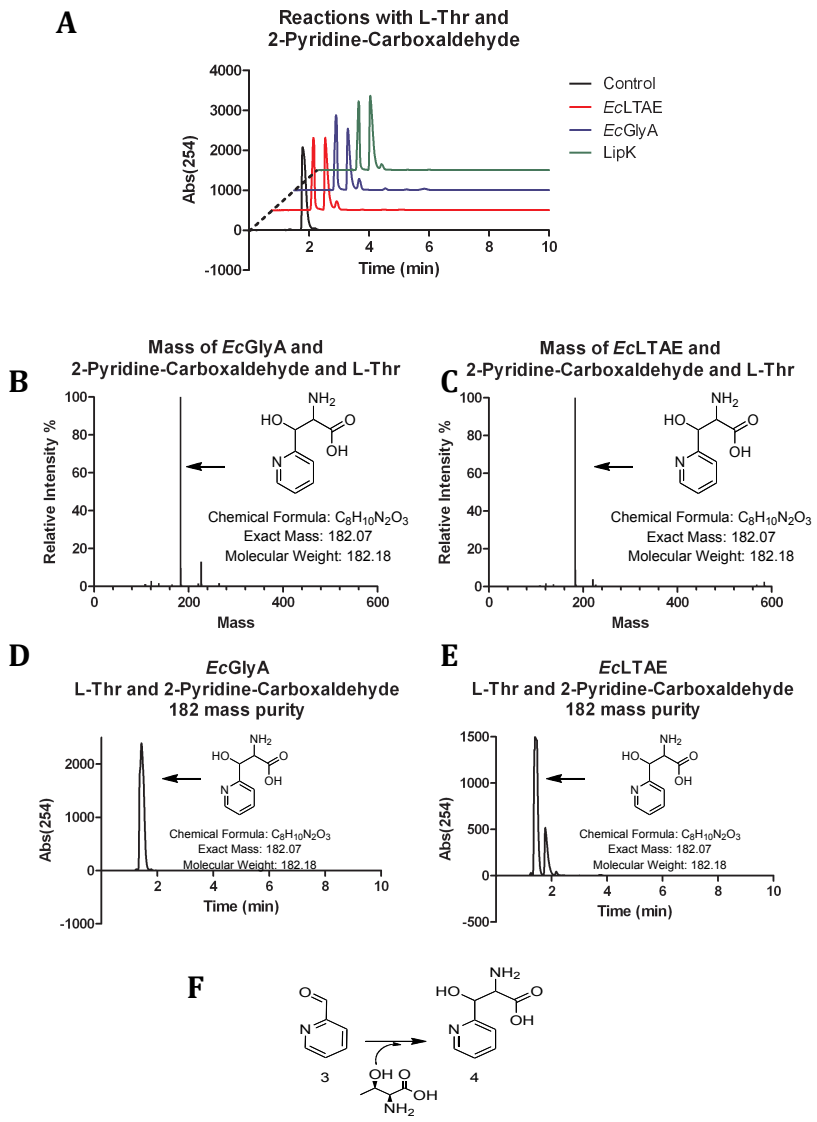

Figure 3.27. HPLC and MS analysis of EcSHMT and EcLTA transaldolase activity utilizing L-Thr and 2-pyridine-carboxaldehyde as primary substrates. (**A**) HPLC analysis of 18 h reactions with no enzyme in the control, 5 μM *Ec*LTA, 5μM *Ec*GlyA, and 5 μM LipK. Abs(254), absorbance at 254 nm. (**B**) Mass spectrum for the peak eluting at t = 1.53 min from the enzymatic product of 2-pyridine-carboxaldehyde, L-Thr, PLP, and *Ec*GlyA. The product yields an ion of mass $(M - H)^+$ consistent with the molecular formula of 4. (**C**) Mass spectrum for the peak eluting at t = 1.53 min from the enzymatic product of 2-pyridine-carboxaldehyde, L-Thr, PLP, and *Ec*LTA. The product yields an ion of mass $(M - H)^+$ consistent with the molecular formula of 4. (**D**) HPLC trace of the *Ec*GlyA enzymatically prepared product following purification using reverse-phase chromatography. (**E**) HPLC trace of the *Ec*LTA enzymatically prepared product following purification using reverse-phase chromatography. (**F**) L-threonine transaldolase activity incorporating L-Thr onto 2–pyridine-carboxaldehyde.

Chapter Four

Summary

The caprazamycin and capuramycin-related compounds A-90289, muraminomicin, A-503083, and A-102395 are potent MraY inhibitor compounds with great potential for antibacterial use within the clinical setting. Their complex and novel structures help to delay the onset of resistance while their non-mammalian homolog targets are specific for gram-positive and gram-negative peptidoglycan cell wall formation. By investigating the biosynthetic pathway utilized in the formation of these compounds, we were able to identify enzymatic homologs suggesting similar biosynthetic pathways in these two families. Characterization of these shared enzymatic homologs revealed novel and interesting chemistry.

Herein we have described the novel chemistry utilized by the putative SHMTs within the caprazamycin and capuramycin-related compounds that catalyze C-C bond formation that is necessary in assembling the high carbon furanoside. The MraY translocase I inhibitor compounds A-90289 isolated from *Streptomyces* sp. SANK 60405, muraminomicin isolated from *Streptosporangium amethystogenes* SANK 60709k, A-503083 isolated from *Streptomyces* sp. SANK 62799, and A-102395 from *Amycolatopsis* sp. SANK 60206 all share this putative SHMT within the biosynthetic gene cluster. Previous research in our group has already shown

the necessity of the putative SHMTs in the formation of the final compound due to the abolishment of product when the SHMT-like gene is deleted from the biosynthetic gene cluster. Therefore, we turned to heterologous expression of the putative SHMTs from each of the above-mentioned compounds for *in vitro* analysis of enzymatic activity and characterization of the enzymatic product. Interestingly we were only able to get soluble protein from Streptomyces host. Perhaps more interesting was the discovery of the true activity of these SHMT homologues as L-Thr UA transaldolases. This is in contrast to our first hypothesis that Gly or Ser was used as a glycyl unit donor.

After identification of (5*S*, 6*S*)-GlyU as the enzymatic product, we tested our next hypothesis that the putative SHMTs could serve as an intermediate in the formation of CarU, the core structure of the capuramycin-related compounds. As expected, based on sequence similarity, Orf25 and CapH had identical activity to LipK and Mra14. Furthermore, isotopically labeled precursors enabled us to identify L-Thr incorporation into the final compound A-503083 and helped us to verify the activity and necessity of the putative SHMTs in formation of the CarU structure. This result suggest more interesting chemistry is yet to be discovered during the conversion of GlyU to CarU during capuramycin biosynthesis.

Finally, identification of the enzymatic activity of the putative SHMTs and the role they play in the biosynthesis of caprazamycin and capuramycin-related

compounds led us to inquire into a potential alternative activity of the canonical SHMT and LTA, GlyA and *Ec*LTA respectively. Analysis of the results from the enzymatic assays using the putative SHMT LipK, as well as *Ec*GlyA and *Ec*LTA, revealed identical HPLC traces as well as the formation of acetaldehyde, the secondary product. Preliminary results indicate that indeed both the *Ec*GlyA and the *Ec*LTA do act in a mechanistic method mimicking that of the transaldolase isolated from the caprazamycin and capuramycin-related compounds. Overall, the heterologous expression, characterization, and in vivo analysis of the putative SHMTs studied in this dissertation offers insight into novel chemistry utilized by organisms to form novel, complex antibacterial compounds.

Chapter Five

Final Thoughts

The continual search for methods enabling the formation of β-hydroxy-α-amino acids continues throughout the scientific community. The requirement of β-hydroxy-α-amino acids in formation of biologically active antibiotics make them ideal scaffolds to build novel antibacterial compounds, however the ability to synthesize enantiomerically pure products still remains challenging (60-63).

This dissertation has revealed the LipK family of L-threonine:uridine-5′-aldehyde transaldolases as putative SHMTs that catalyze an L-Thr-dependent β-substitution reaction by means of a sequential Cα-Cβ bond breaking and re-formation (Fig. 4.1) to form the nonproteinogenic β-hydroxy-α-amino acid (5′*S*, 6′*S*)-GlyU intermediate. Differing in its preference for L-Thr as opposed to L-*allo*-Thr preferred by canonical LTAEs (4), LipK displays activity similar to that of 4-fluorothreonine transaldolase (FTase). Despite sharing only 25% sequence identity within the SHMT-like domain (Fig. 4.2), both LipK and FTase catalyze an L-Thr-dependent β-substitution reaction by means of a Cα-Cβ bond breaking and creation (64, 65). With the Lys residue identified as key in the formation of an external aldimine, and the C-C bond extension capability, LipK paves the way for inquiry into the more canonical enzymes *Ec*GlyA and *Ec*LTA, also utilizing

external aldimine formation and C-C bond extension, which we have tagged as having potential L-Thr transaldolase activity.

Providing another distinct mechanism for C-C bond formation for sugars, LipK differs from the more traditional aldolase and transketolase group of enzymes which employ a carbonyl-group-containing substrate as the donor (66). Instead, LipK uses an amino acid as the donor and yields a β-sugar substituted α-amino acid. Not only could the ability of these novel enzymes for C-C bond formation provide another means of preparing previously un-synthesizable sugars and unusual amino acids, but the amalgamating ability utilizing amino acids into nucleoside antibiotics may provide another means for identifying complex, novel antibacterial compounds.

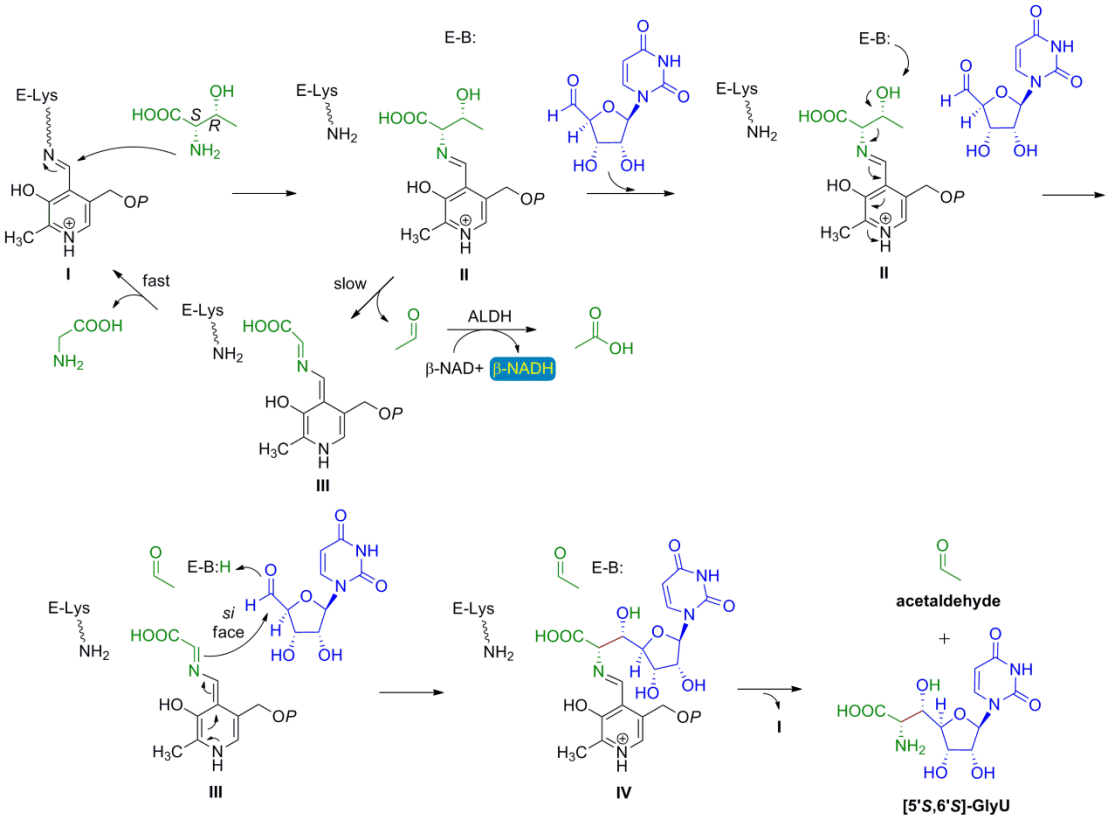

Figure 4.1 Putative chemical mechanism of L-Thr:UA transaldolases. The enzyme in the holo-form (**I**) binds L-Thr to generate the external aldimine (**II**) and **UA** to form a ternary complex. An enzyme base deprotonates the β-hydroxyl to initiate the retro-aldol-type reaction, a step that is likely rate limiting considering no additional UV-active intermediates such as species **III** are detected throughout the course of the reaction. The formed acetaldehyde subsequently diffuses from the active site allowing **UA** to position in the same relative orientation. Attack of **III** on the *si* face in the aldol-type reaction with **UA** generates intermediate **IV** prior to release of the two products and regeneration of the holo-enzyme **I**. In the absence of **UA**, a retro-aldol reaction can occur to putatively generate intermediate **III**, which was not detected by UV/Vis spectroscopy.

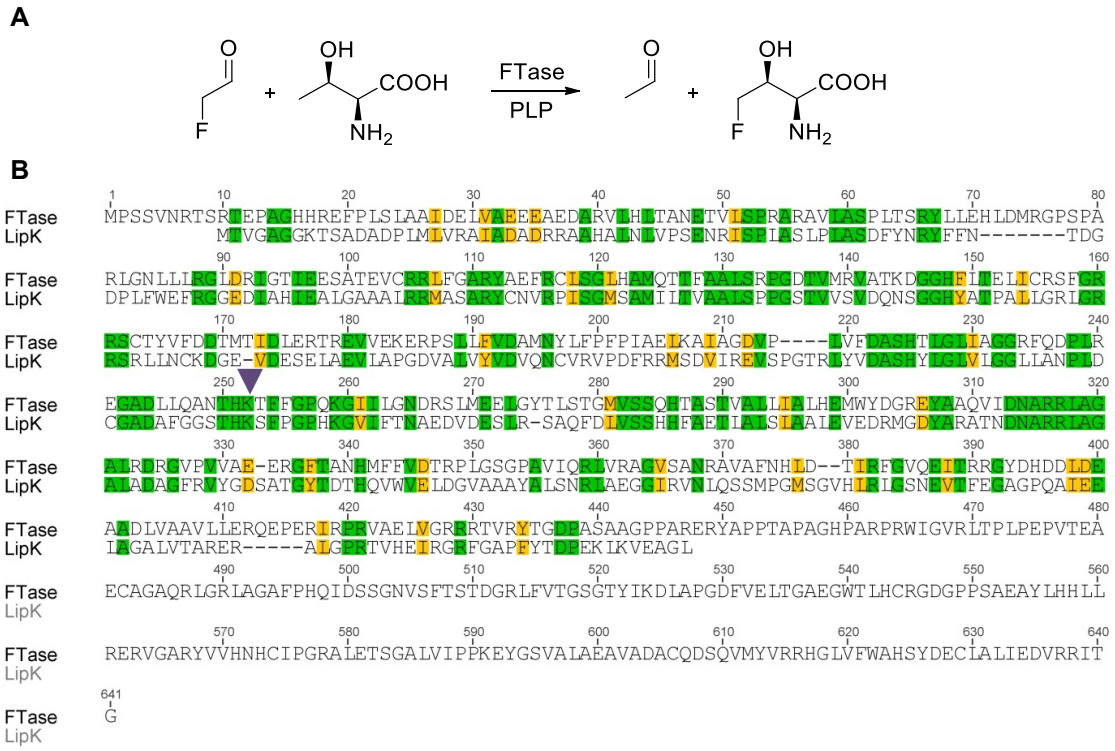

Figure 4.2. Enzymes catalyzing an L-Thr-dependent β-substitution. (**A**) Reaction catalyzed by 4-fluorothreonine transaldolase (FTase). The activity was initially discovered based on isolation of the native enzyme from the 4-fluorothreonine producing-strain *Streptomyces cattleya*. (**B**) Sequence alignment of FTase and LipK. FTase, the sequence of which was identified using reverse genetics, consists of two putative domains: an N-terminal SHMT-like domain and a C-terminal phosphate-binding domain of bacterial sugar epimerases and aldolases. One such epimerase homologue, AraD, catalyzes a reversible retro-aldol reaction with ribulose-1-phosphate. Due to limiting expression levels, recombinant FTase that was partially purified from *Streptomyces lividans* was used solely to reconstitute the biosynthetic pathway of 4-fluorothreonine, thus the exact function of each domain remains undefined. LipK has a relatively low sequence identity of 25% (36% similarity) to the N-terminal domain of FTase, but the results with LipK suggest the transaldolase activity is likely harbored within this domain. ▼, conserved Lys required for formation of the internal aldimine with pyridoxal-5'-phosphate.

References

1. Walsh C. Where will new antibiotics come from? Nat Rev Micro. 2003;1(1):65-70.
2. Newman DJ. Natural Products as Leads to Potential Drugs: An Old Process or the New Hope for Drug Discovery? Journal of Medicinal Chemistry. 2008;51(9):2589-99. doi: 10.1021/jm0704090.
3. Christoffersen RE. Antibiotics[mdash]an investment worth making? Nat Biotech. 2006;24(12):1512-4.
4. Contestabile R, Paiardini A, Pascarella S, di Salvo ML, D'Aguanno S, Bossa F. l-Threonine aldolase, serine hydroxymethyltransferase and fungal alanine racemase. European Journal of Biochemistry. 2001;268(24):6508-25. doi: 10.1046/j.0014-2956.2001.02606.x.
5. Carter AP, Clemons WM, Brodersen DE, Morgan-Warren RJ, Wimberly BT, Ramakrishnan V. Functional insights from the structure of the 30S ribosomal subunit and its interactions with antibiotics. Nature. 2000;407(6802):340-8. doi: http://www.nature.com/nature/journal/v407/n6802/suppinfo/407340a0_S1.html.
6. Hansen JL, Ippolito JA, Ban N, Nissen P, Moore PB, Steitz TA. The Structures of Four Macrolide Antibiotics Bound to the Large Ribosomal Subunit. Molecular Cell. 2002;10(1):117-28. doi: http://dx.doi.org/10.1016/S1097-2765(02)00570-1.
7. Schlunzen F, Zarivach R, Harms J, Bashan A, Tocilj A, Albrecht R, et al. Structural basis for the interaction of antibiotics with the peptidyl transferase centre in eubacteria. Nature. 2001;413(6858):814-21.
8. Yusupov MM, Yusupova GZ, Baucom A, Lieberman K, Earnest TN, Cate JH, et al. Crystal structure of the ribosome at 5.5 A resolution. Science 2001.292(5518):883-96. Epub 2001 Mar 29.
9. Heaslet H, Harris M, Fahnoe K, Sarver R, Putz H, Chang J, et al. Structural comparison of chromosomal and exogenous dihydrofolate reductase from Staphylococcus aureus in complex with the potent inhibitor trimethoprim. Proteins. 2009;76(3):706-17.
10. Falagas ME, Grammatikos AP, Michalopoulos A. Potential of old-generation antibiotics to address current need for new antibiotics. Expert Rev Anti Infect Ther. 2008;6(5):593-600.
11. Pallen MJ, Lam AC, Antonio M, Dunbar K. An embarrassment of sortases – a richness of substrates? Trends in Microbiology. 2001;9(3):97-101. doi: http://dx.doi.org/10.1016/S0966-842X(01)01956-4.
12. Rohdich F, Kis K, Bacher A, Eisenreich W. The non-mevalonate pathway of isoprenoids: genes, enzymes and intermediates. Current Opinion in Chemical Biology. 2001;5(5):535-40. doi: http://dx.doi.org/10.1016/S1367-5931(00)00240-4.
13. Winn M, Goss RJM, Kimura K-i, Bugg TDH. Antimicrobial nucleoside antibiotics targeting cell wall assembly: Recent advances in structure-function studies and nucleoside biosynthesis. Natural Product Reports.27(2):279-304.
14. Stachyra T, Dini C, Ferrari P, Bouhss A, van Heijenoort J, Mengin-Lecreulx D, et al. Fluorescence Detection-Based Functional Assay for High-Throughput Screening for MraY. Antimicrobial Agents and Chemotherapy. 2004;48(3):897-902. doi: 10.1128/aac.48.3.897-902.2004.
15. Kahan FM, Kahan JS, Cassidy PJ, Kropp H. THE MECHANISM OF ACTION OF FOSFOMYCIN (PHOSPHONOMYCIN). Annals of the New York Academy of Sciences. 1974;235(1):364-86. doi: 10.1111/j.1749-6632.1974.tb43277.x.

16. Fan C, Moews P, Walsh C, Knox. Vancomycin resistance: structure of D-alanine:D-alanine ligase at 2.3 A resolution. Science. 1994;266(5184):439-43. doi: 10.1126/science.7939684.
17. Farver DK, Hedge DD, Lee SC. Ramoplanin: A Lipoglycodepsipeptide Antibiotic. The Annals of Pharmacotherapy. 2005;39(5):863-8. doi: 10.1345/aph.1E397.
18. Page MI. The mechanisms of reactions of b-lactam antibiotics. Advances in physical organic chemistry. 1987;23:165-270.
19. Bouhss A, Trunkfield AE, Bugg TDH, Mengin-Lecreulx D. The biosynthesis of peptidoglycan lipid-linked intermediates. FEMS Microbiology Reviews. 2008;32(2):208-33. doi: 10.1111/j.1574-6976.2007.00089.x.
20. Bugg TDH, Lloyd AJ, Roper DI. Phospho-MurNAc-Pentapeptide Translocase (MraY) as a Target for Antibacterial Agents and Antibacterial Proteins. Infectious Disorders - Drug Targets(Formerly Current Drug Targets - Infectious. 2006;6(2):85-106. doi: 10.2174/187152606784112128.
21. Walsh CT, Zhang W. Chemical Logic and Enzymatic Machinery for Biological Assembly of Peptidyl Nucleoside Antibiotics. ACS Chemical Biology. 2011;6(10):1000-7. doi: 10.1021/cb200284p.
22. Bouhss A, Crouvoisier M, Blanot D, Mengin-Lecreulx D. Purification and characterization of the bacterial MraY translocase catalyzing the first membrane step of peptidoglycan biosynthesis. J Biol Chem. 2004;279(29):29974-80.
23. Lloyd AJ, Brandish PE, Gilbey AM, Bugg TD. Phospho-N-acetyl-muramyl-pentapeptide translocase from Escherichia coli: catalytic role of conserved aspartic acid residues. J Bacteriol. 2004;186(6):1747-57.
24. Al-Dabbagh B, Henry X, El Ghachi M, Auger G, Blanot D, Parquet C, et al. Active site mapping of MraY, a member of the polyprenyl-phosphate N-acetylhexosamine 1-phosphate transferase superfamily, catalyzing the first membrane step of peptidoglycan biosynthesis. Biochemistry. 2008;47(34):8919-28.
25. Price NP, Tsvetanova B. Biosynthesis of the tunicamycins: a review. J Antibiot. 2007;60(8):485-91.
26. Yamashita A, Norton E, Petersen PJ, Rasmussen BA, Singh G, Yang Y, et al. Muraymycins, novel peptidoglycan biosynthesis inhibitors: synthesis and SAR of their analogues. Bioorganic & Medicinal Chemistry Letters. 2003;13(19):3345-50. doi: http://dx.doi.org/10.1016/S0960-894X(03)00671-1.
27. Kaysser L, Lutsch L, Siebenberg S, Wemakor E, Kammerer B, Gust B. Identification and Manipulation of the Caprazamycin Gene Cluster Lead to New Simplified Liponucleoside Antibiotics and Give Insights into the Biosynthetic Pathway. Journal of Biological Chemistry. 2009;284(22):14987-96. doi: 10.1074/jbc.M901258200.
28. Igarashi M, Takahashi Y, Shitara T, Nakamura H, Naganawa H, Miyake T, et al. Caprazamycins, Novel Lipo-nucleoside Antibiotics, from Streptomyces sp. J Antibiot. 2005;58(5):327-37.
29. Igarashi M, Nakagawa N, Doi N, Hattori S, Naganawa H, Hamada M. Caprazamycin B, a novel anti-tuberculosis antibiotic, from Streptomyces sp. J Antibiot. 2003;56(6):580-3.
30. Isono KU, M. Kusakabe, H. Kimura, K. Izaki, K. Nelson, C. McCloskey, J. Liposidomycin: Novel Nucleosid Antibiotics Which Inhibit Bacterial Peptidoglycan Synthesis. Journal of Antibiotics. 1985;38:1617-21.
31. Muramatsu Y, Ohnuki T, Ishii MM, Kizuka M, Enokita R, Miyakoshi S, et al. A-503083 A, B, E and F, novel inhibitors of bacterial translocase I, produced by Streptomyces sp. SANK 62799. J Antibiot (Tokyo). 2004;57(10):639-46.

32. Yamaguchi H, Sato S, Yoshida S, Takada K, Itoh M, Seto H, et al. Capuramycin, a new nucleoside antibiotic. Taxonomy, fermentation, isolation and characterization. J Antibiot. 1986;39(8):1047-53.
33. Muramatsu Y, Ishii MM, Inukai M. Studies on novel bacterial translocase I inhibitors, A-500359s. II. Biological activities of A-500359 A, C, D and G. J Antibiot. 2003;56(3):253-8.
34. Muramatsu Y, Muramatsu A, Ohnuki T, Ishii MM, Kizuka M, Enokita R, et al. Studies on novel bacterial translocase I inhibitors, A-500359s. I. Taxonomy, fermentation, isolation, physico-chemical properties and structure elucidation of A-500359 A, C, D and G. J Antibiot. 2003;56(3):243-52.
35. Murakami R, Fujita Y, Kizuka M, Kagawa T, Muramatsu Y, Miyakoshi S, et al. A-102395, a New Inhibitor of Bacterial Translocase I, Produced by Amycolatopsis sp. SANK 60206. J Antibiot. 2007;60(11):690-5.
36. MURAMATSU YJ, FUJITA YJ, AOYAGI AJ, KIZUKA MJ, TAKATSU TJ, MIYAKOSHI SJ, inventors; NOVEL ANTIBIOTIC MURAMINOMICIN. Japan2003 2003.
37. Funabashi M, Baba S, Nonaka K, Hosobuchi M, Fujita Y, Shibata T, et al. The Biosynthesis of Liposidomycin-like A-90289 Antibiotics Featuring a New Type of Sulfotransferase. ChemBioChem.11(2):184-90. doi: 10.1002/cbic.200900665.
38. Yang Z, Chi X, Funabashi M, Baba S, Nonaka K, Pahari P, et al. Characterization of LipL as a Non-heme, Fe(II)-dependent α-Ketoglutarate:UMP Dioxygenase That Generates Uridine-5′-aldehyde during A-90289 Biosynthesis. Journal of Biological Chemistry. 2011;286(10):7885-92. doi: 10.1074/jbc.M110.203562.
39. Chi X, Pahari P, Nonaka K, Van Lanen SG. Biosynthetic Origin and Mechanism of Formation of the Aminoribosyl Moiety of Peptidyl Nucleoside Antibiotics. Journal of the American Chemical Society. 2011;133(36):14452-9. doi: 10.1021/ja206304k.
40. Chi X, Baba S, Tibrewal N, Funabashi M, Nonaka K, Van Lanen SG. The muraminomicin biosynthetic gene cluster and enzymatic formation of the 2-deoxyaminoribosyl appendage. MedChemComm. 2013;4(1):239-43.
41. Lehninger AL. Lehninger principles of biochemistry. 4 ed. New York: W.H Freeman; 2005.
42. Scarsdale JN, Radaev S, Kazanina G, Schirch V, Wright HT. Crystal structure at 2.4 Å resolution of E. coli serine hydroxymethyltransferase in complex with glycine substrate and 5-formyl tetrahydrofolate. Journal of Molecular Biology. 2000;296(1):155-68. doi: http://dx.doi.org/10.1006/jmbi.1999.3453.
43. Schirch V, Hopkins S, Villar E, Angelaccio S. Serine hydroxymethyltransferase from Escherichia coli: purification and properties. Journal of Bacteriology. 1985;163(1):1-7.
44. Schirch V. Mechanism of folate-requiring enzymes in one-carbon metabolism. Comprehensive Biological Catalysis. San Diego, CA.: Academic Press; 1998. p. 211-52.
45. Shostak K, Schirch V. Serine hydroxymethyltransferase: mechanism of the racemization and transamination of D- and L-alanine. Biochemistry. 1988;27(21):8007-14. doi: 10.1021/bi00421a006.
46. Gefflaut T, Blonski C, Perie J, Willson M. Class I aldolases: substrate specificity, mechanism, inhibitors and structural aspects. Prog Biophys Mol Biol. 1995;63(3):301-40.
47. Y. Muramatsu ea, inventor; 2004.
48. Funabashi M, Baba S, Nonaka K, Hosobuchi M, Fujita Y, Shibata T, et al. The Biosynthesis of Liposidomycin-like A-90289 Antibiotics Featuring a New Type of Sulfotransferase. ChemBioChem. 2010;11(2):184-90. doi: 10.1002/cbic.200900665.
49. Funabashi M, Yang Z, Nonaka K, Hosobuchi M, Fujita Y, Shibata T, et al. An ATP-independent strategy for amide bond formation in antibiotic biosynthesis. Nat Chem Biol. 2010;6(8):581-6. doi:

http://www.nature.com/nchembio/journal/v6/n8/abs/nchembio.393.html - supplementary-information.
50. Sambrook J, Russell DW. SDS-Polyacrylamide Gel Electrophoresis of Proteins. Cold Spring Harbor Protocols. 2006;2006(4):pdb.prot4540. doi: 10.1101/pdb.prot4540.
51. Saeed A, Young DW. ChemInform Abstract: Synthesis of L-β-Hydroxyamino Acids Using Serine Hydroxymethyltransferase. ChemInform. 1992;23(27):no-no. doi: 10.1002/chin.199227252.
52. J. Bartos MP. Colorimetric and fluorimetric determination of aldehydes and ketones. Pure and applied Chemistry. 1979;51:1803-14.
53. Segel IH. Enzyme Kinetics. New York: John Wiley and Sons, Inc; 1993.
54. Schirch LV, Tatum CM, Benkovic SJ. Serine transhydroxymethylase: evidence for a sequential random mechanism. Biochemistry. 1977;16(3):410-9. doi: 10.1021/bi00622a011.
55. Ishimaru T. Nippon Kagaku Zasshi1960. 1589 p.
56. Babad H, Zeiler AG. Chemistry of phosgene. Chemical Reviews. 1973;73(1):75-91. doi: 10.1021/cr60281a005.
57. Chang Z, Sitachitta N, Rossi JV, Roberts MA, Flatt PM, Jia J, et al. Biosynthetic Pathway and Gene Cluster Analysis of Curacin A, an Antitubulin Natural Product from the Tropical Marine Cyanobacterium Lyngbya majuscula†. Journal of Natural Products. 2004;67(8):1356-67. doi: 10.1021/np0499261.
58. IMAGAWA T, NAKAMURA T. Properties and Kinetics of Salt Activation of a Membrane-Bound NADH Dehydrogenase from a Marine Bacterium Photobacterium phosphoreum. Journal of Biochemistry. 1978;84(3):547-57.
59. Dückers N, Baer K, Simon S, Gröger H, Hummel W. Threonine aldolases—screening, properties and applications in the synthesis of non-proteinogenic β-hydroxy-α-amino acids. Appl Microbiol Biotechnol. 2010;88(2):409-24. doi: 10.1007/s00253-010-2751-8.
60. Chen H, Hubbard BK, O'Connor SE, Walsh CT. Formation of beta-hydroxy histidine in the biosynthesis of nikkomycin antibiotics. Chem Biol. 2002;9(1):103-12.
61. Chen H, Walsh CT. Coumarin formation in novobiocin biosynthesis: beta-hydroxylation of the aminoacyl enzyme tyrosyl-S-NovH by a cytochrome P450 NovI. Chem Biol. 2001;8(4):301-12.
62. Garneau S, Dorrestein PC, Kelleher NL, Walsh CT. Characterization of the formation of the pyrrole moiety during clorobiocin and coumermycin A1 biosynthesis. Biochemistry. 2005;44(8):2770-80.
63. Fesko K, Giger L, Hilvert D. Synthesis of beta-hydroxy-alpha-amino acids with a reengineered alanine racemase. Bioorg Med Chem Lett. 2008;18(22):5987-90.
64. Deng H, Cross SM, McGlinchey RP, Hamilton JTG, O'Hagan D. In Vitro Reconstituted Biotransformation of 4-Fluorothreonine from Fluoride Ion: Application of the Fluorinase. Chemistry & Biology. 2008;15(12):1268-76.
65. Murphy CD, Schaffrath C, O'Hagan D. Fluorinated natural products: the biosynthesis of fluoroacetate and 4-fluorothreonine in Streptomyces cattleya. Chemosphere. 2003;52(2):455-61.
66. Takayama S, McGarvey GJ, Wong, Chi H. MICROBIAL ALDOLASES AND TRANSKETOLASES:New Biocatalytic Approaches to Simple and Complex Sugars. Annual Review of Microbiology. 1997;51(1):285-310. doi: doi:10.1146/annurev.micro.51.1.285.

Vita

Sandra Hummel Barnard

EDUCATION

Iowa State University, Ames, IA

- B.S. Biochemistry 2007
- Minor in Music 2007

RESEARCH EXPERIENCE

University of Kentucky, Department of Pharmaceutical Science, Lexington, KY
Graduate Student with Dr. Steven Van Lanen,
2008-Present
Researching the biosynthetic pathway of various peptidyl nucleoside and sideromycin antibacterial compounds.

Temporary Research Assistant, Nitrogen Lab, DuPont Pioneer Hi-Bred International, Johnston, Iowa
Supervisor: Dr. Juan Sanchez
May 2007-2008
Executed and analyzed experiments involving the manipulation of plant genomes and the phenotypic results in low nitrogen content soil.

Temporary Research Assistant , Diagnostic Lab, DuPont Pioneer Hi-Bred International, Johnston, Iowa
Supervisor: Barbra Fleener
May 2006-May 2007

ABSTRACTS

Sandra Barnard-Britson, Koichi Nonaka and Steven Van Lanen. The Discovery of an L-Threonine: Uridine-5'-Aldehyde Transaldolase in Caprazamycin like Antibiotics. Abstracts of the Zing Biocatalyst Conference. 2012.

Axel Vazquez, **Sandra Barnard-Britson**, and Steven Van Lanen. Characterization of the Enzymatic Chemistry that Catalyzes the Biosynthesis of the Core Skeleton of Capuramycin-type Antibiotics. Abstracts of the SACNAS National Conference, 2012.

PUBLICATIONS

Barnard-Britson, S.; Chi, X.; Nonaka, K.; Spork, A. P.; Tibrewal, N.; Goswami, A.; Pahari, P.; Ducho, C.; Rohr, J.; Van Lanen, S. G. *Journal of the American Chemical Society* **2012**, *134*, 18514.